

Particles and Cosmology:
Scale-Symmetric Theory (SST)

Sylwester Kornowski

2021

Poland, Western Pomerania, Szczecin

First publication:

The first version of the book was entitled “*General Theory of Singularities*”,

Szczecin: Tajgeta, ISBN 83-901005-1-7 (1997);

Available in Polish National Library: Signature: NR_BBN: PB 9041/2000

or in Jagiellonian Library: Signature: B 250180.

The first publication contains the foundations of the Scale-Symmetric Theory i.e. the phase transitions of the inflation field and the atom-like structure of baryons.

The first version of the atom-like structure of baryons appeared in 1996 (Polish edition).

Technical Notes: The book is divided into chapters (e.g. 2 or 2.), sections (e.g. 2.1.) and paragraphs (e.g. 2.1.1.). The main topics described are listed at the beginning of each chapter. The figures and tables are numbered with consecutive natural numbers. The numbering of the formulas is as follows: (chapter.section.current-number). Literature is provided at the end of each of the first three chapters and at the end of each Paragraph in the remaining chapters. The Index leads to a page containing the main information about the search term.

Preface

This book is an attempt to organize the main ideas and to unify the descriptions that were included in my letters, papers and books written in 1976-2021 on particle physics, cosmology, astrophysics, atomic nucleus physics, atomic physics, brain-mind interactions, chaos theory, or quantum physics. But it also includes many new elements. It is a book about the missing part of the theory of everything (ToE). The Scale-Symmetric Theory (SST) is based on two pillars. The first pillar describes the four successive phase transitions of the initial inflation field composed of practically non-gravitating tachyons and it is the basis of the ToE. The second pillar is the atom-like structure of baryons, which is due to the electroweak and nuclear strong interactions.

Contents

1. Introduction	4
2. Particle Physics	21
3. Cosmology	73
4. Applications	92
5. Interdisciplinary Problems	133
6. Harbingers of a revolution in physics	140
7. Appendices	143
Index	148

Chapter 1

Introduction

1.1. Need for new methods	5
1.2. Nomenclature used in SST	6
1.3. Initial conditions used in SST	10
1.4. Derivation of the very frequently applied formulas and laws	15
1.5. Electron	19
1.6. Uncertainty of experimental results from virtual phenomena	20
References	20

1.1. Need for new methods

For decades we are still not able to solve dozens of basic problems in physics and cosmology. Why?

The most common error in theories is not separating the definitions from the laws of Nature. The definitions can be freely chosen and do not require justification. On the other hand, the laws of Nature, i.e. mathematical formulas that describe the internal structures of objects or their dynamics, must always be justified on the basis of possible physical phenomena resulting from the initial conditions.

If, for example, differential equations appear in theory as some hocus-pocus, and then we add a large enough number of free parameters to fit the theoretical results with the experimental data, this is quackery that has nothing with real physics.

The laws of conservation of some physical quantities (or symmetries) are laws of Nature, so they must be derived from the initial conditions. For example, in mainstream physics there is no justification why an electric charge is invariant. The claim that this is due to the symmetry of a gauge transformation is not an explanation because such a transformation is a mathematical operation and not a physical phenomenon.

So gauge transformations are not the right way to formulate the missing part of the theory of everything (ToE).

Physics needs new methods and here we present them.

Here, due to the viscosity that results from smoothness of surfaces of the inertial masses, due to the possible quantum entanglement and/or confinement of the components of the Scale-Symmetric-Theory (SST) absolute spacetime (SST-As), instead of solving differential equations of motion or looking for symmetries resulting from the gauge transformations, we are looking for stable or metastable dynamical distributions of the components of such spacetime. The distributions lead to the coupling constants which are the core of the dynamical description. Most of such distributions cannot result from solutions of the equations of motion because the observed particles have too rich internal structure which requires the use of various methods for single particles.

The General Theory of Relativity (GR) starts from the assumptions that the inertial mass and gravitational mass, M_{inertial} and $M_{\text{gravitational}}$ respectively, have the same value

$$M_{\text{inertial}} = M_{\text{gravitational}} \quad (1.1.1)$$

and that there is an upper speed limit $v_{\text{upper}} = c = 299,792,458 \text{ m/s}$. Such a theory leads to the relativistic masses which are consistent with experimental results – for the upper speed limit, there appears a relativistic-mass singularity so within GR we cannot describe phenomena concerning such a singularity and tachyons i.e. objects that are moving with superluminal speeds.

The four fundamental phase transitions of the inflation field lead to the five levels of Nature: to the tachyons the SST Higgs field (SST-Hf) consists of, to the superluminal quantum-entanglement objects (entanglons), neutrino-antineutrino pairs the SST absolute spacetime (SST-As) consists of, to the core of baryons, and to the cosmological Protoworld – dynamics of the last three objects is similar. The strength of SST comes from the fact that it contains only 7 parameters and 2 iterative parameters and leads to physical constants and all the basic physical quantities used in particle physics and cosmology, and many used in other areas of physics. SST is the classical non-perturbative theory.

Here we will show that the Quantum Mechanics (QM) is the result of neglecting the exchanges of the spin-1 superluminal objects (the entanglons) the GR and QM matter consists

of (i.e. matter with the upper speed limit equal to c). In SST, there appear the entanglons so we do not apply the QM formalism. The quantum behaviour of a particle (i.e. the disappearance in one place of a field and appearance in another one, and so on) has a classical but superluminal origin.

Generally, the matter and energy behave classically so the SST is the pure classical theory with physical quantities quantized classically.

Each spinning object immersed in a granular field curves the field, i.e. creates a gradient with non-spherical symmetry. We assume that objects with inertial mass much higher than their gravitational mass

$$M_{\text{inertial}} \gg M_{\text{gravitational}} \quad (1.1.2)$$

can be tachyonic.

Tachyonic objects (here they are called the tachyons and entanglons) which are characterized by infinitesimal gravitational constants, we can call the imaginary objects because we can detect them only indirectly as a gravitational field and quantum entanglement respectively. But we can precisely define their properties because when we apply the minimum number of initial conditions, only the unique set of initial physical quantities leads to the experimental data.

1.2. Nomenclature used in SST

The definitions of structures, physical quantities and their units are not laws of nature, but the language of description. Using the same definitions allows you to compare the theoretical results obtained in different theories with experimental data. Let us emphasize, however, that new and extended definitions must emerge in the broader theories. SST is the missing core of ToE, so new and extended definitions are needed. Redundant definitions appear in incomplete and at least partially erroneous theories.

External helicity and internal helicity: external helicity is defined by toroidal motion and kinetic velocity while internal helicity is defined by poloidal motion and toroidal motion (Fig.1). Thin torus (loop) and other tori with central hole are the simplest objects that can have internal helicity. We will show that the poloidal motions lead to the low violation of the CP symmetry, where C denotes the charge conjugation, and P is the parity transformation.

Tachyon: a spinning internally structureless inertial mass (it is a physical volume with the same inertial-mass density at all points inside it) with a radius about 29 orders of magnitude lower than the Planck length. Spinning inertial masses create some non-spherical gradients in fields composed of inertial masses but they do not cause a relativistic mass of the inertial mass to appear.

Closed string: a circle-like superluminal spin-1/2 loop made of one layer of touching tachyons with a radius about 10 orders of magnitude lower than the Planck length.

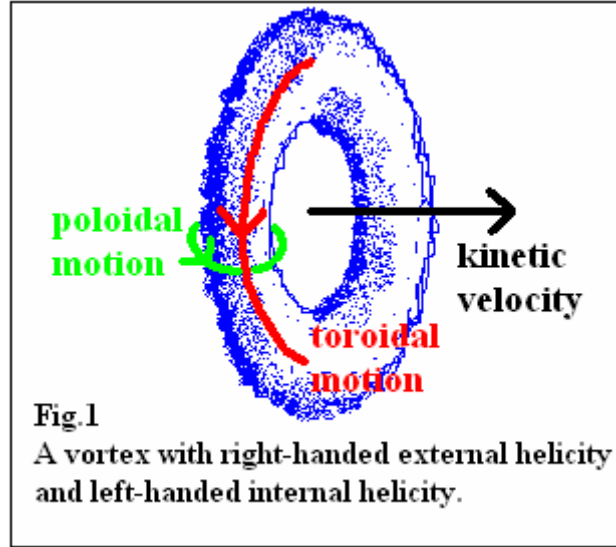
Entanglon: a superluminal spin-1 binary system of the closed strings responsible for quantum entanglement.

SST Higgs field (SST-Hf): a field composed of tachyons.

Initial inflation field: the field with left-handed external helicity composed of tachyons packed to maximum.

SST absolute spacetime (SST-As): a field composed of the non-entangled and non-rotating-spin-1 neutrino-antineutrino pairs moving with their natural speed c in relation to such absolute spacetime. The SST-As behaves as superfluid.

SST spacetime (SST-S): the two-component spacetime composed of the SST Higgs field and the SST absolute spacetime (SST-Hf and SST-As).



Quantum entanglement: the entanglement of the components of the SST absolute spacetime caused by exchanges of the superluminal entanglons. Distance between entangled components can change. But there are the two very stable states for the two shortest-distance quantum entanglement.

Confinement: it is the confinement of the spin-1 components of the SST absolute spacetime (or neutrinos) caused by the SST Higgs potential created by them. Distance of such confinement is invariant.

Photons and gluons: photons and gluons are the rotational energies of single or entangled components of the SST absolute spacetime. In fields that have internal helicity (the nuclear strong fields have such helicity), because of the three internal helicities of the components of the SST absolute spacetime, the photons behave as gluons so instead of the one type of photons we have the 8 types of gluons. In SST, the gluons are not confined.

Baryons and electrically charged leptons: cores of such fermions consist of a spin-1/2 torus/electric-charge and a spin-0 central ball/condensate both composed of the components of the SST absolute spacetime (Fig.2). We know that following equation defines a torus:

$$(x^2 + y^2 + z^2 - a^2 - b^2)^2 = 4 b^2 (a^2 - z^2) . \quad (1.2.1)$$

The spin-1/2 tori are most stable when $b = 2a$ because then the distance between points in the same state on the torus in the plane of the equator is $4a = \lambda$, where λ is the classical radius of a fermion (it is the 4/3 of the quantum radius). Then the maximal changes in amplitude of the standing wave coincide with the centre of the condensate and a point on the circular axis of the torus, while its three nodes are placed on the torus. The spin speed on the equator is c so the mean spin speed of the torus is $2c/3$ – it forces the radial and poloidal motions of the SST-As components so there appears the spin-0 condensate in the centre of the torus. Mean radius of the tori is the 2/3 of their equatorial radius.

Outside the core of baryons is obligatory the Titius-Bode law for the nuclear strong interactions.

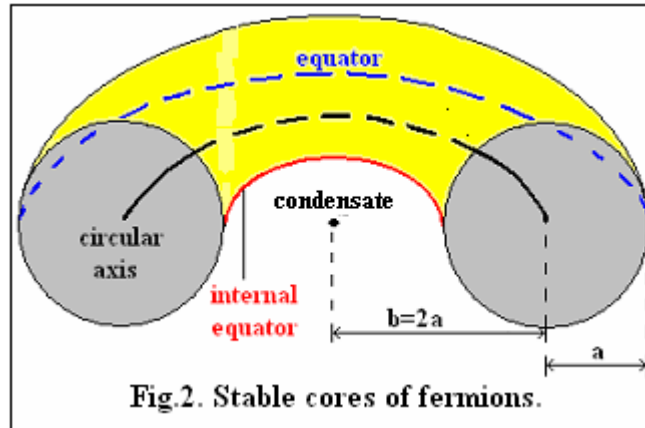


Fig.2. Stable cores of fermions.

Neutrinos: there are three species of neutrinos, i.e. the 6 different neutrinos. The tau-neutrino consists of 3 different smallest neutrinos so we have 4 different smallest neutrinos, i.e. 2 species of smallest neutrinos (the electron-neutrino and muon-neutrino). Cores of smallest neutrinos look as both the core of baryons and cores of electrically charged leptons but instead the SST-As components there are the superluminal spin-1 entanglons. It means that the smallest neutrinos carry the weak charge. The smallest neutrinos differ by orientation of the spins of entanglons on their torus and by the internal helicity. Their radius is close to the Planck length. The neutrino-antineutrino pairs are moving with the speed c despite the fact that they have the gravitational masses – it follows from the fact that they cannot attach entanglons because there are not free entanglons in the SST spacetime. On the other hand, for example, a moving proton can attach SST-As components so there appears the relativistic mass – it follows from the conservation of the spin of the torus/electric-charge of the proton and from the fact that the natural speed of the SST-As components in the SST absolute spacetime is c . Due to the tremendous non-gravitating energy frozen in each neutrino, neutrinos are the very stable particles. Oscillations of neutrinos are an illusion resulting from the switching of neutrino positions in collisions of free neutrinos with free or bound neutrinos.

Zero-energy field: the zero-energy field is associated with the excited states of the SST absolute spacetime. Rotational motions of photons and gluons and other ordered motions decrease dynamic pressure in the local SST-As so local density of it must increase. Mass of such additional compaction of spacetime is equivalent to the carried energy – it leads to the origin of the Einstein formula $E = mc^2$. We see that momentum density and momentum flux both increase the local energy density, i.e. they increase density of the zero-energy field. The same concerns the shear stress because it forces creation of the particle-antiparticle pairs. Such is the origin of replacement of the Newtonian mass density with the Einsteinian stress-energy-momentum tensor. We can say that such a tensor leads to the *granular* SST absolute spacetime and vice versa. But emphasize that contrary to the Einstein's spacetime, the SST-As is not elastic but granular and it does not concern the gravitational fields.

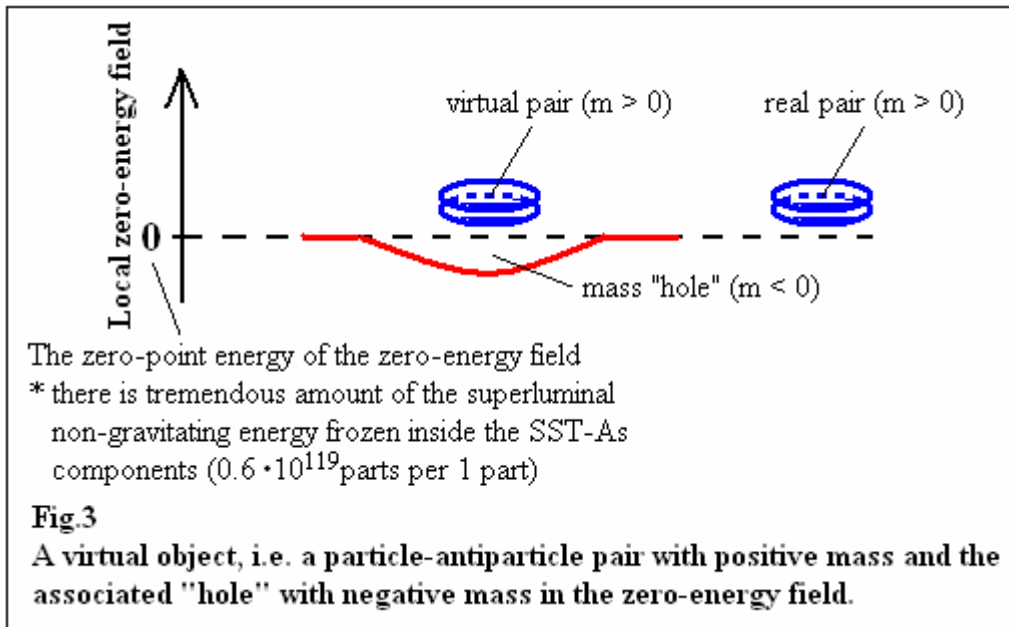
Unification of GR and QM: In SST, gravitating masses create gradients in the SST Higgs field, i.e. create the gravitational fields. Such gradients cause that the GR time is not absolute. On the other hand, gradients are not produced in the SST absolute spacetime – there are created the virtual pairs. It means that time in QM, which is associated with the

SST absolute spacetime, is absolute. It is impossible to merge the not absolute time with absolute time within the same methods so unification of GR and QM is impossible – we can “unify” such theories only via the phase transitions of the initial inflation field.

Dark matter (DM) loops: they are a circle-like loops composed of the SST-As components with spins tangent to the loop. Such loops cannot interact electromagnetically because the spins of the SST-As components cannot rotate. We show in this book that mass of the DM-loop with shortest-distance quantum entanglement has mass about $2.08 \cdot 10^{-47}$ kg. A DM-torus built of such DM-loops has mass equal to 727.4387 MeV.

Dark energy (DE): dark energy must increase dynamic pressure of the ground state (i.e. of the not excited state) of the SST-As, i.e. its components must move with the speed c – the DE components/segments were building blocks of the DM loops and DM tori created at the end of the SST inflation.

Our Cosmos: from the succeeding phase transitions of the inflation field follows that radius of our Cosmos is about $2.3 \cdot 10^{30}$ m.



Virtual particles: They are the objects created spontaneously in the SST absolute spacetime – there appear the bare (i.e. without the radiation masses) particle-antiparticle pairs with positive mass and the associated with them “holes” in the SST-As with negative mass in such a way that the total mass is equal to zero (Fig.3).

Speed c : It is the natural speed of the non-entangled SST-As components in relation to the SST absolute spacetime, and it is the speed of photons and gluons in relation to the object with which they interacted for the last time. In the Michelson-Morley experiment, the interferometer is the last-interaction object so it always will measure the speed c . Photons and gluons are entangled with the last-interaction object, i.e. there are exchanged the superluminal entanglons between the photons or gluons and the last-interaction object. The Special Theory of Relativity (SR) is valid only for particles that are entangled with the frame of reference we are considering. Here we calculated the speed c from our initial conditions. The protogalaxies were surrounded by the photons entangled with them so because the SST-As behaves as a superfluid, some protogalaxies in the initial protuberances in the early Universe have reached radial velocities many times higher than the c . Some similar phenomena appear in other superfluids. For

example, we know that a wire rod moving through a helium-3 superfluid does not break apart the Cooper pairs above the critical Landau velocity [1]. It is because particles in the superfluid stick to the rod. Of course, the superluminal cosmological protuberances were damped – galaxies whose relative speed in relation to the Earth has fallen below the speed c can be observed by us but due to the quantum entanglement, we measure the initial redshift, i.e. the redshift higher than 1.

SST quarks: they are the loops or condensates built of the SST-As components with the masses equal to the masses of quarks in the Standard Model (SM). Other properties of the SM quarks are not important. Here the masses of the SST quarks are derived from our initial conditions.

Neutron black holes (NBHs): they are the neutron stars with the spin speed equal to c on their equator.

1.3. Initial conditions used in SST

Due to a collision of the externally left-handed initial inflation field with a much bigger cosmological inertial mass, there appeared the inflation inside the bigger object. As a result there was created the SST spacetime with a stable boundary.

1.3.1. The 7 SST parameters

The 7 parameters applied in SST are as follows.

The mean radius of the tachyons is

$$r_t = 4.7571055 \cdot 10^{-65} \text{ m},$$

mean linear speed of tachyons is

$$v_t = 2.386343972 \cdot 10^{97} \text{ m/s},$$

mean spin speed on equator of tachyons is

$$v_{st} = 1.725741 \cdot 10^{70} \text{ m/s},$$

mean inertial mass of tachyons is

$$m_t = 3.752673 \cdot 10^{-107} \text{ kg},$$

dynamic viscosity resulting from smoothness of surfaces of tachyons is

$$\eta_t = 1.87516465001657 \cdot 10^{138} \text{ kg m}^{-1} \text{ s}^{-1},$$

the present-day mean inertial mass density of the SST Higgs field is

$$\rho_{Hf} = 2.645834 \cdot 10^{-15} \text{ kg m}^{-3},$$

and mean gravitational mass density of the SST absolute spacetime is

$$\rho_{As} = 1.102200989196 \cdot 10^{28} \text{ kg m}^{-3}. \quad (1.3.1)$$

1.3.2. The 2 additional iterative parameters

To simplify to maximum the calculations, we additionally use two iterative parameters. Iteration is the repeated application of a process in which the output of each step is used as the input for the next iteration. The two iterative parameters are as follows.

The electric charge of electron is

$$e = 1.60217643101205 \cdot 10^{-19} \text{ C}$$

and mass of the core of baryons is

$$H^\pm = 727.438703205527 \text{ MeV}. \quad (1.3.2)$$

In this book, the symbols of particles denote also their masses.

1.3.3. The 5 new symmetries and one new asymmetry

Four closed-strings symmetry (four-object/particle/fermion symmetry): it follows from the fact that internal helicity and spin of the inflation field was conserved. The tachyons

rotate so the created closed strings have internal helicity and spin. To create an object with zero internal helicity and zero spin, the closed strings must be created as binary systems of binary systems. The constituents of the single binary systems have parallel spins and opposite internal helicities whereas the binary systems in a binary system have opposite spins. Such four-object symmetry can be adopted by other objects on higher levels of Nature.

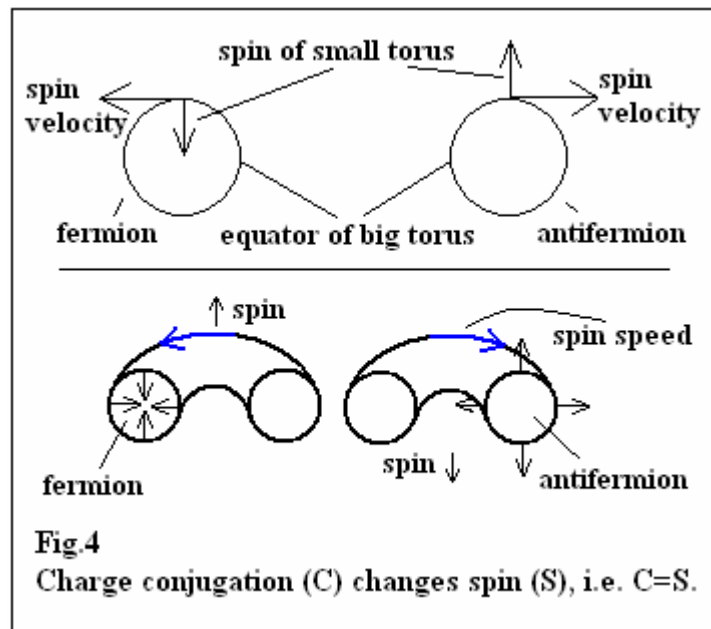
Saturation symmetry: it follows from collisions of the free and bound tachyons. Consider an object composed of four parts each composed of four elements. Then three elements of each part are exchanged between a part and the three other parts while the fourth element represents the part. We see that if a smaller object contains N elements then the next bigger one contains N^2 elements.

Invariant surface-density symmetry: surface density of different tori created due to the phase transitions of the expanding inflation field is invariant so Nature can immediately repair damages to the tori.

Adoption symmetry: on the higher levels of Nature, the half-integral spin of the closed strings and the unitary spin of the binary closed strings are adopted by other particles/objects. Tori are the simplest surfaces which can adopt the internal helicity and spin of the closed strings.

Decay symmetry: there are the symmetrical decays of bosons in the fields surrounding the objects with the spin speed equal to the c on their equator. Such processes lead to the Titius-Bode law which is valid in the plane of the equator.

Half-jet asymmetry: the poloidal motion in fermions (there is torus/charge) creates in the SST spacetime a half-jet that is the cause of the C , P and T violations, where T is the time reversal. Poloidal motions follow from the spin speed of tachyons which is very low in comparison with its linear velocity – it causes that the violation of symmetries is also very low.



The tachyons have infinitesimal spin so all fermions have internal helicity (helicities) which distinguishes fermion from antifermion. On surface of the tori/electric-charges, all spins of the SST-As components point towards the

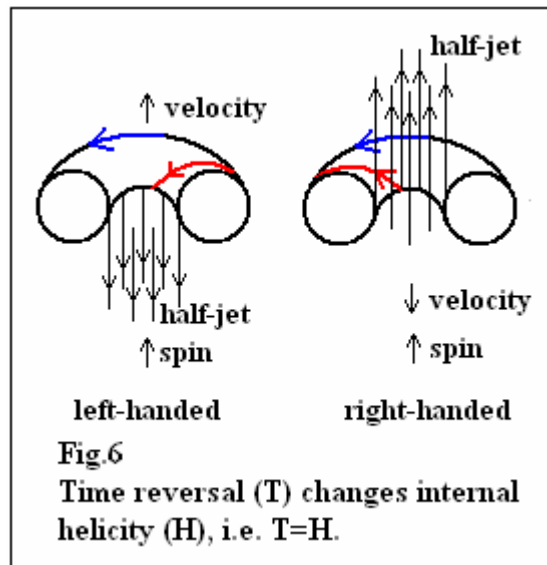
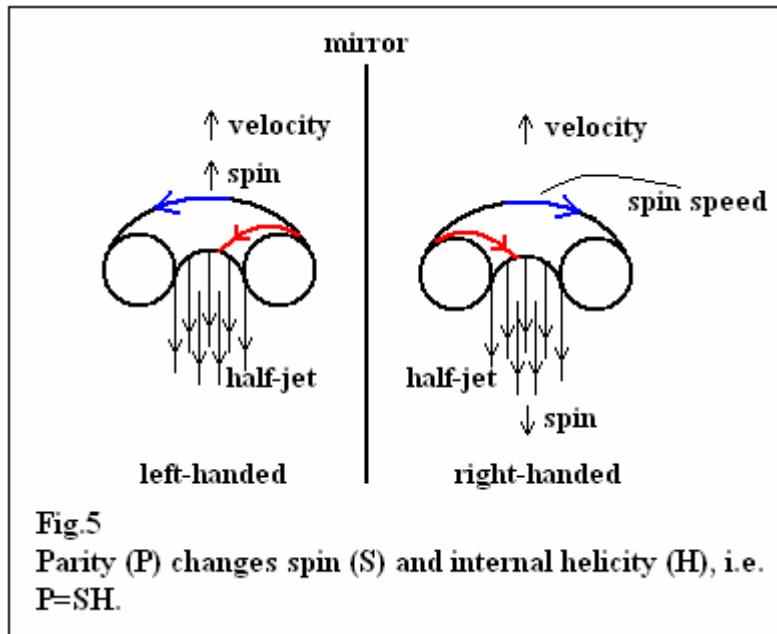
circular axis of the torus (Fig.2) or all point in the opposite direction which distinguishes electric charge from opposite one.

Due to the half-jets, there appears an asymmetry between parallel and antiparallel orientations of spin of fermions in relation to their velocity.

From Figures 4, 5 and 6 follows that the *CPT* symmetry is always valid

$$CPT = S SH H = S^2 H^2 = 1^2 1^2 = (-1)^2 (-1)^2 = 1 \text{ (always)}. \quad (1.3.3)$$

This means that symmetry-breaking of a system composed of fermion-antifermion pairs is impossible. The observed in our Universe the baryon-antibaryon asymmetry does not follow from a *CPT*-symmetry violation. Asymmetry follows from the fact that the initial inflation field had the left-handed external helicity.



The nuclear strong interactions are CP -invariant. It results from the fact that single neutral pion, which is responsible for the nuclear strong interactions of baryons, is composed of two loops that simultaneously create antiparallel half-jets so asymmetry does not appear.

The origin of the symmetries used in mainstream physics will be reported on an ongoing basis during the calculations performed.

1.3.4. The three fundamental equations

Assume that the closed string is composed of K^2 adjoining tachyons (the square of the K means that calculations are far simpler). The saturation symmetry causes that the tori created during the succeeding phase transitions of the Higgs field should contain K^2 , K^4 , K^8 , K^{16} tachyons (the K^{16} tachyons is the upper limit that follows from the size of our Cosmos). The mass of the tori are directly proportional to the number of closed strings. This means that the stable objects contain the following number of closed strings: K^0 , K^2 , K^6 , K^{14} , and means that the mass of the stable objects are directly proportional to $K^{2(d-1)}$, where $d = 1$ for closed strings, $d = 2$ for neutrinos which consist of the binary closed strings (entanglons), $d = 4$ for the cores of baryons which consist of the neutrino-antineutrino pairs), and $d = 8$ for a cosmological torus (the core of the Protoworld) which consisted of the DM particles – their masses were the same as the core of baryons. The early Universe arose inside the Protoworld as the double cosmic loop composed of the neutron black holes (NBHs) grouped in protogalaxies. The evolution of the Protoworld leads to the dark matter, dark energy, and to the expanding Universe.

The radii of the tori are

$$r_d = r_1 K^{d-1}, \quad (1.3.4)$$

whereas the rest masses of the tori are

$$m_d = m_1 K^{2(d-1)}, \quad (1.3.5)$$

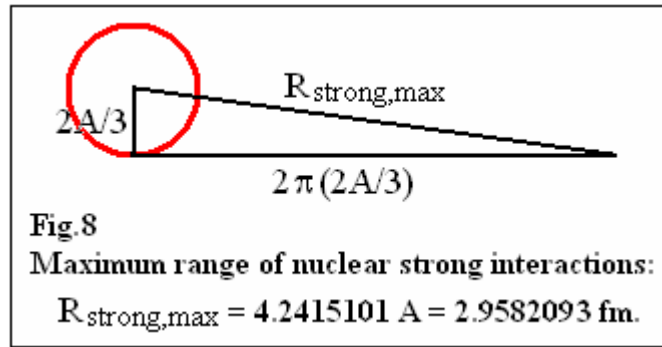
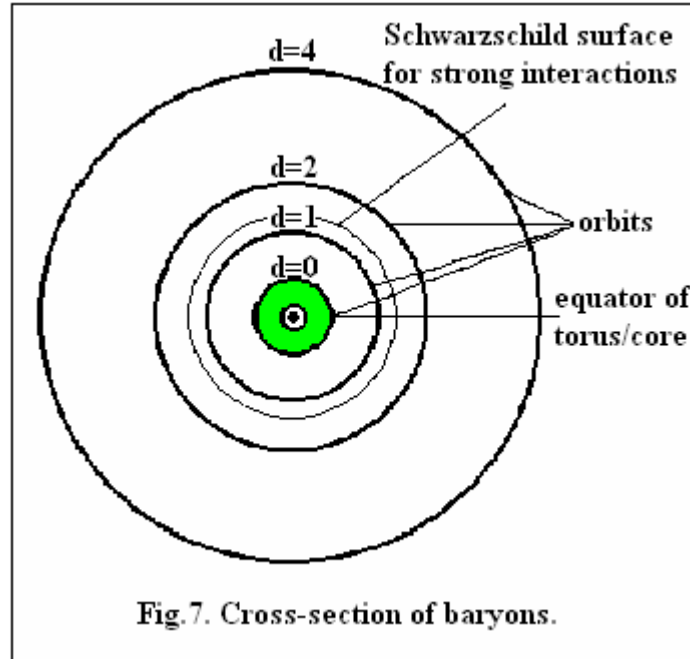
where r_1 and m_1 are for the closed string.

On equator of the core of baryons, there appear virtual bosons that to equalize their number density in spacetime are emitted. Assume that the radius of the equator of the core of baryons is A , and that the range of a virtual boson is B . At distance $A + B$ there is symmetrical decay of the virtual boson to two identical parts. One part is moving towards the equator whereas the second one is moving in the opposite direction. It means that in the place of decay there is produced a hole in the field surrounding the core. When the first part reaches the equator then the second one stops and decays to two identical parts – it takes place in distance $A + 2B$. In the place of decay is created “hole” in the zero-energy field. Next decay takes place in distance $A + 4B$. A statistical distribution of the holes in the field in the plane of the equator (of the circular tunnels in field) is defined by following formula

$$R_d = A + d B, \quad (1.3.6)$$

where R_d denotes the radii of the circular tunnels, the A denotes the external radius of the torus/core, $d = 0, 1, 2, 4$; the B denotes the distance between the second tunnel ($d = 1$) and

the first tunnel ($d = 0$). The first tunnel is in contact with the equator of the torus. Formula (1.3.6) is the Titius-Bode (TB) law for the nuclear strong interactions (Fig.7).



The gluon loop overlapping with the circular axis of the torus (Fig.2) in the core of baryons, we will call the fundamental gluon loop (FGL) – from Fig.2 we have that its radius is $R_{\text{FGL}} = 2A/3$.

Circumference and radius of FGL determine the maximum range of the nuclear strong interactions in baryons (Fig.8) – it is

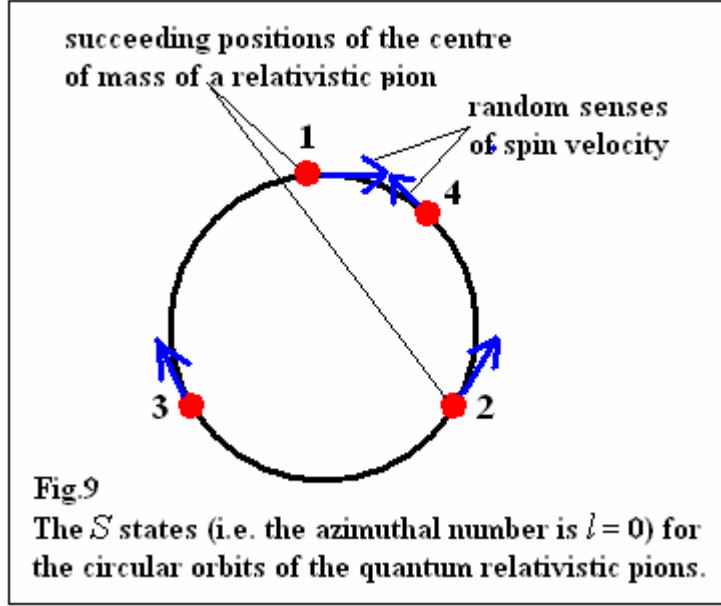
$$R_{\text{strong,max}} = 4.2415101 A . \quad (1.3.7)$$

Our calculations will show that $A = 0.697442472994 \text{ fm}$ so $R_{\text{strong,max}} = 2.9582093 \text{ fm.}$

Our calculations also will show that value of the B and the maximum range of the strong interactions in baryons cause that the $d = 4$ in formula (1.3.6) define the radius of the last TB orbit (i.e. the radius of the last tunnel in the zero-energy field) for the strong interactions.

Why all the d states of the relativistic pions in baryons are the S states i.e. why all the azimuthal/secondary quantum numbers of the relativistic pions are $l = 0$? It results from the fact that a pion in defined d state behaves as follows. Centre of mass of a relativistic pion

disappears in one point of defined circular orbit/tunnel and appears in another one, and so on, but senses of the spin velocities of the pion change randomly – it causes that resultant angular momentum on the circular orbit is equal to zero (Fig.9).



1.4. Derivation of the very frequently applied formulas and laws

In this book, we apply some laws used in mainstream physics. But SST is the supreme theory so we have to show that they can also be derived from the SST initial conditions.

1.4.1. Formula for relativistic mass

It is not true that pure energy, i.e. rotational energy of something or kinetic energy of something can directly transform into inertial or gravitational mass. The Einstein's formula $E = mc^2$ is valid because with each pure energy (it does not gravitate), E , is associated a local poor compaction of the SST absolute spacetime. The gravitational mass of it, m , is equivalent to the energy and such gravitational mass is a part of the zero-energy field.

Consider a rigid loop composed of the entangled SST-As components. Assume that linear/relativistic velocity of it is parallel to its spin – then the spin is conserved. The resultant speed of the SST-As components must be equal to c . Their spin speed we denote by v_{spin} while their linear/relativistic speed by v . Then for the rigid loop is

$$v_{\text{spin}}^2 + v^2 = c^2. \quad (1.4.1)$$

We can multiply it by $N_{\text{Rel}}^2 m^2$, where N_{Rel} and m denote the number of the SST-As components and mass of single component in relativistic loop respectively

$$N_{\text{Rel}}^2 m^2 v_{\text{spin}}^2 + N_{\text{Rel}}^2 m^2 v^2 = N_{\text{Rel}}^2 m^2 c^2. \quad (1.4.2)$$

Spin of the rigid loop is

$$\mathbf{spin} = N_i m v_{\text{spin}} r, \quad (1.4.3)$$

where N_i denotes number of the SST-As components.

Since spin and radius of the rigid loop and the mass of the SST-As components, m , are invariant, we have

$$N_0 c = N_{\text{Rel}} v_{\text{spin}}, \quad (1.4.4)$$

$$m_{\text{Rel}} = N_{\text{Rel}} m, \quad (1.4.5)$$

$$m_0 = N_0 m, \quad (1.4.6)$$

where N_0 denotes number of the SST-As components in the resting rigid loop, m_{Rel} is the relativistic mass of the loop, and m_0 is the rest mass of the loop.

From formulae (1.4.1)-(1.4.6) we obtain

$$m_{\text{Rel}} = m_0 / (1 - v^2 / c^2)^{1/2}. \quad (1.4.7)$$

We can see that when we accelerate such a rigid loop, it attaches more and more the SST-As components, i.e. the relativistic mass is real.

Emphasize that in a particle, there is the non-gravitating energy, E , and the particle has the bare mass M_{Bare} equal to the E (it is when units of E and M are the same) so the sum of absolute values of energies of virtual particles created outside the bare particle cannot be greater than $E + M_{\text{Bare}} = 2M_{\text{Bare}}$.

1.4.2. The Stefan-Boltzmann law and the Wien's displacement law

In SST, we very frequently apply the Stefan-Boltzmann law and the Wien's displacement law so we must derive them from our initial conditions.

The Stefan-Boltzmann law states that the radiated total energy (per unit surface area), denoted by $-\Delta E^*$, is directly proportional to the fourth power of the black body's thermodynamic temperature T

$$-\Delta E^* \sim T^4. \quad (1.4.8)$$

Wien's displacement law states that the black-body-radiation curve for different temperatures, T , peaks at different wavelengths, λ_{Peak} , and λ_{Peak} is inversely proportional to T

$$\lambda_{\text{Peak}} \sim 1 / T. \quad (1.4.9)$$

We can define the temperature T as inversely proportional to the radius R of a circle-like loop composed of the entangled SST-As components, so the T , because there is $\lambda = 2\pi R$, is also inversely proportional to the wavelength of the loop λ

$$T \sim 1 / R \sim 1 / (2 \pi R) \sim 1 / \lambda. \quad (1.4.10)$$

For a vortex composed of such loops with a peak radius, R_{Peak} , we have

$$T \sim 1 / (2 \pi R_{\text{Peak}}) \sim 1 / \lambda_{\text{Peak}}. \quad (1.4.11)$$

By comparing (1.4.9) and (1.4.11), we see that the Wien's displacement law that follows from experimental data suggests that black bodies consist of vortices composed of loops built

of the entangled SST-As components. We will show that it is true. For example, in the baryons can be produced such loops with different radii – in higher temperatures, number density of created loops with smaller radii is higher. The atom-like structure of baryons and the creations of such loops in them lead to the black body spectrum and to the temperature fluctuations in CMB. The structure of baryons suggests that for sufficiently high temperature of a black body, the smallest wavelengths should be two times smaller than λ_{Peak} and we should see a threshold for density of the longest wavelengths for $\lambda = 2\pi\lambda_{\text{Peak}}$ (see Chapter “Cosmology”).

In reality, formula (1.4.11) and our considerations suggest that the Wien’s displacement formula is a definition of thermodynamic temperature of a black body.

Consider a spinning circle-like loop, composed of the SST-As components, that collapses to a spin-0 condensate/ball with a loop on its equator that is emitted. Assume that the final condensate has radius r . Then for the initial loop is

$$\mathbf{spin} = M v_{\text{spin}} R . \quad (1.4.12)$$

For the final loop is

$$\mathbf{spin} = \Delta M v_{\text{spin}}^* r . \quad (1.4.13)$$

For the condensate/ball we have

$$M - \Delta M \sim r^3 . \quad (1.4.14)$$

From (1.4.12)-(1.4.14) is

$$1 / (v_{\text{spin}} R) - 1 / (v_{\text{spin}}^* r) \sim r^3 \quad (1.4.15)$$

or

$$r / (v_{\text{spin}} R) - 1 / v_{\text{spin}}^* \sim r^4 . \quad (1.4.16)$$

For $r \ll R$ and from (1.4.10) is

$$- v_{\text{spin}}^* \sim T^4 . \quad (1.4.17)$$

Energy of the final loop is

$$\Delta E^* = \Delta M v_{\text{spin}}^{*2} . \quad (1.4.18)$$

From (1.4.13) and (1.4.18) we have

$$\Delta E^* \sim v_{\text{spin}}^* \quad (1.4.19)$$

so from (1.4.17) and (1.4.19) we obtain the Stefan-Boltzmann law

$$- \Delta E^* \sim T^4 . \quad (1.4.20)$$

1.4.3. Lifetimes of particles and stars

Dynamic pressure of a field, p_{Dyn} , is defined as directly proportional to its energy density ρ_{Energy}

$$p_{\text{Dyn}} = \rho_{\text{Energy}} c^2 / 2 . \quad (1.4.21)$$

Since photons and gluons raise the zero-point of the zero-energy field, so the radiation pressure, p_{Rad} , is directly in proportion to the four powers of absolute temperature T

$$p_{\text{Rad}} \sim T^4 . \quad (1.4.22)$$

We see that the theory of stars follows from the dynamics of loops created in baryons.

Since absolute temperature of a loop is inversely proportional to its radius (so to radius of the final condensate as well) so for mass inversely proportional to radius of a loop we have that absolute temperature is directly proportional to mass m

$$T \sim m . \quad (1.4.23)$$

Spin of a virtual loop we can define as the product of its energy ($-E^*$) and period of spinning which is the lifetime, τ_{Lifetime} , of the virtual loop

$$\tau_{\text{Lifetime}} \sim 1 / -E^* . \quad (1.4.24)$$

From formulae (1.4.20), (1.4.23) and (1.4.24) we have

$$\tau_{\text{Lifetime}} \sim 1 / m^4 , \quad (1.4.25)$$

where m is the mass of a condensate or loop composed of the SST-As components or of a star.

In SST, coupling constants, α_i , are defined as follows

$$\alpha_i = G_i M m / (c \hbar) , \quad (1.4.26)$$

where G_i are the constants of interactions (such as, for example, the gravitational constant G), M is mass of source of interactions, m is mass of carrier of interactions, and \hbar is the reduced Planck constant.

The following formula defines the energy of an interaction

$$\Delta E_i = G_i M m / r . \quad (1.4.27)$$

Then from (1.4.26) and (1.4.27) we obtain

$$\Delta E_i = \alpha_i c \hbar / r = m_i c^2 . \quad (1.4.28)$$

From (1.4.24) and (1.4.28) we obtain

$$\tau_{\text{Lifetime}} \sim 1 / \alpha_i . \quad (1.4.29)$$

Emphasize that we derived all formulae in this Paragraph from our initial conditions.

1.5. Electron

The electron plays an important role in our theory so we described its internal structure (which follows from properties of the SST-As) in this separated Section. In our book, we show that such a simple structure leads to the correct value for the anomalous magnetic moment.

Electron is created as a spin-1/2 loop with the spin-0 central condensate both composed of the SST-As components. Due to the superluminal quantum entanglement, there is created immediately the torus/electric-charge in such a way that its equatorial radius is equal to radius of the loop $\lambda_{e,bare}$ (it is the reduced Compton wavelength of the bare electron) while its circular axis has radius equal to $2\lambda_{e,bare}/3$ (Fig.2). So the mass of the electric charge is on the equator while the mean radius of the torus/electric-charge is $2\lambda_{e,bare}/3$. All spins of the SST-As components on surface of the torus point towards the circular axis of the torus (Fig.2) or all point in the opposite direction – it distinguishes the positive electric charge from negative one. The SST-As components swap places, which causes them to rotate on the circular axis of the torus, i.e. there is raised the local zero-point of the zero-energy field. But emphasize that such processes do not change mass and the half-integral spin of the electron electric charge.

Knowing mass density of the SST-As and mass of neutrino, we can calculate mass of the electron torus – it is equal to the mass of the electric charge in the core of baryons: ~ 318.3 MeV so both electric charges are the same! **But emphasize that the electron torus is only the polarized part of the SST absolute spacetime so such mass cannot be measured – just it behaves as a virtual object.**

Outside the torus/electric-charge, there is created only one the virtual bare electron-positron pair (the virtual dipole) which behaves in a quantum way i.e., it disappears in one place and, due to the superluminal entanglons, appears in another one, and so on. The virtual dipole is polarised along the electric lines of forces that converge on the circular axis of the electron torus (Fig.2).

Masses of the loop and the central condensate are the same, i.e. they are equal to $m_{e,bare}/2 = 0.255203454653129$ MeV (it is derived from our initial conditions) – in the core of baryons, because there is much higher mass density, masses of the real torus and central condensate are not the same.

We see that the half-integral spin of the loop satisfies following equation

$$(m_{e,bare} / 2) c \lambda_{e,bare} = \hbar / 2 . \quad (1.5.1)$$

In this book we have:

e denotes electric charge of the electron or positron,

m_e is the mass of electron or positron, and

$m_{e,bare}$ is the bare mass of electron or positron.

Electron as a whole also behaves in a quantum way (i.e. it disappears in one place and appears in another one, and so on) so in QM is introduced the wavelength of electron.

Mean mass density of the bare electron is about 21 orders of magnitude lower than the SST absolute spacetime so it is very difficult to examine the internal structure of electron. It is not true that the bare electron is a point-like particle.

Electric charge: We define the elementary electric charge (EEC) as the type-Fig.2 torus composed of the $8.50713889377113 \cdot 10^{38}$ SST-As components – we will show that this number follows from properties of the SST absolute spacetime and the core of baryons.

1.6. Uncertainty of experimental results from virtual phenomena

Here we write for the most important results the 15 significant digits. But emphasize that to obtain perfect results we should eliminate the spontaneous virtual phenomena in the SST-As what is impossible. For example, there are the spontaneous weak interactions of the virtual bare electron-positron pairs in presence of dark matter (DM) defined by the coupling constant $\alpha'_{w(e-p),DM}$ calculated in this book

$$\alpha'_{w(e),DM} \approx 1.119446 \cdot 10^{-5} . \quad (1.6.1)$$

It causes that in the SST-As, there are the spontaneous temperature fluctuations with a mean value equal to

$$2.726 \text{ [K]} \alpha'_{w(e),DM} \approx 3.05 \cdot 10^{-5} \text{ K} = 30.5 \text{ } \mu\text{K} , \quad (1.6.2)$$

where 2.726 K is the present-day temperature of the Universe.

We see that the mean temperature fluctuation is about 30 parts per 3 million parts. Moreover, the value of the zero-point of the zero-energy field changes with time. Thus, it is not possible to obtain perfect experimental results.

There are also activated virtual processes because of the applied methods in the experiments.

If we do not take into account the gravitational interactions, then the weak interactions of the virtual electron-positron pairs (we are unable to control them) are the weakest ones. Then the lowest mass distance between the upper limit and lower limit for measured mass, \mathbf{M} , is $2\alpha_{w(e)}\mathbf{M}$, where $\alpha_{w(e)} = 0.951118612099992 \cdot 10^{-6}$ is the coupling constant for the weak interactions of the virtual electron-positron pairs (the factor 2 is because there is the virtual pair, not a single particle).

When we want to specify value of the central mass then our result will be written as follows

$$\approx \mathbf{M}(\alpha_{w(e)}\mathbf{M}) \equiv \mathbf{M} \pm \alpha_{w(e)}\mathbf{M} , \quad (1.6.3)$$

where $(\alpha_{w(e)}\mathbf{M}) \equiv \pm \alpha_{w(e)}\mathbf{M}$ is the theoretical uncertainty of the central mass.

For example, our mass of electron is

$$\begin{aligned} m_e &= 0.510998803789532 \text{ MeV} \approx \\ &\approx 0.51099880(49) \text{ MeV} . \end{aligned} \quad (1.6.4)$$

References

- [1] D. I. Bradley, *et al.* (18 July 2016). “Breaking the superfluid speed limit in a fermionic condensate”
Nature Physics **12**, 1017-1021 (2016)

Chapter 2

Particle Physics

2.1. Classical thermodynamics and phase transitions of inflation field and physical constants	22
2.2. Dynamics of the core of baryons	25
2.3. Energy frozen inside the SST-absolute-spacetime components	29
2.4. Weak interactions and magnetic moment of electron	29
2.5. The atom-like structure of baryons at low energy	31
2.6. Masses and magnetic moments of nucleons	35
2.7. Uncertainties	36
2.8. Muon	37
2.9. Neutral pion	39
2.10. Tauon and fine-structure constant at high energies	40
2.11. Photons, gluons and selected properties of fundamental particles	40
2.12. The mass of W^\pm and Z^0 bosons	41
2.13. Degrees of freedom	42
2.14. The seven types of interactions	43
2.15. Higgs boson and a prediction of new particle	48
2.16. Frequency of the hydrogen spin-flip transition	49
2.17. Lamb-Retherford shift	50
2.18. Lifetimes	51
2.19. Radius of proton	54
2.20. Selected mesons	56
2.21. Hyperons	58
2.22. Selected resonances	59
2.23. Masses of quarks	60
2.24. The PMNS neutrino-mixing matrix	61
2.25. The CKM quark-mixing matrix	63
2.26. Larger structures	65
2.27. The ultimate equation	66
2.28. Turning points in the formulation of the Scale-Symmetric Theory	66
2.29. Summary	67
2.30. Tables	68
References	72

2.1. Classical thermodynamics and phase transitions of inflation field, physical constants, and dark-matter (DM) particles

In this Section, we apply the formulae (1.3.4) and (1.3.5).

The definition of the Reynolds number N_R for the SST Higgs field with tachyons packed to maximum looks as follows

$$N_R = \rho_t v_t (2 r_t) / \eta_t = 1.00760468808565 \cdot 10^{-19} . \quad (2.1.1)$$

where ρ_t is the inertial-mass density of single tachyon

$$\rho_t = m_t / (4 \pi r_t^3 / 3) = 8.32192436201086 \cdot 10^{85} \text{ kg m}^{-3} . \quad (2.1.2)$$

The radius of closed string which can be produced due to the value of the Reynolds number is (it consists of tachyons which are in direct contact)

$$r_1 = (2r_t) / N_R = 0.944240445930837 \cdot 10^{-45} \text{ m} . \quad (2.1.3)$$

We can calculate the number of tachyons, K^2 , a closed string consists of

$$K^2 = 2 \pi r_1 / (2 r_t) = (0.789668554836067 \cdot 10^{10})^2 . \quad (2.1.4)$$

The spin of each closed string is half-integral while of the entanglons is unitary

$$\hbar = 2 K^2 m_t v_t r_1 = 1.05457154835254 \cdot 10^{-34} \text{ Js} . \quad (2.1.5)$$

Spins of all objects defined by formulae (1.3.4) and (1.3.5) are half-integral so from definition of spin

$$\text{Spin} = M v R \quad (2.1.6)$$

we can calculate the speed of light in “vacuum” c

$$c = 3 \hbar / (4 m_4 r_4) = 3 \hbar / (4 m_t r_1 K^{11}) = 299792458.00000 \text{ m/s} . \quad (2.1.7)$$

Mass of the superluminal closed string is

$$m_1 = m_t K^2 = 2.34007841915134 \cdot 10^{-87} \text{ kg} . \quad (2.1.8)$$

Speed of the closed string is

$$v_1 = 3 \hbar / (4 m_t r_1 K^5) = 0.726925275260465 \cdot 10^{68} \text{ m/s} . \quad (2.1.9)$$

We can calculate the factor which changes kg into MeV

$$F = 10^6 e / c^2 = 1.7826616957332 \cdot 10^{-30} \text{ kg/MeV} . \quad (2.1.10)$$

In formula (2.1.10), there is the input of the first iterative parameter $e = 1.60217643101205 \cdot 10^{-19} \text{ C}$.

Mass of the torus/electric-charge in the core of baryons is

$$X^\pm = m_4 / F = m_1 K^6 / F = 318.2955341124 \text{ MeV} . \quad (2.1.11)$$

The ratio of the masses of the lightest neutrino, m_{neutrino} , and its torus, m_2 , and the ratio of the masses of the electrically charged core of baryons, H^\pm , and its torus, X^\pm , and the ratio of the masses of the core of the Protoworld, $M_{\text{Pw,core}}$, and its torus, $M_{\text{Pw,torus}}$, are the same

$$F_{\text{H/X}} = m_{\text{neutrino}} / m_2 = H^\pm / X^\pm = M_{\text{Pw,core}} / M_{\text{Pw,torus}} = 2.28541913173261 . \quad (2.1.12)$$

In formula (2.1.12), there is the input of the second iterative parameter $H^\pm = 727.438703205527 \text{ MeV}$.

Mass of the lightest neutrinos is (its torus and central condensate are built of the entanglons, i.e. of the spin-1 binary systems of the superluminal closed strings)

$$m_{\text{neutrino}} = F_{\text{H/X}} m_1 K^2 = 3.33492413655866 \cdot 10^{-67} \text{ kg} . \quad (2.1.13)$$

Mass of the local zero-energy field around a neutrino depends on frequency of its spin rotation so measured masses of neutrinos can be even tens of orders of magnitude higher than of the non-rotating-spin neutrinos.

The equatorial radius of the lightest neutrinos is

$$r_{\text{neutrino}} = 3 r_1 K / 2 = A / K^2 = 1.11845548253395 \cdot 10^{-35} \text{ m} , \quad (2.1.14)$$

where A is the equatorial radius of the torus/electric-charge in the core of baryons

$$A = 3 r_4 / 2 = 3 r_1 K^3 / 2 = 0.697442472994368 \text{ fm} . \quad (2.1.15)$$

By an analogy, the core of the cosmological Protoworld, i.e. the cosmological torus and its central condensate, should be built of the cores of baryons. But the cores of baryons are the SST black holes in respect of the nuclear strong interactions, so they capture relativistic pion which is in the $d = 1$ state (see formula (1.3.6)) – it is because such TB orbit is below the Schwarzschild surface for the nuclear strong interactions. Masses of nucleons do not satisfy the formulae (1.3.4) and (1.3.5). We need a stable particle with a mass equal to H^\pm . Consider a torus composed of K^2 entangled loops each composed of K^2 entangled lightest neutrinos with spins tangent to the loops – we will call such a torus and such a loop the dark-matter (DM) objects because due to the orientations of the spins of neutrinos, they cannot interact electromagnetically. Then the shortest-distance quantum entanglement causes that two nearest neutrinos in a loop are in distance equal to

$$L_{\text{Neutrinos}} = 2 \pi r_{\text{neutrino}} / 3 . \quad (2.1.16)$$

Such distance results from the geometry of the torus of lightest neutrino.

We assume that the distance between neutrinos in the nearest loops on the equator of the DM torus is also defined by the geometry of the torus of lightest neutrinos, so it is

$$L_{\text{Neutrinos,loops}} = 2 \pi r_{\text{neutrino}} . \quad (2.1.17)$$

The above remarks lead to a conclusion that the radius of a single DM loop is

$$R_{\text{DM-loop}} = K^2 L_{\text{Neutrinos}} / (2 \pi) = K^2 r_{\text{neutrino}} / 3 = r_1 K^3 / 2 = A / 3 . \quad (2.1.18)$$

On the other hand, the equatorial radius of the DM torus is

$$R_{\text{DM-torus}} = K^2 L_{\text{Neutrinos,loops}} / (2 \pi) = K^2 r_{\text{neutrino}} = 3 r_1 K^3 / 2 = A . \quad (2.1.19)$$

We see that sizes of the DM torus are the same as of the torus/electric-charge in the core of baryons.

Mass of the DM loop is

$$\begin{aligned} M_{\text{DM-loop}} &= K^2 m_{\text{Neutrino}} = 2.07958007571345 \cdot 10^{-47} \text{ kg} \approx \\ &\approx 2.0795801(20) \cdot 10^{-47} \text{ kg} . \end{aligned} \quad (2.1.20)$$

$$\begin{aligned} M_{\text{DM-loop}} &= 10^6 K^2 m_{\text{Neutrino}} / F = 1.16655901713944 \cdot 10^{-11} \text{ eV} \approx \\ &\approx 1.1665590(12) \cdot 10^{-11} \text{ eV} . \end{aligned} \quad (2.1.21)$$

Mass of the DM torus is

$$M_{\text{DM-torus}} = K^4 m_{\text{Neutrino}} / F = H^\pm \approx 727.43870(70) \text{ MeV} . \quad (2.1.22)$$

Emphasize that the masses of the charged core of baryons and the DM torus are the same, both tori have the same sizes, but in centre of the DM torus is no condensate, and contrary to the core of baryons, the DM torus does not interact electromagnetically.

Mass of the charged core of baryons is

$$H^\pm = F_{\text{H/X}} m_1 K^6 . \quad (2.1.23)$$

The Protoworld was the stable cosmological object because its core, i.e. the cosmological torus and the central condensate both were built of the binary systems of the DM tori.

Mass of the core of the Protoworld was

$$\begin{aligned} H^+_{\text{Protoworld}} &= F_{\text{H/X}} m_1 K^{14} = 1.96075843626826 \cdot 10^{52} \text{ kg} \approx \\ &\approx 1.9607584(19) \text{ kg} . \end{aligned} \quad (2.1.24)$$

The equatorial radius of the core of the Protoworld was

$$\begin{aligned} A_{\text{Protoworld}} &= 3 r_8 / 2 = 3 r_1 K^7 / 2 = 2.71198803642873 \cdot 10^{24} \text{ m} = \\ &= 286.663483403373 \text{ million light-years [Mly]} . \end{aligned} \quad (2.1.25)$$

The internal helicity of the closed string resulting from the infinitesimal spin of the tachyons and their viscosity means that the entanglons a neutrino consists of transform, outside the neutrino, the chaotic motions of tachyons into divergently moving tachyons. The direct collisions of divergently moving tachyons with tachyons the SST Higgs field consists of produce a gradient in this field. The gravitational constant, G , results from behaviour of all closed strings a neutrino consists of. Constants of interactions are directly proportional to the mass densities of fields carrying the interactions then the G we can calculate from following formula

$$G = g \rho_{Hf} = 6.67400068894098 \cdot 10^{-11} \text{ m}^3/(\text{kg s}^2), \quad (2.1.26)$$

where the g has the same value for all interactions and is equal to

$$g = v_{st}^4 / \eta^2 = 25,224.5631772099 \text{ m}^6/(\text{kg}^2 \text{ s}^2). \quad (2.1.27)$$

Notice that gravitational field produced by the entanglons is residual and has not spherical symmetry. Its residual gravitational constant is

$$G_{\text{entanglon,residual}} = (m_1 / m_{\text{neutrino}}) G \approx 7 \cdot 10^{-21} G. \quad (2.1.28)$$

Residual gravitational constant for a tachyon is about 40 orders of magnitude lower than the G . We can treat the single SST tachyons and entanglons as imaginary objects, i.e. as objects which are directly not detectable.

2.2. Dynamics of the core of baryons

The virtual or real fundamental gluon loop (FGL) is created on the circular axis (Fig.2) of the torus/electric-charge in the core of baryons (they initially overlap) from the SST-As components. Masses of spinning virtual objects can be calculated from the definition

$$E T_{\text{Period}} = \hbar, \quad (2.2.1)$$

where $E = mc^2$.

Mass of the resting FGL is

$$\begin{aligned} m_{\text{FGL}} &= 3 \hbar / (4 \pi A c F) = 67.5444101574179 \text{ MeV} \approx \\ &\approx 67.544410(65) \text{ MeV}. \end{aligned} \quad (2.2.2)$$

The central condensate, Y , is created due to the transition of the FGL from its circumference to its radius so the mass increases 2π times. In such a process is emitted energy/mass defined by formula (1.4.20), i.e. by the Stefan-Boltzmann law. From the Wien's displacement law follows that temperature is inversely proportional to radius so the emitted energy is directly proportional to $1/(2\pi)^4$, so we have

$$\begin{aligned} Y &= 2 \pi m_{\text{FGL}} \{1 - 1 / (2\pi)^4\} = 424.121744124454 \text{ MeV} \approx \\ &\approx 424.12174(41) \text{ MeV}. \end{aligned} \quad (2.2.3)$$

The condensate Y is the SST black hole for the nuclear weak interactions so the spin speed on its surface is c .

The number of the neutrino-antineutrino pairs, N_{NA} , on the torus in the core of a baryon is

$$N_{NA} = X^{\pm} F / (2 m_{\text{neutrino}}) = 8.50713889377113 \cdot 10^{38} . \quad (2.2.4)$$

Mean distance, L_{NA} , of the neutrino-antineutrino pairs on the torus in the core of a baryon is

$$L_{NA} = (8 \pi^2 A^2 / (9 N_{NA}))^{1/2} = 7.08255965743672 \cdot 10^{-35} \text{ m} . \quad (2.2.5)$$

Mean distance, L_{As} , of the neutrino-antineutrino pairs in the SST-As is

$$\begin{aligned} L_{As} &= (2 m_{\text{neutrino}} / \rho_{As})^{1/3} = 3.92601287403043 \cdot 10^{-32} \text{ m} = \\ &= 3510.20933362115 r_{\text{neutrino}} . \end{aligned} \quad (2.2.6)$$

The ratio, N^* , of the mean distances is

$$N^* = L_{As} / L_{NA} = 554.321186678335 . \quad (2.2.7)$$

The Compton length, $\lambda_{e,\text{bare}}$, of the bare electron is

$$\lambda_{e,\text{bare}} = A N^* = 3.86607139270111 \cdot 10^{-13} \text{ m} . \quad (2.2.8)$$

The bare mass of electron is

$$m_{e,\text{bare}} = \hbar / (c \lambda_{e,\text{bare}}) = 9.09882846478312 \cdot 10^{-31} \text{ kg} , \quad (2.2.9)$$

$$\begin{aligned} m_{e,\text{bare}} &= \hbar / (c \lambda_{e,\text{bare}} F) = 0.510406909306258 \text{ MeV} \approx \\ &\approx 0.51040691(49) \text{ MeV} . \end{aligned} \quad (2.2.10)$$

On comparing the two definitions of the fine-structure constant for low energies, α_{em} , we arrive at the relation

$$k e^2 / (\hbar c) = G_{\text{em}} m_e^2 / (\hbar c) , \quad (2.2.11)$$

where $k = c^2 / 10^7$ whereas G_{em} is

$$G_{\text{em}} = G \rho_{As} / \rho_{Hf} = 2.78025384859577 \cdot 10^{32} \text{ m}^3 / (\text{kg s}^2) . \quad (2.2.12)$$

From formula (2.2.11), we can calculate the mass of electron

$$m_e = e c / (G_{\text{em}} 10^7)^{1/2} = 9.10937994101586 \cdot 10^{-31} \text{ kg} , \quad (2.2.13)$$

$$m_e = \{ e c / (G_{\text{em}} 10^7)^{1/2} \} / F = 0.510998803789532 \text{ MeV} \approx$$

$$\approx 0.51099880(49) \text{ MeV} . \quad (2.2.14)$$

and next the fine-structure constant, α_{em} ,

$$\alpha_{em}^{-1} = 10^7 \hbar / (e^2 c) = 137.035998889019 . \quad (2.2.15)$$

Notice that the ratio of the mass of electron and its bare mass is

$$F_{1+a} = m_e / m_{e,bare} = 1.00115965217649 . \quad (2.2.16)$$

But this result has no physical value because we obtained it applying the first iterative parameter. We later will calculate the anomalous magnetic moment from our model of electron.

The ratio of the binding energy of two FGLs, ΔE_{FGL} (it results from creations of the virtual electron-positron pairs), to the mass of FGL, m_{FGL} , is (energy is inversely proportional to a length, and m_{FGL} is associated with A while ΔE_{FGL} with $\lambda_{e,bare}$)

$$\Delta E_{FGL} / m_{FGL} = A / \lambda_{e,bare} . \quad (2.2.17)$$

From this formula we obtain $\Delta E_{FGL} = 0.121850673906522 \text{ MeV}$.

During creation of the bound neutral pion from two fundamental gluon loops, due to the electromagnetic interactions, there is released additional energy equal to $\alpha_{em} \Delta E_{FGL}$. The total binding energy of the bound neutral pion is

$$\Delta E_{\text{pion}(o),\text{bound}} = \Delta E_{FGL} (1 + \alpha_{em}) = 0.122739861236087 \text{ MeV} . \quad (2.2.18)$$

This means that the mass of bound neutral pion (i.e. placed in nuclear strong field) is

$$\pi_{\text{bound}}^0 = 2 m_{FGL} - \Delta E_{\text{pion}(o),\text{bound}} = 134.966080453600 \text{ MeV} . \quad (2.2.19)$$

Notice that from the mass of a virtual $X^+ X^-$ pair can be simultaneously created 9 virtual fundamental gluon loops. It forces a creation of an electron with a relativistic mass 9 times higher than its rest mass that attaches radiation mass and next such object interacts with the bound neutral pion. Then the mass of charged pion is

$$\begin{aligned} \pi^\pm &= \pi_{\text{bound}}^0 + 9 m_e F_{1+a} = 139.570402915580 \text{ MeV} \approx \\ &\approx 139.57040(14) \text{ MeV} . \end{aligned} \quad (2.2.20)$$

Masses of bound and free charged pions are the same.

We very frequently will use the mass distance between the charged pion and the bound neutral pion

$$\Delta \pi = \pi^\pm - \pi_{\text{bound}}^0 = 4.60432246198079 \text{ MeV} . \quad (2.2.21)$$

Mass of a loop is inversely proportional to its radius (or circumference) so we have

$$2 \pi r_{C(p)} \sim 1 / Y , \quad (2.2.22)$$

where $r_{C(p)}$ is the radius of a loop with a mass Y overlapping with the equator of the condensate Y .

Assume that emission of $\Delta\pi$ by X^\pm (the mean radius of it is $2A/3$) forces its transition from circumference to its radius (so its radius decreases 2π times), so we have

$$(2 A / 3) / (2 \pi) \sim 1 / (X^\pm - \Delta\pi) . \quad (2.2.23)$$

From (2.2.22) and (2.2.23) is

$$r_{C(p)} = A (X^\pm - \Delta\pi) / (6 \pi^2 Y) = 0.871102397108628 \cdot 10^{-17} \text{ m} . \quad (2.2.24)$$

The Y is responsible for the nuclear weak interactions and it is the weak SST black hole so we have

$$r_{C(p)} = G_w Y F / c^2 . \quad (2.2.25)$$

From (2.2.25) we obtain value of the constant of the weak interactions, G_w , for baryons

$$G_w = r_{C(p)} c^2 / (Y F) = 1.03550247948936 \cdot 10^{27} \text{ m}^3/(\text{kg s}^2) . \quad (2.2.26)$$

The characteristic feature of the nuclear weak interactions is that Y is both the source and the carrier of interactions so from formula (1.4.26) is

$$\alpha_{w(p)} = G_w (Y F)^2 / (c \hbar) = 0.0187229092873063 , \quad (2.2.27)$$

where $\alpha_{w(p)}$ is the coupling constant for the nuclear weak interactions.

We can test our dynamics of the core of baryons because there is the second formula for $\alpha_{w(p)}$. Transition of the FGL from its circumference to its radius (because of the nuclear weak interactions) causes that we can rewrite the formula (2.2.22) as follows

$$2 \pi (2 A / 3) \sim 1 / (\alpha_{w(p)} 2 \pi m_{FGL}) . \quad (2.2.28)$$

From (2.2.23) and (2.2.28) is

$$\alpha_{w(p)} = (X^\pm - \Delta\pi) / ((2 \pi)^3 m_{FGL}) = 0.0187229092873063 . \quad (2.2.29)$$

The values from (2.2.27) and (2.2.29) are the same.

Mass density of Y follows from the confinement of the SST-As components – we have devoted a separate Section to this issue.

Mass density of Y is

$$\rho_Y = Y F / (4 \pi r_{C(p)}^3 / 3) = 2.73063237955490 \cdot 10^{23} \text{ kg/m}^3 . \quad (2.2.30)$$

Surface density of X^\pm is

$$\rho_{X,\text{surface}} = X^\pm F / (8 \pi^2 A^2 / 9) = 1.32964428715601 \cdot 10^2 \text{ kg/m}^2 . \quad (2.2.31)$$

A single SST-As component occupies a cube with a side equal to (see formula (2.2.6))

$$L_{As} = 3.92601287403043 \cdot 10^{-32} \text{ m} , \quad (2.2.32)$$

so surface density of a plane in the SST-As is

$$\rho_{As,\text{surface}} = 2 m_{\text{neutrino}} / L_{As}^2 = 4.32725527335245 \cdot 10^{-4} \text{ kg/m}^2 . \quad (2.2.33)$$

From (2.2.31) and (2.2.33) results that surface density of the torus X^\pm is $N_{X/As}$ times higher than in the SST-As

$$N_{X/As} = \rho_{X,\text{surface}} / \rho_{As,\text{surface}} = 3.07271978000478 \cdot 10^5 = N^{*2} . \quad (2.2.34)$$

We see that surface density of the torus in the core of baryons is about 300,000 times higher than in SST-As – it is very important in the theory of the neutron black holes (NBHs).

2.3. Energy frozen inside the SST-absolute-spacetime components

The SST-As consists of the non-rotating-spin-1 neutrino-antineutrino pairs. Gravitational energy of a single lightest neutrino is

$$E_G = m_{\text{neutrino}} c^2 . \quad (2.3.1)$$

On the other hand, the not observed non-gravitating superluminal energy of the entanglons the lightest neutrino consists of is (see formula (2.1.9))

$$E_S = m_{\text{neutrino}} v_1^2 . \quad (2.3.2)$$

The ratio of these energies is

$$E_S / E_G = v_1^2 / c^2 \approx 0.6 \cdot 10^{119} . \quad (2.3.3)$$

We see that inside the SST-As is frozen tremendous amount of unobserved energy about $0.6 \cdot 10^{119}$ parts per 1 part of the observed gravitating energy.

2.4. Weak interactions and magnetic moment of electron

Mass of the condensate in the centre of electron is a half of its bare mass so it is $N_{Y/m(e)\text{-bare}}$ times lower than Y

$$N_{Y/m(e)\text{-bare}} = Y / (m_{e,\text{bare}} / 2) = 1661.89656288516 . \quad (2.4.1)$$

The ratio, $N_{p/e}$, of the radii of the Y and the condensate in electron is

$$N_{p/e} = r_{C(p)} / r_{C(e)} = \{ Y / (m_{e,\text{bare}} / 2) \}^{1/3} = 11.8449890398865 , \quad (2.4.2)$$

then

$$r_{C(e)} = 0.735418491461073 \cdot 10^{-18} \text{ m} . \quad (2.4.3)$$

From formulae (2.2.26) and (2.2.27) results that the ratio of the coupling constants is directly proportional to both the ratio of masses of the condensates and the ratio of their radii, so the coupling constant of the weak interactions of the charged leptons is

$$\alpha_{w(e)} = \alpha_{w(p)} / (N_{Y/m(e)\text{-bare}} N_{p/e}) = 0.951118612099992 \cdot 10^{-6} . \quad (2.4.4)$$

Electron is a pure quantum particle because its torus/electric charge behaves as a virtual particle. We cannot say it about the torus/electric-charge inside the core of baryons because its surface density is about 300,000 times higher than in the SST absolute spacetime. Such scenario causes that an electron disappears in one place and appears in another one, and so on. It causes that outside hadrons we must take into account the dark matter. From observational data we know that density of dark matter is about 5.4 times higher than the baryonic matter. On the other hand, in SST is assumed that the baryonic matter of our Universe appeared similarly to the two fundamental gluon loops (it leads to the bound neutral pion) in the core of baryons – there were two cosmological loops overlapping with the circular axis of the core of the Protoworld. Each loop was composed of the protogalaxies built of the NBHs. These remarks lead to

$$\xi^* = M_{Pw,core} / M_{Baryonic} = H^\pm / (2 m_{FGL}) = 5.38489196596855 , \quad (2.4.5)$$

where $M_{Baryonic}$ is the baryonic mass of the Universe.

The formula (2.4.5) concerns a binary system such as, for example, two gluon loops or the electron-positron pair. For a single electron is

$$\xi = 2 \xi^* = H^\pm / m_{FGL} = 10.7697839319371 . \quad (2.4.6)$$

Coupling constants, α_i , are directly proportional to constants of interaction, G_i , and from (2.1.26) we have that G_i are directly proportional to densities of fields, so for an electron in presence of dark matter we have

$$\alpha'_{w(e),DM} = \alpha_{w(e)} (1 + \xi) = 1.11944605580608 \cdot 10^{-5} . \quad (2.4.7)$$

We can introduce the symbol

$$\gamma = \alpha_{em} / (\alpha'_{w(e),DM} + \alpha_{em}) = 0.998468305602133 , \quad (2.4.8)$$

where γ denotes the mass fraction in the bare mass of the electron that can interact electromagnetically, whereas $1-\gamma$ denotes the mass fraction in the bare mass of the electron that can interact weakly. Whereas the electromagnetic mass of a bare electron is equal to its weak mass.

For photon loops, mass is inversely proportional to radius, and αM denotes a mass which is responsible for an interaction. Since the distance between the constituents of a virtual electron-positron pair (virtual dipole) is equal to the length of the equator of the electron torus (because such is the length of the virtual photons) so the ratio of the radiation mass (created

by the virtual pair), $\Delta m^{**}_{\text{rad}}$, to the bare mass of electron is (it concerns only the virtual dipole)

$$\begin{aligned} \delta &= \Delta m^{**}_{\text{rad}} / m_{e,\text{bare}} = \gamma \alpha_{\text{em}} / 2\pi + (1 - \gamma) \alpha'_{w(e),\text{DM}} / 2\pi = \\ &= 0.00115963353870338 . \end{aligned} \quad (2.4.9)$$

The virtual dipole is polarized in such a way that its electric line converges on the circular axis of the electron torus so the distance of such axis to the electron condensate is equal to $2/3$ of the equatorial radius of the electron torus – such a factor must appear for the weak interactions of the virtual dipole with the real bare electron. The ratio of the total mass of an electron to its bare mass, which is equal to the ratio of the magnetic moment of the electron to the Bohr magneton for the electron, without the virtual-field correction described below, is (it concerns the virtual dipole and its weak interactions with the real bare electron (the $\Delta m^{**}_{\text{rad}}$ is a part of the total radiation mass Δm_{rad}^*))

$$\begin{aligned} \varepsilon &= (\Delta m_{\text{rad}}^* + m_{e,\text{bare}}) / m_{e,\text{bare}} = m_e^* / m_{e,\text{bare}} = 1 + \delta + \delta \alpha'_{w(e),\text{DM}} / (2 / 3) = \\ &= 1.00115965301091 . \end{aligned} \quad (2.4.10)$$

Each real electron is entangled with proton and it is the virtual proton field that increases the density of the zero-energy field, so measured mass of electron is a little lower than it would be for a free electron (i.e. for electron not entangled with proton). There are the weak interactions of the Y with the two condensates in the virtual electron-positron pair (its total mass is equal to the bare mass of electron). It causes that we must subtract from ε following value

$$\Delta \varepsilon_{\text{electron}} = (\varepsilon - 1) (\alpha'_{w(e),\text{DM}} m_{e,\text{bare}}) / (\alpha_{w(p)} Y) = 8.34418459663742 \cdot 10^{-10} . \quad (2.4.11)$$

The final ratio of the magnetic moment of the electron to the Bohr magneton for the electron, describes the formula

$$\varepsilon' = 1 + a_e = m_e / m_{e,\text{bare}} = \varepsilon - \Delta \varepsilon_{\text{electron}} = 1.00115965217649 . \quad (2.4.12)$$

From (2.4.12), which defines the ratio of the electron mass to its bare mass, and from $m_{e,\text{bare}}$ (see formula (2.2.10)), we can calculate the mass of electron. Emphasize that the bare mass of electron was derived without the first iterative parameter e . Next, applying formula (2.2.13), we can calculate the electron electric charge

$$e = 1.60217643101205 \cdot 10^{-19} \text{ C} . \quad (2.4.13)$$

It is the output of the first iterative parameter.

2.5. The atom-like structure of baryons at low energy

Hyperons arise very quickly because of the nuclear strong interactions. Due to the electroweak interactions, they decay slowly on the TB orbits (in the “tunnels” in the SST-As).

The relativistic pions in the tunnels “circulate” the torus (they are the S states i.e. $l = 0$). Such pions we refer to as $W_{(+o),d}$ pions because they are associated with the strong-electroWeak interactions.

The distance B we can calculate on the condition that the relativistic charged pion in the $d = 1$ state, which is responsible for the properties of nucleons, should have unitary angular momentum (this state is the ground state for the $W_{(+o),d}$ pions)

$$W_{(+),d=1} (A + B) v_{d=1} = \hbar , \quad (2.5.1)$$

where $v_{d=1}$ denotes the orbital speed of the $W_{(+),d=1}$ pion in the $d = 1$ state.

We can calculate the relativistic mass of the $W_{(+o),d}$ pions using Einstein’s formula (see our derivation in Paragraph 1.4.1)

$$W_{(+o),d} = \pi^{\pm o}_{\text{bound}} / (1 - v_d^2 / c^2)^{1/2} . \quad (2.5.2)$$

For the SST black holes, the square of the orbital speed is inversely proportional to the radius R_d and for A we have c^2 so we have

$$v_{d=1}^2 / c^2 = A / (A + B) . \quad (2.5.3)$$

From (2.5.2) and (2.5.3) is

$$W_{(+o),d} = \pi^{\pm o}_{\text{bound}} (1 + A / (d B))^{1/2} . \quad (2.5.4)$$

The formulae (2.5.1)–(2.5.4) give two solutions for the B . The first solution is

$$B = 0.501839476788152 \text{ fm} . \quad (2.5.5)$$

Then

$$A / B = 1.38977203917497 . \quad (2.5.6)$$

The second solution is $B^* = 0.969286047900613 \text{ fm}$ but this solution is not realized by Nature. It follows from the fact that after creation of a baryon, inside the core dominates the nuclear weak interaction while outside it there dominates the electroweak interaction. We know that coupling constant is directly proportional to exchanged mass while the mass is inversely proportional to its range so we have

$$(A / B)_\alpha = (\alpha_{\text{em}} + \alpha_{w(p)} + \alpha_{w(e)}) / \alpha_{w(p)} = 1.38980607053558 . \quad (2.5.7)$$

The A/B^* differs very much from (2.5.7) so the value B^* is not realized in baryons. From (2.5.6) and (2.5.7) we obtain the mean value

$$(A / B)_{\text{mean}} = 1.38978905485527 , \quad (2.5.8)$$

so the B_{mean} is

$$\mathbf{B}_{\text{mean}} = 0.501833332589454 \text{ fm} . \quad (2.5.9)$$

Creation of a resonance is possible when gluon loops overlap with the tunnels. Such bosons we call $S_{(+0),d}$ bosons because they are associated with the nuclear Strong interactions. The spin speeds of the $S_{(+0),d}$ bosons (they are equal to the c) differ from the speeds calculated on the basis of the Titius-Bode law for the strong interactions.

The masses of the charged and neutral core of resting baryons are denoted by $H^{\pm 0}$. The maximum mass of a virtual $S_{(+0),d}$ boson cannot be greater than the mass of the core so we assume that the mass of the $S_{(+0),d}$ boson, created in the $d = 0$ tunnel, is equal to the mass of the core. As we know, the ranges of virtual particles are inversely proportional to their mass. As a result, we obtain

$$H^{\pm 0} A = S_{(+0),d} (A + d B_{\text{mean}}) . \quad (2.5.10)$$

There is some probability that a virtual $S_{(+0),d}$ boson arising in the $d = 0$ tunnel decays to two parts. One part covers the distance A whereas the remainder covers the distance $4B_{\text{mean}}$.

Notice that there is

$$4 \pi_{\text{bound}}^0 / (H^{\pm} - 4 \pi_{\text{bound}}^0) = 4 B_{\text{mean}} / A = 2.878134 , \quad (2.5.11)$$

so for the remainder we have

$$S_{(+),d=4} = H^{\pm} - 4 \pi_{\text{bound}}^0 . \quad (2.5.12)$$

The formulae (2.5.10) and (2.5.12) lead to

$$H^{\pm} = \pi_{\text{bound}}^0 \{ (A / B)_{\text{mean}} + 4 \} = 727.438703205527 \text{ MeV} . \quad (2.5.13)$$

It is the output of the second iterative parameter.

The nucleons and pions are respectively the lightest baryons and mesons interacting strongly, so there should be some analogy between the carrier of the electric charge interacting with the core of baryons (it is the mass distance between the charged and neutral core) and the carrier of an electric charge interacting with the charged pion (this is the electron). It leads to following formula

$$(H^{\pm} - H^0) / H^{\pm} = m_e / \pi^{\pm} . \quad (2.5.14)$$

From (2.5.14) we obtain

$$H^0 = 724.775385629572 \text{ MeV} . \quad (2.5.15)$$

The mass distance $\Delta H = H^{\pm} - H^0$ is

$$\Delta H = H^{\pm} - H^0 = 2.66331757595538 \text{ MeV} . \quad (2.5.16)$$

For electron (plus electron antineutrino) placed on the circular axis of the core (i.e. the centre of the electron condensate is placed on this axis) we obtain that the electromagnetic binding energy is

$$\Delta E_{em} = 3 k e^2 / (2 A c^2 F) = 3.09695298260205 \text{ MeV} . \quad (2.5.17)$$

The results are collected in Table 1 (the masses are provided in **MeV**).

Table 1 *Relativistic mass on the TB orbits*

d	S_{(+),d}	S_{(o),d}	W_{(+),d}	W_{(o),d}
0	H[±] = 727.438703	H^o = 724.775386		
1	423.04418	421.49532	215.76108	208.64329
2	298.24462	297.15268	181.70408	175.70980
4	187.57438	186.88763	162.01276	156.66808

The binding energy of the core of baryons is

$$\Delta E_{core} = X^{\pm} + Y - H^{\pm} = 14.9785750313267 \text{ MeV} . \quad (2.5.18)$$

There is the four-object symmetry so the symmetrical decays of a virtual boson with a mass four times higher than the remainder

$$M_{TB} = M_4 = 4 S_{(+),d=4} = 750.297525564514 \text{ MeV} \quad (2.5.19)$$

lead to the Titius-Bode law for the strong interactions. The group of four virtual remainders reaches the **d = 1** state. There, it decays to two identical bosons. One of these components is moving towards the equator of the torus whereas the other one is moving in the opposite direction. When the first component reaches the equator of the torus, the other one is stopping and decays into two particles, and so on. In place of the decay, a “hole” appears in the SST absolute spacetime. A set of such holes is some “tunnel”.

The **d = 4** orbit is the last orbit for the strong interactions.

The probability of the occurrence in the proton of the state $H^+W_{(o),d=1}$ is **y** while the probability of the occurrence of $H^oW_{(+),d=1}$ is **1–y**. The probabilities **y** and **1–y**, which are associated with the lifetimes of protons in the above-mentioned states, are inversely proportional to the relativistic masses of the $W_{(+o),d}$ pions so we have

$$y = \pi^{\pm} / (\pi^{\pm} + \pi_{bound}^o) = 0.508385629489887 , \quad (2.5.20)$$

$$1-y = \pi_{bound}^o / (\pi^{\pm} + \pi_{bound}^o) = 0.491614370510113 . \quad (2.5.21)$$

The probability of the occurrence in the neutron of the state $H^+W_{(-),d=1}$ is **x** while the probability of the occurrence of H^o , π_{bound}^o and Z^o is **1–x**, where $Z^o = W_{(o),d=1} - \pi_{bound}^o$ (the pion $W_{(o),d=1}$ decays because in this state both particles, i.e. the torus and the $W_{(o),d=1}$ pion, are electrically neutral). Since the $W_{(o),d=1}$ pion only occurs in the **d = 1** state and because the mass of the resting bound neutral pion is greater than the mass of Z^o (so the neutral pion lives shorter) then

$$x = \pi_{bound}^o / W_{(-),d=1} = 0.625534863496851 , \quad (2.5.22)$$

$$1 - x = 0.374465136503149 . \quad (2.5.23)$$

The mean square charge for the proton is

$$\langle Q_{\text{proton}}^2 \rangle = e^2 [y^2 + (1 - y)^2] / 2 = 0.25e^2 \text{ (quark model gives } 0.33e^2 \text{)} . \quad (2.5.24)$$

The mean square charge for the neutron is

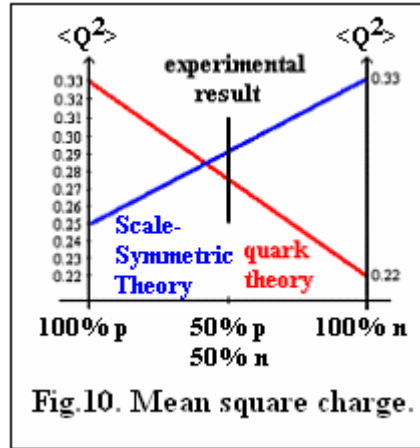
$$\begin{aligned} \langle Q_{\text{neutron}}^2 \rangle &= e^2 [x^2 + (-x)^2] / (2x + 3(1 - x)) = \\ &= 0.33e^2 \text{ (quark model gives } 0.22e^2 \text{)} , \end{aligned} \quad (2.5.25)$$

where $(2x + 3(1 - x))$ defines the mean number of particles in the neutron.

The mean square charge for a nucleon is

$$\langle Q^2 \rangle = [\langle Q_{\text{proton}}^2 \rangle + \langle Q_{\text{neutron}}^2 \rangle] / 2 = 0.29e^2 \text{ (quark model gives } 0.28e^2 \text{)} . \quad (2.5.26)$$

The results are collected in Fig.10.



When the virtual condensates \bar{Y} appear on the equator then there is a natural width of the $d = 0$ orbit – its effective radius is equal to $A + r_{C(p)}$ so the ratio of relativistic mass to rest mass in such state is (see formulae (2.5.2) and (2.5.3))

$$M_{\text{Rel}} / M_0 = 1 / \{(1 - A / (A + r_{C(p)}))\}^{1/2} = 9.00357429607990 . \quad (2.5.27)$$

2.6. Masses and magnetic moments of nucleons

The mass of a baryon is equal to the sum of the masses of the components because the binding energy associated with the strong interactions cannot abandon the strong field – it follows from the fact that the periods of changes in masses that result from the strong interactions are shorter than lifetimes of the baryons and from the fact that the $d = 0$ and $d = 1$ TB orbits are placed under the Schwarzschild surface for the strong interactions.

The mass of the proton is

$$p = (H^+ + W_{(o),d=1}) y + (H^0 + W_{(+),d=1}) (1 - y) = 938.271877349237 \text{ MeV} \approx$$

$$\approx 938.27188(90) \text{ MeV} . \quad (2.6.1)$$

The mass of the bound neutron is

$$\begin{aligned} n_{\text{bound}} &= (H^+ + W_{(-),d=1}) x + (H^0 + \pi_{\text{bound}}^0 + Z^0)(1-x) = 939.537101665991 \text{ MeV} \approx \\ &\approx 939.53710(90) \text{ MeV} . \quad (2.6.2) \end{aligned}$$

The proton magnetic moment in the nuclear magneton is

$$\mu_{\text{proton}} / \mu_0 = p y / H^+ + p (1 - y) / W_{(+),d=1} = +2.793595154 . \quad (2.6.3)$$

The neutron magnetic moment in the nuclear magneton is

$$\mu_{\text{neutron}} / \mu_0 = p x / H^+ - p x / W_{(-),d=1} = -1.913405950 . \quad (2.6.4)$$

2.7. Uncertainties

The four formulas that define the masses and magnetic moments of protons and neutrons are very simple and give very good results. It is easy to notice that even through direct changes of the masses occurring in these formulas, it is impossible to obtain four results simultaneously perfectly consistent with the average experimental results, i.e. with the world average values.

Note that the problems increase with the increasing mass of the particles, i.e. with the increase of the internal energy/mass density. This suggests that real and virtual phenomena that we cannot control during the measurements have a greater and greater impact on the obtained experimental results with the increase of energy.

The main reason is electroweak phenomena occurring in the region of spacetime coinciding with the effective areas occupied by particles. For lightest particles, the uncertainties are $\pm\alpha_{w(e)}M \approx \pm 0.95 \cdot 10^{-6} M$ or $\pm\alpha'_{w(e)}M \approx \pm 1.12 \cdot 10^{-5} M$, for heavier particles they can be $\pm\alpha_{em}\alpha_{w(p)}M \approx \pm 1.37 \cdot 10^{-4} M$, and for the heaviest ones, such as the W^\pm and Z^0 bosons or the H^0 Higgs boson/scalar, they can be $\pm\alpha_{w(p)}M \approx \pm 1.87 \cdot 10^{-2} M$.

The influence of uncontrolled phenomena can be seen in the lifetime of the neutron, which we will describe later in this book.

Here we suggest what uncontrolled phenomena may affect the masses and magnetic moments of nucleons.

From the SST follows that uncharged particles, and especially spinless particles, are less resistant to mass changes in their bound states because they are less stable.

Probably, mass of free neutron is higher because of the state $H^0\pi_{\text{bound}}^0Z^0$ that is free from charged particles. There probably for the relative time $(1 - x)$ is added the weak mass of the $(\Delta\pi - m_{e,\text{bare}})$ which is also electrically neutral

$$\Delta M_w = (1 - x) \alpha_{w(p)} (\Delta\pi - m_{e,\text{bare}}) = 0.0287027562788546 \text{ MeV} . \quad (2.7.2)$$

It leads to the following mass of the free neutron

$$n = n_{\text{bound}} + \Delta M_w = 939.565804422269 \text{ MeV} \approx$$

$$\approx 939.56580(90) \text{ MeV}. \quad (2.7.3)$$

Then, the mass distance between neutron and proton is

$$\mathbf{n} - \mathbf{p} = 1.2939271(13) \text{ MeV}. \quad (2.7.4)$$

On the other hand, assume that changes in magnetic moments during their measurement are associated with the states containing one or more charged particles and that it forces an emission of the lightest part in the bare electron – it is $m_{e,bare}/2$. Then the factor for the magnetic moment of proton is

$$F_p = (\mathbf{p} - m_{e,bare}/2) / \mathbf{p}, \quad (2.7.5)$$

while of neutron is

$$F_n = (\mathbf{p} - x m_{e,bare}/2) / \mathbf{p}, \quad (2.7.6)$$

Then the magnetic moments are as follows.

The proton magnetic moment in the nuclear magneton is

$$(\mu_{\text{proton}} / \mu_o)^* = F_p (\mu_{\text{proton}} / \mu_o) = +2.7928353. \quad (2.7.7)$$

The neutron magnetic moment in the nuclear magneton is

$$(\mu_{\text{neutron}} / \mu_o)^* = F_n (\mu_{\text{neutron}} / \mu_o) = -1.9130804. \quad (2.7.8)$$

But emphasize that it is only our proposal.

2.8. Muon

Muon is the electrically charged fermion. Mass of muon is close to the mass distance between \mathbf{Y} and \mathbf{X}^\pm so such mass distance and some interaction should define the mass of muon. Notice also that mass of a spin-0 charge-0 quadrupole of muons ($4\mu^\pm = 422.64 \text{ MeV}$) is a little lower than \mathbf{Y} so in the central condensate of baryons there can be realized the four-muon symmetry.

Assume that between a muon in \mathbf{Y} and the torus/electric-charge \mathbf{X}^\pm is exchanged a virtual bare electron-positron pair (i.e. there are the radial motions) that during the emission of the muon undergoes the radius-orbit transition i.e. there is emitted the energy equal to $E^* = 2m_{e,bare}/(2\pi) = m_{e,bare}/\pi$. Moreover, the muon inside the core of baryon interacts weakly with the \mathbf{Y} (it is defined by $\alpha_{w(p)}$) and weakly with other muons (it is defined by $\alpha_{w(e)}$). After emission, the muon interacts only with \mathbf{Y} . It leads to following mass of the muon

$$\mu^\pm = (\mathbf{Y} - \mathbf{X}^\pm - E^*) [\alpha_{w(p)} / (\alpha_{w(p)} + \alpha_{w(e)})] = 105.6583750306 \text{ MeV}. \quad (2.8.1)$$

This result is perfect [4] as it should be for electrically charged fermion.

Muon looks similar to electron, i.e. there is a torus/electric-charge and central condensate – outside such a system, there are created the virtual electron-positron pairs. The two energetic neutrinos that appear in decay of muon are inside the central condensate – it leads to the

difference in magnetic behaviour of muon and electron. Such complex muon condensate behaves as the SST black hole in respect of the weak interactions.

By using the formula

$$c^2 = G_w M F / r_{C(e)}, \quad (2.8.2)$$

we can calculate the virtual or real energy/mass E of two neutrinos which should be absorbed by the condensate of electron (the two neutrinos means that the structure is stable) to create the SST black hole in respect of the weak interactions

$$M = E + m_{e,bare} / 2 = 35.8060056194461 \text{ MeV} . \quad (2.8.3)$$

$$E = 2 E_{\text{neutrino}} = 35.5508021647930 \text{ MeV} . \quad (2.8.4)$$

$$E_{\text{neutrino}} = 17.7754010823965 \text{ MeV} . \quad (2.8.5)$$

Emphasize that the total mass of the muon condensate is a half of its bare mass so the weak black hole of muon is surrounded by a part of the mass of the condensate equal to about 17.2 MeV.

The anomalous relative magnetic moment of electron and muon are different because their electroweak interactions are different, i.e. their central condensates do not look similar.

We can define mass of muon as follows

$$\mu^\pm = \mu^{*\pm} + \Delta\mu^\pm , \quad (2.8.6)$$

where $\Delta\mu^\pm$ causes that muon does not behave as electron, so we have

$$a_\mu = a_e \mu^\pm / \mu^{*\pm} , \quad (2.8.7)$$

where $a_e = 0.00115965217649$ (see (2.4.12)).

From definition of coupling constants results that they are directly proportional to the product of masses of source of interaction and of carrier of interaction, so we have

$$F_{\text{correction}} = \alpha_1 / \alpha_2 = M_1 m_1 / (M_2 m_2) . \quad (2.8.8)$$

We can define the $\Delta\mu^\pm$ as follows

$$\Delta\mu^\pm = F_{\text{correction}} (m_e - m_{e,bare}) , \quad (2.8.9)$$

where $(m_e - m_{e,bare})$ is the radiation mass of electron. How we should interpret the expression $m\alpha_1/\alpha_2$? When $\alpha_1 < 1$ and $\alpha_2 < 1$ then mass m initially increases $1/\alpha_2$ times and next decreases α_1 times and such a resultant mass can be emitted or attached/absorbed.

Muon interacts with the torus/electric-charge X^\pm . On the other hand, an electron interacts with the virtual bare electron-positron pair and virtual photon loop with a mass equal to the mass of the fundamental gluon loop m_{FGL} , so from (2.8.8) and (2.8.9) we have

$$\Delta\mu^\pm = [X^\pm / (m_{\text{FGL}} + 2 m_{e,bare})] (\mu^\pm / m_e) (m_e - m_{e,bare}) =$$

$$= 0.568139496546 \text{ MeV} . \quad (2.8.10)$$

From (2.8.6) we obtain

$$\mu^{*\pm} = 105.0902355341 \text{ MeV} . \quad (2.8.11)$$

From (2.8.7) is

$$a_{\text{SST},\mu^\pm} = 11659214.95431 \cdot 10^{-10} \approx 0.0011659215(11) . \quad (2.8.12)$$

We can compare the SST result with experimental data.

In the E821 experiment at Brookhaven National Lab (BNL), they found [2]

$$a_{\text{EXP},\mu^-} = 0.0011659215(8)(3) , \quad (2.8.13)$$

$$a_{\text{EXP},\mu^+} = 0.0011659204(6)(5) . \quad (2.8.14)$$

We see that our result is consistent with experimental data.

The theoretical Standard-Model (SM) result [3] is inconsistent with experimental data

$$a_{\text{SM},\mu} = 0.00116591810(43) . \quad (2.8.15)$$

2.9. Neutral pion

Contrary to the charged particles, masses of the bound neutral particles are lower than free particles because in the bound state there appears the binding energy that results from the nuclear weak interactions.

It is difficult to determine the mass attached to bound neutral pion when it is emitted. We can suppose that it is the result of decay of the charged pion and the attached mass is the nuclear weak mass of the mass which differentiates the anomalous magnetic moment of the muon and electron (see (2.8.10)), so we have

$$\begin{aligned} \pi^0 &= \pi^0_{\text{bound}} + \alpha_{w(p)} \Delta\mu^\pm = 134.97671768 \text{ MeV} \approx \\ &\approx 134.97672(13) \text{ MeV} . \end{aligned} \quad (2.9.1)$$

The SST mass distance between the charged pion and free neutral pion is

$$\Delta\pi^* = \pi^\pm - \pi^0 = 4.5936852(44) \text{ MeV} . \quad (2.9.2)$$

There is the second possibility i.e. there is attached the mass $W_{(-),d=1} \alpha_{w(e)}/\alpha_{w(p)}$

$$\begin{aligned} \pi^0 &= \pi^0_{\text{bound}} + W_{(-),d=1} \alpha_{w(e)}/\alpha_{w(p)} = 134.9766795 \text{ MeV} \approx \\ &\approx 134.97668(13) \text{ MeV} . \end{aligned} \quad (2.9.3)$$

Then the SST mass distance between the charged pion and free neutral pion is

$$\Delta\pi^* = \pi^\pm - \pi^0 = 4.5937234(44) \text{ MeV} . \quad (2.9.4)$$

2.10. Tauon and fine-structure constant at high energies

Assume that the tauon is a result of transition of the FGL onto the orbit with a radius equal to its circumference ($2\pi \cdot 2A/3 = 4\pi A/3$) and next to a circle with a radius 2π times smaller than the equatorial radius of the torus of baryons ($R_{\text{resultant}} = A/(2\pi)$). With the tauon, which is electrically charged, is created the bare electron-positron pair which is responsible for the electromagnetic interactions.

From the conservation of angular momentum we have

$$m_{\text{FGL}} (4 \pi A / 3) c = (m_{\text{tauon}} + 2 m_{\text{e,bare}}) \{A / (2 \pi)\} c . \quad (2.10.1)$$

It leads to the tauon mass

$$\begin{aligned} m_{\text{tauon}} &= 8 \pi^2 m_{\text{FGL}} / 3 - 2 m_{\text{e,bare}} = 1776.67680687108 \text{ MeV} \approx \\ &\approx 1776.6768(17) \text{ MeV} . \end{aligned} \quad (2.10.2)$$

The second solution follows from the fact that the mean distance between the entangled SST-As components on surface of the torus in the core of baryons is a little higher than the circumference of the equatorial radius of the lightest neutrino (see formulae (2.2.5)-(2.2.7))

$$L_{\text{NA}} / (2 \pi r_{\text{neutrino}}) = L_o = 1.00784018392085 = 1 + \alpha_{\text{em,high}} , \quad (2.10.3)$$

where $\alpha_{\text{em,high}} = 1 / 127.54802822179$ is the fine-structure constant at high energies.

Let us calculate mass of the tauon on the assumption that the distances between the neutrino-antineutrino pairs in it is $L_o r_{\text{neutrino}}$ instead the $2\pi N^* L_o r_{\text{neutrino}}$ as it is in the bare electron. We obtain following relation

$$(m_{\text{tauon}} + 2 m_{\text{e,bare}}) / m_{\text{e,bare}} = 2 \pi N^* . \quad (2.10.4)$$

From (2.10.4) results that mass of the tauon lepton is

$$\begin{aligned} m_{\text{tauon}} &= 2 (\pi N^* - 1) m_{\text{e,bare}} = 1776.67680687108 \text{ MeV} \approx \\ &\approx 1776.6768(17) \text{ MeV} . \end{aligned} \quad (2.10.5)$$

2.11. Photons, gluons and properties of fundamental particles

The neutrinos interact with the condensates in centres of the fermions. Physical states of them should be different. Components of a fermion should differ by internal helicity and, if not by it, by the sign of the electric charge and/or the weak charge carried by neutrinos. The possible bound states are as follows

$$\mu^-_{\text{R}} \equiv e^-_{\text{R}} \nu_{\text{e(anti)L}^+} \nu_{\mu\text{L}^-} ,$$

$$\mu^+_{\text{L}} \equiv e^+_{\text{L}} \nu_{\text{eR}^-} \nu_{\mu(\text{anti})\text{R}^+} ,$$

$$\pi^-_{\text{R}} \equiv e^-_{\text{R}} \nu_{\text{e(anti)L}} \mathbf{L}_{\text{L}} \mathbf{L}_{\text{LA}} \rightarrow \mu^-_{\text{R}} \nu_{\mu(\text{anti})\text{R}^+} ,$$

where \mathbf{L}_{LA} denotes the FGL with the left helicity and antiparallel spin.

$$\pi^+_{\text{L}} \equiv e^+_{\text{L}} \nu_{\text{eR}^-} \mathbf{L}_{\text{R}} \mathbf{L}_{\text{RA}} .$$

There are in existence the following 8 states of the rotating-spin neutrino-antineutrino pairs

$$\begin{aligned}\gamma_{L1} &\equiv (v_{eR-} v_{e(\text{anti})L+})_L, \\ \gamma_{L2} &\equiv (v_{\mu L-} v_{\mu(\text{anti})R+})_L, \\ \gamma_{L3} &\equiv (v_{eR-} v_{\mu(\text{anti})R+})_L, \\ \gamma_{L4} &\equiv (v_{\mu L-} v_{e(\text{anti})L+})_L, \\ \gamma_{R1} &\equiv (v_{eR-} v_{e(\text{anti})L+})_R, \\ \gamma_{R2} &\equiv (v_{\mu L-} v_{\mu(\text{anti})R+})_R, \\ \gamma_{R3} &\equiv (v_{eR-} v_{\mu(\text{anti})R+})_R, \\ \gamma_{R4} &\equiv (v_{\mu L-} v_{e(\text{anti})L+})_R.\end{aligned}$$

In fields with internal helicity, they behave as gluons (8 different types) whereas in field without internal helicity, they behave as photons (1 type only).

Table 2 *New symbols*

* Particle	Internal helicity	Electric charge	Weak charge	* New symbol
* $v_{e(\text{anti})}$	L (left)		+	* $v_{e(\text{anti})L+}$
* v_e	R (right)		-	* v_{eR-}
* $v_{\mu(\text{anti})}$	R		+	* $v_{\mu(\text{anti})R+}$
* v_{μ}	L		-	* $v_{\mu L-}$
* e^-	R	-		* e^-_R
* e^+	L	+		* e^+_L
* p^+	L	+		* p^+_L
* p^-	R	-		* p^-_R
* n	L¹⁾		+	* n_L
* $n(\text{anti})$	R¹⁾		-	* $n(\text{anti})_R$
* μ^-	R¹⁾	-		* μ^-_R
* μ^+	L¹⁾	+		* μ^+_L
* π^-	R¹⁾	-	+	* π^-_R
* π^+	L¹⁾	+	-	* π^+_L

¹⁾The resultant internal helicity is the same as the internal helicity of the torus having highest mass.

2.12. The mass of W^\pm and Z^0 bosons

The ratio of the coupling constant for the nuclear weak interactions to the coupling constant for the weak interactions of electrons is

$$X_{w(p/e)} = \alpha_{w(p)} / \alpha_{w(e)} = 19685.1465727998. \quad (2.12.1)$$

Assume that due to the four-fermion symmetry, a spin-0 charge-0 quadrupole of bare electron-positron pairs ($8m_{e,\text{bare}}$) transits from the weak interactions of electrons to the nuclear weak interactions and then to such an object is added the spin-1 virtual pair composed of electron (positron) and electron-antineutrino (electron-neutrino). Mass and spin of such a particle is equal to the mass and spin of the W^\pm boson

$$W^\pm = 8 m_{e,\text{bare}} X_{w(p/e)} + \{m_{e,\text{bare}} + v_{e(\text{anti})}\}_{\text{virtual}} = 80.3794785717075 \text{ GeV} \approx$$

$$\approx 80.379479(77) \text{ GeV} . \quad (2.12.2)$$

The ratio of the fine-structure constant to the coupling constant for the weak interactions of electrons in presence of dark matter is

$$X_{\text{em/w(e),DM}} = \alpha_{\text{em}} / \alpha'_{\text{w(e),DM}} = 651.871748693794 . \quad (2.12.3)$$

Assume that an object composed of the positively charged pion (or negative one) and a spin-1 pair composed of the bare electron (bare positron) and electron-antineutrino (electron-neutrino) ($\pi^+ + m_{\text{e,bare}} + \nu_{\text{e(anti)}}$) transits from the weak interactions of electrons in presence of dark matter to the electromagnetic interactions and then from such an object is created a pair composed of the spin-1 Z^0 boson and bound neutral pion

$$Z^0 = (\pi^+ + m_{\text{e,bare}} + \nu_{\text{e(anti)}}) X_{\text{em/w(e),DM}} - \pi^0_{\text{bound}} = 91.179756378538 \text{ GeV} \approx \\ \approx 91.179756(87) \text{ GeV} . \quad (2.12.4)$$

2.13. Degrees of freedom

To describe position, shape and motions of a spinning loop without internal structure, but with poloidal motion, we need 10 degrees of freedom: the three coordinates of its centre, mean radius of the loop, its thickness, toroidal/spin speed, poloidal speed, linear speed (i.e. time), and two angles describing rotation of the spin of the loop. A non-rotating-spin loop has 8 degrees of freedom.

To describe in such a way our core composed of a torus with central condensate (both components without internal structure) we also need 10 degrees of freedom. It follows from the fact that thickness of the torus depends on its mean radius so instead two sizes we have one size. But there appears the radius of the central condensate. A non-rotating-spin core has 8 degrees of freedom.

Emphasize that we should not take into account sizes which depend on some other size.

Table 3 *Degrees of freedom of fundamental objects*

Stable object	Co-ordinates and quantities needed to describe position, shape and motions
Tachyon	6 (they always are spinning)
Closed string Entanglon	10 or 8
Neutrino Neutrino-antineutrino (NA) pair	26 or 24 : 8 for entanglons on torus 8 for entanglons in condensate 8 (or 10) for the core as a whole
Core of baryons Electron	58 or 56 : 24 for NA pairs on torus 24 for NA pairs in condensate 8 (or 10) for the core as a whole
An abstract core of Protoworld composed of the baryonic core-anticore (CA) pairs	122 or 120 : 56 for CA on torus 56 for CA in condensate 8 (or 10) for the core as a whole

If N denotes the degrees of freedom then for non-rotating-spin loops/string and our cores is

$$N = 8 (2d - 1), \quad (2.13.1)$$

where $d = 1, 2, 4, 8$ are the TB numbers.

For the rotating-spin our objects we have

$$N = | 8 (2d - 1) + 2 |, \quad (2.13.2)$$

where $d = 0, 1, 2, 4, 8$.

2.14. The seven types of interactions

There are seven types of interactions.

Viscosity of tachyons and viscosity between the tachyons and entanglons follows from smoothness of surfaces of the tachyons – such viscosity causes that the entanglons are the stable objects and that neutrinos curve the SST Higgs field, i.e. they produce the elementary gravitational fields. We call such forces *the viscid interactions*.

The neutrinos and the SST-As components can be entangled due to the exchanges of the superluminal entanglons they consist of. We call such directional forces *the directional entanglement*.

The gravitational interactions follow from the gradients produced in the SST Higgs field. Around the neutrinos there is a region filled with the emitted and absorbed entanglons – binary systems of entanglons are the spin-2 objects. We can call them the SST gravitons but emphasize that they are the superluminal objects. We already calculated the gravitational constant.

The emissions and absorptions of some groups of the SST gravitons cause that around the neutrinos is created the SST Higgs potential which leads to *the volumetric confinement* of neutrinos and of the SST-As components. In next Paragraph, we calculated its range.

The creations and annihilations of the virtual bare electron-positron pairs and their polarization are responsible for *the electromagnetic interactions*. We already calculated the fine-structure constants at low and high energies.

The scalar condensates are responsible for *the weak interactions*. We already calculated the three fundamental coupling constants for the weak interactions.

The FGL and its binary systems (the pions) are responsible for *the nuclear strong interactions*. In this Section we calculated the running coupling constant for such interactions.

2.14.1. Range of the volumetric confinement for neutrinos (the SST Higgs potential)

For the side of a mean cube occupied by one neutrino-antineutrino (NA) pair in the condensate Y (we denote it by $L_{Y+As} = R_{\text{Confinement,Neutrino}}$ – it is the range of the confinement for neutrinos and for the NA pairs which defines also their effective radius, $R_{\text{Neutrino,NA,effective}}$), we obtain (we must take into account also the pairs in the SST absolute spacetime)

$$\begin{aligned} L_{Y+As} = R_{\text{Confinement,Neutrino}} = R_{\text{Neutrino,NA,effective}} &= \{ 2 m_{\text{neutrino}} / (\rho_Y + \rho_{As}) \}^{1/3} = \\ &= 3.92598045308082 \cdot 10^{-32} \mathbf{m} = \\ &= 3510.18034637033 r_{\text{neutrino}}. \end{aligned} \quad (2.14.1)$$

where $\rho_Y = 2.73063237955490 \cdot 10^{23} \text{ kg/m}^3$ is the density of the condensate Y (see formula (2.2.30)), and ρ_{As} is the density of the SST absolute spacetime. But our result does not explain the origin of the range of the confinement, i.e. of the range of the SST Higgs potential for neutrinos and their pairs.

We already calculated the side of a mean cube occupied by one neutrino-antineutrino pair in the SST absolute spacetime (see formula (2.2.6)): $L_{As} = 3510.20933362115 r_{\text{neutrino}}$.

We can see that the difference $\Delta L = L_{As} - L_{Y+As} = 0.028987 r_{\text{neutrino}}$ is very small in comparison with L_{As} so it should be very easy to produce condensates in the SST As.

Notice that the density of the condensate Y of baryons is $f = 40,364.3125818004$ times lower than the density of the SST As. It leads to conclusion that the mean distance between the neutrino-antineutrino pairs, L_{Y+As} , in the Y condensate is

$$L_{Y+As} = L_{As} \{f / (f + 1)\}^{1/3} = 3510.18034637033 r_{\text{neutrino}} \quad (2.14.2)$$

as it should be.

The theories of the core of lightest neutrinos and core of baryons are similar so the ratios of similar quantities in both theories have the same values. Instead to consider neutrinos we are considering the core of baryons.

The ranges of the SST Higgs potential of the lightest neutrino or of the core of baryons should result from the binding energy which should have a spherical symmetry.

Consider the core of baryons. The binding energy of X^\pm and Y is $\Delta E_{\text{core}} = X^\pm + Y - H^\pm = 14.9785750313267 \text{ MeV}$ (see formula (2.5.18)). This binding energy lowers the zero-point of the zero-energy field. In such a region, the transitions from circular motions (circumference is $2\pi R$) to motions along the diameter ($2R$), and vice versa, cause that according to the formulae (1.4.10) and (1.4.20) there are emitted and absorbed virtual condensates composed of the SST-As components – their mass is

$$\begin{aligned} \Delta m^* &= \Delta E_{\text{core}} / \pi^4 = 0.153769785472058 \text{ MeV} \approx \\ &\approx 0.15376979(15) \text{ MeV} . \end{aligned} \quad (2.14.3)$$

We need some boundary condition to determine the range of such virtual condensates. We know that the range of the mass $M_{TB} = 750.297525564514 \text{ MeV}$ that leads to the TB orbits (see (2.5.19)) is B_{mean} (see (2.5.9)). Assume that such a mass emits a virtual mass $\Delta m \approx \Delta m^*$ with a range equal to $L_b = 3510.18034637033A$ – it is some baryonic analog to (2.14.1). It means that the range of $(M_{TB} - \Delta m)$ should be a little bigger than B_{mean} , say, it is equal to $B = 0.501839476788152 \text{ fm}$ (see (2.5.5)). It leads to following formula (notice that range is inversely proportional to mass)

$$(M_{TB} - \Delta m) B = \Delta m L_b . \quad (2.14.4)$$

From it we obtain

$$\Delta m = 0.153769958910634 \text{ MeV} \approx$$

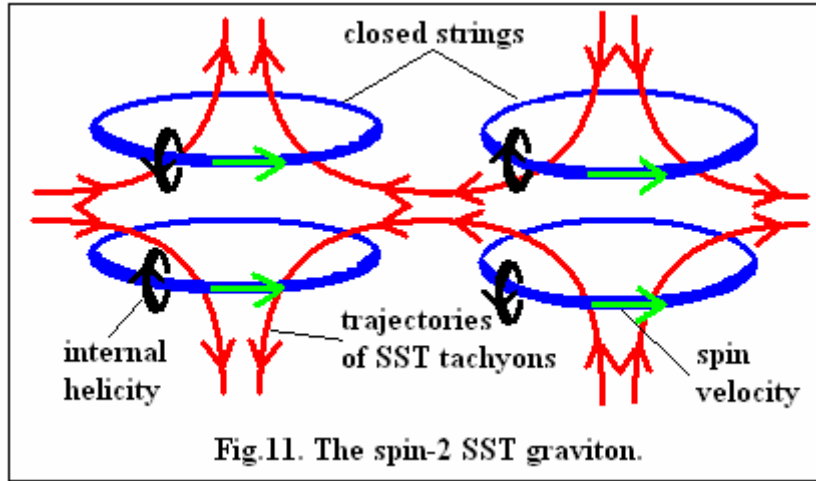
$$\approx 0.15376996(15) \text{ MeV} . \quad (2.14.5)$$

Since the masses in (2.14.3) and (2.14.5) are consistent so we can say that we showed the origin of the SST Higgs mechanism that leads to the volumetric confinement of the cores of baryons.

Similar phenomena take place in the SST-As components and neutrinos but the virtual SST-As condensates we must replace for groups/quanta composed of the superluminal entanglons the neutrinos consist of.

Gravitational fields are the result of the viscid interactions of the SST Higgs field with the entanglons the neutrinos consist of. Inside the region of the SST Higgs potential, the spin-2 binary systems of entanglons (we call them the SST gravitons) are emitted and absorbed so such a region is described by the SST quantum gravity. The flows of the SST tachyons in a SST graviton we present in Fig.11.

The SST Higgs mechanism presented in this Paragraph (which leads to the volumetric confinement) leads to the SST scalar condensates composed of the SST gravitons and to the SST-As scalar condensates which in SST are responsible for the weak interactions.



We described three phenomena that cause that particles acquire their gravitational masses, i.e. the SST is the theory with mass gaps. The first phenomenon shows how neutrinos acquire their masses – it is due to the viscid interactions between the SST Higgs field and the entanglons the neutrinos consist of. The second phenomenon shows how the SST-As condensates acquire their masses – it is due to the volumetric confinement of the neutrinos and their pairs forced by the circle-diameter transitions within the regions with lowered density of the zero-energy fields. The third phenomenon shows how the tori/charges acquire their masses – it is due to the two shortest-distance quantum entanglement, i.e. $2\pi R$ and $2\pi R/3$ where R is the equatorial radius of the tori.

Notice also that the SST Higgs-potential range for the baryons, $L_b = 2448.14886142875 \text{ fm}$ is very close to the Compton wavelength of the bare electron multiplied by $(1 + \alpha_{em,high})$

$$2 \pi \lambda_{C(e),bare} (1 + \alpha_{em,high}) = 2448.16907836865 \text{ fm} . \quad (2.14.6)$$

The perfect consistency we obtain for value of the electromagnetic coupling constant equal to

$$\alpha_{\text{em,high}}^* = (L_{Y+\text{As}} / r_{\text{neutrino}}) / (2 \pi N^*) - 1 = 1 / 127.683570396528 \quad (2.14.7)$$

because then we obtain

$$2 \pi \lambda_{C(e),\text{bare}} (1 + \alpha_{\text{em,high}}^*) = 2448.14886142875 \text{ fm} = L_b . \quad (2.14.8)$$

The difference between (2.14.6) and (2.14.8) follows from the fact that $\alpha_{\text{em,high}}$ is the value for the torus/electric-charge of the baryons in absence of the virtual condensates Y , while $\alpha_{\text{em,high}}^*$ is the value in presence of the virtual condensates Y that decrease the radiation mass of the charge. Emphasize that $\alpha_{\text{em,high}}$ is the upper limit.

2.14.2. Homogeneous description of all interactions

Constants of interactions, G_i , are directly proportional to the inertial mass densities of fields carrying the interactions. The following formula defines the coupling constants of all interactions

$$\alpha_i = G_i M_i m_i / (c \hbar) = v_{\text{spin}}^2 r m_i / (c \hbar) = v_{\text{spin}} / c , \quad (2.14.9)$$

where M_i defines the sum of the mass of the sources of interaction being in touch via a field plus the mass of the component of the field whereas m_i defines the mass of the carrier of interactions.

We know that the bound neutral pion is a binary system of FGLs composed of the rotating-spin-1 neutrino-antineutrino (NA) pairs. This means that inside the bound neutral pion the NA pairs are exchanged whereas between the bound neutral pions the FGLs are exchanged. We can neglect the mass of the neutrino-antineutrino pairs in comparison to the mass of the neutral pion. On the other hand, from (2.14.9) it follows that coupling constant for the FGL is unitary because its spin speed, v_{spin} , is equal to the c . For strongly interacting bound neutral pion is

$$\alpha_S^{\pi\pi,\text{FGL}} = G_S (2 \pi^{\circ}_{\text{bound}}) m_{\text{FGL}} F^2 / (c \hbar) = v_{\text{spin}} / c = 1 . \quad (2.14.10)$$

Then the constant of the strong interactions is $G_S = 5.45650858081491 \cdot 10^{29} \text{ m}^3 \text{ s}^{-2} \text{ kg}^{-1}$. Coupling constant for strongly interacting proton at low energies is

$$\alpha_S^{\text{pp},\pi} = G_S (2 p + m_{\text{FGL}}) \pi^{\circ}_{\text{bound}} F^2 / (c \hbar) = 14.3911847059219 . \quad (2.14.11)$$

In a relativistic version, the G_S is invariant. When we accelerate a baryon, then there decreases the spin speed of FGL so its energy decreases as well

$$E_{\text{Loop}} 2 \pi r_{\text{loop}} / v_{\text{spin}} = \hbar . \quad (2.14.12)$$

This condition leads to the conclusion that the value of the strong coupling decreases when energy increases, i.e. it is the running coupling constant for the nuclear strong interactions.

2.14.3. The running coupling constant for the nuclear strong interactions

For colliding nucleons, we cannot separate the nuclear weak and strong interactions of the cores of baryons. The nuclear weak interactions are realized by exchanges of the virtual or real Y condensates so there appears the factor 2. This means that the running coupling constant for the strong-weak interactions, α_{sw} , is defined by following formula

$$\alpha_{sw} = 2 \alpha_{w(p)} \alpha_{s,running} , \quad (2.14.13)$$

where $\alpha_{s,running}$ is the running coupling constant for the nuclear strong interactions.

For virtual FGL which is responsible for the nuclear strong interactions we have

$$\begin{aligned} E_{FGL,running} T_{Period,FGL} &= m_{FGL,running} v_{spin}^2 \cdot 2 \pi r_{FGL} / v_{spin} = \\ &= 2 \pi r_{FGL} m_{FGL,running} v_{spin} = \hbar , \end{aligned} \quad (2.14.14)$$

where $m_{FGL,running}$ is the running mass of FGL.

We see that when we accelerate nucleons then their spin speed (so also the spin speed of the FGLs) must decrease because the resultant speed of the neutrino pairs the mentioned objects consist of is invariant. From formula (2.14.14) results that with increasing energy of colliding nucleons, the running mass of FGLs decreases, i.e. value of the running coupling constant also decreases.

We can calculate the mass of the carrier of interactions, $m_{running}$, using the following formula

$$m_{running} = F \pi^0_{bound} \beta , \quad (2.14.15)$$

where

$$\beta = (1 - v^2 / c^2)^{1/2} , \quad (2.14.16)$$

where v denotes the relativistic speed of the nucleon.

Define energy of collision as $Q = Np$ then

$$\beta = 1 / N = p / Q . \quad (2.14.17)$$

When the energy of colliding protons increases, more sources interacting strongly appear. The sources are in contact because there is a liquid-like substance composed of the cores of baryons. There is the destruction of the atom-like structure of baryons so instead a collision of two protons we have a collision of two cores of baryons. This means that a colliding nucleon and the new sources behave as one source. Strong interactions are associated with the torus X^\pm whereas the mass of the core is H^\pm . The mass of the source, M_{sw} , for colliding proton is

$$M_{sw} = F \{ 2 H^\pm + \pi^0_{bound} \beta / 2 + X^\pm (p / H^\pm) / \beta \} . \quad (2.14.18)$$

The torus-antitorus pairs are produced from the energy Q but number of the tori is not proportional to number of protons but to the ratio p/H^\pm .

The formula

$$\alpha_{sw} = F^2 2 \alpha_{w(p)} G_S M_{sw} m_{\text{running}} / (c \hbar) \quad (2.14.19)$$

leads to

$$\alpha_{sw} = a_u \beta^2 + b_u \beta + c_u, \quad (2.14.20)$$

where $a_u = 0.0187059$, $b_u = 0.403283$, $c_u = 0.113801$.

Within the Standard Model the parton shower (PS) is not good understood so the phenomena associated with the PS can change the experimental data concerning the running coupling for the strong interactions.

In SST, PS is produced due to the weak decays of condensates composed of the carriers of gluons and photons i.e. of the neutrino-antineutrino pairs.

Table 4 *Running strong coupling constant*

Q [GeV]	$\alpha_{SST}(Q)$
2,000	0.08030
$Z^0 = 91.180$	0.11795
50	0.12477
20	0.14019
10	0.16157
p	0.55044

In the collisions of nucleons there are produced the Z^0 bosons. For energies lower than Z^0 there are produced the SST-As condensates that increase the density of the zero-energy field so they increase value of the running coupling. For energy equal to Z^0 , the α_{sw} should be defined by formula (2.14.20) while for higher energies the created additional Z^0 bosons decrease the density of the zero-energy field so α_{sw} is lowered. From formula (2.14.9) we have that coupling constants are directly proportional to spin speeds so from the conservation of spin we have that α is inversely proportional to radius of a loop. The above remarks lead to

$$\alpha_{SST} = \alpha_{sw} + \alpha_{w(p)} \{ 1 - (Q / Z^0)^{1/3} \}. \quad (2.14.21)$$

Calculate a few results that follow from formula (2.14.21) – they are collected in Table 4.

2.14.4. Range of the gravitational interactions

Gravitational fields are the gradients produced in the superluminal Higgs field by neutrinos. The total cross section of all tachyons in volume of a rectangular prism $1\mathbf{m} \cdot 1\mathbf{m} \cdot 2 \cdot 10^{36}\mathbf{m}$ is $1\mathbf{m}^2$ so all divergently moving tachyons sooner or later are scattered. It leads to conclusion that range of the gravitational interactions is about $2 \cdot 10^{36}\mathbf{m}$.

2.15. Higgs boson and a prediction of new particle

Mass of the region of the SST absolute spacetime, H_{Higgs} , which overlaps with the electromagnetic binding energy of the bare electron on the circular axis of the torus in the core of baryons, $\Delta E_{\text{em}} = 3.09695298260205 \text{ MeV}$ (see formula (2.5.17)), is

$$\begin{aligned} \mathbf{H}_{\text{Higgs}} &= f \Delta E_{\text{em}} = 125.006378240888 \text{ GeV} \approx \\ &\approx 125.00638(12) \text{ GeV} . \end{aligned} \quad (2.15.1)$$

where $f = 40,364.3125818004$ (see formula (2.14.2)). It is the Higgs boson – it is the composite scalar particle composed of the confined SST-As components.

There should be in existence a scalar (we call it the Higgs boson-high), $\mathbf{H}_{\text{Higgs-high}}$, or/and spin-1 charged/neutral particle, \mathbf{H}^* , \mathbf{H}^{**} , with a mass equal to mass of the region of the SST-As, which overlaps with the condensate \mathbf{Y}

$$\mathbf{H}_{\text{Higgs-high}} = f \mathbf{Y} \approx 17.119383(17) \text{ TeV} . \quad (2.15.2)$$

Notice that similar value we obtain applying three other formulae

$$\mathbf{H}^* = f 2 \pi m_{\text{FGL}} \approx 17.1304 \text{ TeV} , \quad (2.15.3)$$

$$\mathbf{H}^{**} = 4 W^+ / \alpha_{\text{w(p)}} \approx 17.1726 \text{ TeV} . \quad (2.15.4)$$

$$\mathbf{H}^{***} = \mathbf{H}_{\text{Higgs}} / \alpha_{\text{em}} \approx 17.1304 \text{ TeV} . \quad (2.15.5)$$

2.16. Frequency of the hydrogen spin-flip transition

The parallel polarisation of two vortices increases the binding energy of a system

$$E_{\text{par}} = E + \Delta E_i , \quad (2.16.1)$$

whereas the antiparallel polarisation decreases the binding energy

$$E_{\text{ant}} = E - \Delta E_i . \quad (2.16.2)$$

Since $\Delta E_i = \alpha_i c \hbar / r$ (see formula (2.14.9)) so the change of the mutual orientation of spins causes that the emitted energy is

$$E_i = 2 \alpha_i c \hbar / r = h \nu , \quad (2.16.3)$$

and therefore

$$\nu = \alpha_i c / (\pi r) , \quad (2.16.4)$$

where ν denotes the frequency.

Here the coupling constant is the weak coupling constant for electron in presence of dark matter, i.e. $\alpha_i = \alpha'_{\text{w(e),DM}}$.

The mechanism forcing the transition is as follows. There is the circle-radius transition of the electron on the Bohr orbit. The electron does not reach the centre of the proton but the surface of its strong-electroweak field with a radius $\mathbf{R}_{\text{s-w-em}}$ defined as follows

$$\mathbf{R}_{\text{s-w-em}} = \mathbf{R}_{\text{strong}} \alpha_s / (\alpha_s - \alpha_{\text{w(p)}} - \alpha_{\text{em}}) , \quad (2.16.5)$$

where $\mathbf{R}_{\text{strong}} = 2.9582092848041 \text{ fm}$ is the range of the strong interactions (see (1.3.7) and Fig.8), and $\alpha_s = 1$ is the coupling constant for the nuclear strong interactions at low

energy. The electroweak interactions weaken the strong field so range of the mixture of them is bigger.

From (2.14.9) results that for a circle-like loops is $\alpha_i = v_{\text{spin}} / c$. On the other hand, from the conservation of spin follows that spin speed is inversely proportional to radius so radius is inversely proportional to coupling constant. The weak interactions during the circle-radius transition increase the resultant radius so the final formula for the radius r in formula (2.16.4) is

$$R^* = \{R_B / (2 \pi) - R_{s-w-em}\} / \alpha'_{w(e),DM} = 7.52075628847542 \cdot 10^{-7} \text{ m}, \quad (2.16.6)$$

where the Bohr radius calculated within SST is

$$R_B = \hbar / (m_e F c \alpha_{em}) = 5.29177293474929 \cdot 10^{-11} \text{ m}. \quad (2.16.7)$$

The experimental value is $5.29177210903(80) \cdot 10^{-11} \text{ m}$ (source: 2018 CODATA). The seven significant digits in the SST result and the CODATA value are the same. We can rewrite formula (2.16.4) as follows

$$\begin{aligned} v &= \alpha'_{w(e),DM} c / (\pi R^*) = 1420.40595773115 \text{ MHz} \approx \\ &\approx 1420.4060(14) \text{ MHz}. \end{aligned} \quad (2.16.8)$$

This value is consistent with the experimental result: $1420.4057517667(9) \text{ MHz}$ [1].

2.17. Lamb-Retherford shift

The Lamb shift is the difference in energy between the $^2S_{1/2}$ and $^2P_{1/2}$ energy levels. It was not predicted by the Dirac equation because from it follows that these two states should have the same energy. Now, in the mainstream physics, it is assumed that it is a result of interaction of the hydrogen electron with vacuum energy fluctuations.

We can calculate the Lamb shift using following formula

$$\Delta E_i = \alpha_i c \hbar / r = m_i c^2. \quad (2.17.1)$$

The Lamb shift concerns the second orbit so we have $r = 4 R_B$. We can rewrite (2.17.1) as follows

$$v_{L-R} = \alpha_i c / (2 \pi \cdot 4 R_B). \quad (2.17.2)$$

From the definition we have

$$\alpha_{w(p)} \sim Y^2. \quad (2.17.3)$$

We claim that the Lamb shift is the result of the nuclear weak interactions of the energy which is equal to the energy distance between the relativistic mass of the charged pion in the $d = 1$ state and its rest mass with the radiation mass of the electron on the second shell in the hydrogen atom, so from the definition we have

$$\alpha_i \sim (W_{(+),d=1} - \pi^\pm) (m_e - m_{e,bare}), \quad (2.17.4)$$

The last two formulae lead to

$$\alpha_i = \alpha_{w(p)} (W_{(+),d=1} - \pi^\pm) (m_e - m_{e,bare}) / Y^2, \quad (2.17.5)$$

so from (2.17.2) is

$$\nu_{L-R} = 1058.0789 \text{ MHz}. \quad (2.17.6)$$

The second solution is as follows.

From (2.14.9) results that for spherical symmetry is $\alpha \sim R$ so we have

$$\alpha_{w(p)} \sim A. \quad (2.17.7)$$

A change in the radius of the second orbit in the hydrogen atom, dr , should be because of the electromagnetic and weak interactions in presence of dark matter of the electron with proton so we have

$$dr / A = (\alpha'_{w(e),DM} + \alpha_{em}) / \alpha_{w(p)}. \quad (2.17.8)$$

From this $dr = 2.72248882025292 \cdot 10^{-16} \text{ m}$.

For the second shell of the hydrogen atom the frequency associated with such a shift is

$$\nu_{L-R} = R_H c [1 / 4 - 1 / (4 + dr / R_B)] = 1057.83840825705 \text{ MHz}, \quad (2.17.9)$$

where the Rydberg constant calculated within SST is

$$R_H = F m_e e^4 c^3 / (4 \pi \hbar^3 10^{14}) = 1.09737298714366 \cdot 10^7 \text{ m}^{-1}. \quad (2.17.10)$$

The two different phenomena lead to two different (but very close) frequencies. It suggests that the Lamb shift should be split unless the second mechanism dominates because it relates to the lower involved energy.

2.18. Lifetimes

Lifetimes we can calculate applying formulae (1.4.25) and (1.4.29)

$$\tau_{\text{Lifetime}} \sim 1 / m^4, \quad (2.18.1)$$

$$\tau_{\text{Lifetime}} \sim 1 / \alpha_i. \quad (2.18.2)$$

If the same mass can interact in different ways (i.e. the involved masses are $\alpha_1 m$ and $\alpha_2 m$) then from (2.18.1) we obtain

$$\tau_1 / \tau_2 = (\alpha_2 / \alpha_1)^4. \quad (2.18.3)$$

If one of the interactions is the nuclear strong interaction at low energy, say $\alpha_2 = \alpha_s = 1$, then from (2.18.2) we have

$$\tau_1 / \tau_2 = (1 / \alpha_i), \quad (2.18.4)$$

or from (2.18.3) is

$$\tau_1 / \tau_2 = (1 / \alpha_i)^4. \quad (2.18.5)$$

Contrary to appearances there is practically no ambiguity in the calculated lifetimes of particles.

Muons are created as quadrupoles from the Y condensates. It causes that they conserve the zero-electric-charge and the zero-spin of the condensate Y . Then the muon torus and the torus in the core of the baryon overlap, which fixes the spinning period which is the initial lifetime of the muon

$$T_o = 2\pi A/c = 1.4617314 \cdot 10^{-23} \text{ s}. \quad (2.18.6)$$

The weak interactions of the muon increase its initial lifetime. There is the transition from the nuclear weak interactions (the involved mass is $m_{w,1} = \alpha_{w(p)} \mu^\pm$) to weak interaction of electron (the involved mass is $m_{w,2} = \alpha_{w(e)} \mu^\pm$). Such transition increases the muon lifetime. Since $X_{w(p/e)} = \alpha_{w(p)} / \alpha_{w(e)} = 19685.147$ (see formula (2.12.1)) so the lifetime of muon is (see (2.18.3))

$$\tau_{\text{muon}} = T_o X_{w(p/e)}^4 = 2.194937 \cdot 10^{-6} \text{ s}. \quad (2.18.7)$$

The weak interactions are responsible for the decay of the hyperons and because of these interactions they behave as a nucleon, whereas the muon behaves as an electron, so the lifetimes of the hyperons should be close to (there is a transition from weak interaction of electron to the nuclear weak interaction) – see (2.18.2)

$$\tau_{\text{hyperon}} = \tau_{\text{muon}} (1 / X_{w(p/e)}) = 1.115022 \cdot 10^{-10} \text{ s}. \quad (2.18.8)$$

The tauon decays because of the transition from the nuclear weak interaction to the nuclear strong interaction (see (2.18.3))

$$\tau_{\text{taun}} = \tau_{\text{muon}} (\alpha_{w(p)} / \alpha_s)^4 = 2.697209 \cdot 10^{-13} \text{ s}. \quad (2.18.9)$$

The lifetime of the charm hyperon $\Lambda_c^+(2260)$ is (see (2.18.1))

$$\tau_{\Lambda(2260)} = \tau_{\text{hyperon}} (Y / Y_{\Lambda(2260)})^4 = 1.82 \cdot 10^{-13} \text{ s}, \quad (2.18.10)$$

where $Y_{\Lambda(2260)} = 2286 - 1115 + 940 = 2111 \text{ MeV}$.

The lifetime of the FGL created on the circular axis of the torus of the nucleon can be calculated using the formula $E_{\text{FGL}} \cdot \tau_{\text{FGL}} = \hbar$, where $m_{\text{FGL}} = 67.54441 \text{ MeV}$

$$\tau_{\text{FGL}} = 9.745 \cdot 10^{-24} \text{ s}. \quad (2.18.11)$$

The neutral pion decays in respect of the transition from the strong interactions to the nuclear weak interaction. The weak mass of virtual particles produced by the FGL we can calculate using the formula $m_{\text{FGL(weak)}} = \alpha_{\text{w(p)}} m_{\text{FGL}} = 1.26463 \text{ MeV}$. Consequently the lifetime of the neutral pion is (see (2.18.5))

$$\tau_{\text{pion(o)}} = \tau_{\text{FGL}} (1 / \alpha_{\text{w(p)}})^4 = 0.793 \cdot 10^{-16} \text{ s} . \quad (2.18.12)$$

The charged pion decays because of the transition from the nuclear strong interaction to the electromagnetic interaction of the weak mass, therefore (see (2.18.5))

$$\tau_{\text{pion(+-)}} = \tau_{\text{pion(o)}} (1 / \alpha_{\text{em}})^4 = 2.797 \cdot 10^{-8} \text{ s} . \quad (2.18.13)$$

In neutron, there is the transition from the FGL interacting with $\Delta\pi = \pi^{\pm} - \pi^{\text{o}}_{\text{bound}}$ to the bare electron (see (2.18.1))

$$\tau_{\text{neutron}} = \tau_{\text{muon}} \{ (m_{\text{FGL}} + \Delta\pi) / m_{\text{e,bare}} \}^4 = 876.34 \text{ s} . \quad (2.18.14)$$

Ordered motions of neutrons at low energy decrease local density of field so neutrons attached the smallest possible mass, i.e. the electron condensate, so we have

$$\tau^*_{\text{neutron}} = \tau_{\text{muon}} \{ (m_{\text{FGL}} + \Delta\pi + m_{\text{e,bare}} / 2) / m_{\text{e,bare}} \}^4 = 888.80 \text{ s} . \quad (2.18.15)$$

2.18.1. Lifetimes of the W^{\pm} and Z^0 bosons and of the H Higgs boson

The H, W^{\pm} and Z^0 bosons decay due to their weak mass, M_{weak} ,

$$M_{\text{weak}} = \alpha_{\text{w(p)}} M = \Gamma / c^2 , \quad (2.18.16)$$

where M is the mass of a condensate whereas the $M_{\text{weak}} c^2$ is the decay width Γ .

On the other hand, lifetime of a condensate is defined as follows

$$\tau = \hbar / \Gamma = \hbar / (M_{\text{weak}} c^2) = \hbar / (\alpha_{\text{w(p)}} M c^2) . \quad (2.18.17)$$

Applying formula (2.18.17) we obtain the rigorous theoretical lifetimes – they are the upper limits for experimental data. It follows from the fact that theoretical decay width always has higher accuracy than experimental ones (it is due to the systematic and statistical errors)

$$\Gamma_{\text{H,theory(SST)}} \approx 2.34 \text{ GeV} / c^2 \rightarrow \tau_{\text{H,theory}} = 2.82 \cdot 10^{-25} \text{ s} , \quad (2.18.18)$$

$$\Gamma_{\text{W,theory(SST)}} \approx 1.51 \text{ GeV} / c^2 \rightarrow \tau_{\text{W,theory}} = 4.38 \cdot 10^{-25} \text{ s} , \quad (2.18.19)$$

$$\Gamma_{\text{Z,theory(SST)}} \approx 1.71 \text{ GeV} / c^2 \rightarrow \tau_{\text{Z,theory}} = 3.86 \cdot 10^{-25} \text{ s} . \quad (2.18.20)$$

Applying formula (2.18.17) and knowing the decay widths, [4], we obtain the experimental lifetimes

$$\Gamma_{\text{H,exp.}} \approx 3.4 \text{ GeV} / c^2 \rightarrow \tau_{\text{H,exp.}} = 1.94 \cdot 10^{-25} \text{ s} , \quad (2.18.21)$$

$$\Gamma_{W,\text{exp.}} \approx 2.1 \text{ GeV} / c^2 \rightarrow \tau_{W,\text{exp.}} = 3.16 \cdot 10^{-25} \text{ s} , \quad (2.18.22)$$

$$\Gamma_{Z,\text{exp.}} \approx 2.5 \text{ GeV} / c^2 \rightarrow \tau_{Z,\text{exp.}} = 2.64 \cdot 10^{-25} \text{ s} . \quad (2.18.23)$$

Notice that

$$\tau_{\text{theory}} / \tau_{\text{exp.}} = \Gamma_{\text{exp.}} / \Gamma_{\text{theory}} = 2^{1/2} . \quad (2.18.24)$$

It suggests that the energy responsible for decay, Γ_{theory} , appears on the Schwarzschild surface for the weak or nuclear strong interactions. Then, its relativistic mass is $\Gamma_{\text{exp.}} = 2^{1/2} \Gamma_{\text{theory}}$ – it leads to the perfect consistency of the SST with experimental data concerning the lifetimes.

2.19. Radius of proton

Here we show that the charge radius of proton depends on kind of measurement.

We know that range/radius of interaction is inversely proportional to mass so an increase in mass due to some additional interactions causes that effective radius (for example, of proton), R_{eff} , decreases. It follows from the conservation of the angular momentum of a loop for an invariant spin speed of the loop – it can be a virtual photon loop or virtual gluon loop with energy equal to a characteristic mass that carries an interaction. It leads to following relationship

$$R_{\text{eff}} = R_o M_o / (M_o + \Sigma_i m_i) , \quad (2.19.1)$$

where R_o is the initial radius, M_o is the initial mass carrying an initial interaction, and $\Sigma_i m_i$ is the sum of masses of carriers of additional interactions.

On the other hand, coupling constants, α_i , are directly proportional to masses of carriers of interactions, m_i , (see (2.14.9))

$$\alpha_i \sim m_i . \quad (2.19.2)$$

From (2.19.1) and (2.19.2) we have

$$R_{\text{eff}} = R_o \alpha_o / (\alpha_o + \Sigma_i \alpha_i) , \quad (2.19.3)$$

where α_o is the initial coupling constant, and $\Sigma_i \alpha_i$ is the sum of coupling constants for additional interactions.

In the proton, there is occupied only the $d = 1$ state, i.e. $R_{d=1} = A + B_{\text{Mean}} = 1.199276 \text{ fm}$ – it is occupied by the positively charged relativistic pion, π^+ or relativistic bound neutral pion $\pi^{\text{o}}_{\text{bound}}$.

From the sizes of the torus/electric-charge follows that the charge radius of proton along the z-axis is

$$R_z = A / 3 . \quad (2.19.4)$$

The charged pion in the $d = 1$ state causes that the charged radius of proton along the x-axis and y-axis is

$$R_x = R_y = A + B_{\text{mean}} . \quad (2.19.5)$$

The virtual gluons are emitted especially in directions parallel to the plane of the equator of the torus/electric-charge so the nuclear strong field has a shape of a cylinder.

The arithmetic mean of the orthogonal radii, which is the real mean charge radius of proton, $R_{o,p}$, is

$$R_{o,p} = (R_x + R_y + R_z) / 3 = [2 (A + B_{\text{mean}}) + A / 3] / 3 = \mathbf{0.87701081 \text{ fm}} . \quad (2.19.6)$$

This value is consistent with the result obtained by Fleurbaey, *et al.* (2018) [5] – the result is $r_p = 0.877(13) \text{ fm}$. It is based on the 1S – 3S transition in hydrogen.

This value is consistent also with the result obtained by Sick (2018) [6] – the result is $r_p = 0.887(12) \text{ fm}$. It is based on the electron scattering.

The virtual nuclear strong field creates the virtual charged pion-antipion pairs (the $\pi^- \pi^+$ pairs). Decays of such pairs into muons cause that there appear the muon-antimuon pairs (the $\mu^- \mu^+$ pairs). On the other hand, the decays of the $\pi^- \pi^+$ pairs into the neutral pions cause that there appears a virtual cloud composed of the electron-electron antineutrino pairs and the positron-electron neutrino pairs – they are the $e^- \nu_{e,\text{anti}} e^+ \nu_e$ lepton quadrupoles with a mass of $\Delta\pi = \pi^\pm - \pi_{\text{bound}}^0$.

In measurements based on, for example, the muonic hydrogen Lamb shift, the virtual leptonic quadrupoles are forced to interact with the virtual $\mu^- \mu^+$ pairs. It causes that the effective charge radius of proton decreases. The mean muon charge radius, $R_{p(\mu)}$, of proton is

$$R_{p(\mu)} = R_{o,p} \mu^\pm / (\mu^\pm + \Delta\pi) = \mathbf{0.84038927 \text{ fm}} . \quad (2.19.7)$$

This value is very close to the result obtained by Antognini, *et al.* (2013) [7] – the result is $r_p = 0.84087(39) \text{ fm}$. It is based on the $\mu^+ p$ – atom Lamb shift.

Applying formula (2.19.3) we obtain

$$R_{p(\text{lower-limit})} = R_{o,p} \alpha_s / [\alpha_s + 2 (\alpha_{w(p)} + \alpha_{em})] = \mathbf{0.83362836 \text{ fm}} , \quad (2.19.8)$$

where $\alpha_s = 1$ is the coupling constant for the nuclear strong interactions inside baryons at low energy. The factor 2 in formula (2.19.8) appears because the virtual leptonic field interacts with proton via the particle-antiparticle pairs, not via single particles.

This value is consistent with the result obtained by Bezginov, *et al.* (2019) [8] – the result is $r_p = 0.833(10) \text{ fm}$. It is based on the 2S-2P transition in hydrogen.

On the basis of the atom-like structure of baryons, we showed that the effective charge radii of proton strongly depend on the kinds of measurements.

We claim that the measurements based on the $nS - mS$ transitions in hydrogen, where n and m are the natural numbers, and based on the elastic electron-proton scattering in the low momentum transfer region, practically eliminate the electroweak interactions of the virtual leptonic field with proton. It causes that the nuclear strong interactions lead to the real charge radius of proton equal to 0.87701081 fm – it is the upper limit.

The electroweak interactions of proton with the virtual leptonic field composed of the muon-antimuon pairs ($\mu^- \mu^+$) and the lepton quadrupoles ($e^- \nu_{e,\text{anti}} e^+ \nu_e$) from the decays of the virtual charged pion-antipion pairs ($\pi^- \pi^+$), cause that the effective charge radius of proton decreases to **0.84038927 fm** so we indeed can call such a radius the muon charge radius of proton.

The lower limit for the effective charge radius of proton we obtain using the coupling constants for the nuclear-strong, nuclear-weak and electromagnetic interactions – it is **0.83362836 fm**.

The calculated values should dominate but there can be also some mixtures of them.

2.20. Selected mesons

Mesons, meanwhile, are binary systems of gluon loops that are created inside and outside the torus of baryons. They can also be mesonic nuclei that are composed of the other mesons and the FGLs, or they can be binary systems of mesonic nuclei and/or other binary systems.

We can build three of the smallest unstable neutral objects containing the carriers of strong interactions i.e. the pions (134.96608 MeV (the bound state) and 139.57040 MeV) and the FGLs (67.54441 MeV). Each of those objects must contain the FGL because only then it can interact strongly.

The letter **a** denotes the mass of the object built of a bound neutral pion and one FGL

$$\mathbf{a} = 202.51 \text{ MeV.}$$

The parity of this object is equal to $P = +1$ because both the pion and the FGL have a negative parity so as a result the product has a positive value.

The letter **b** denotes the mass of the two bound neutral pions and one FGL

$$\mathbf{b} = 337.48 \text{ MeV.}$$

And **b'** denotes the mass of the two charged pions and one FGL

$$\mathbf{b}' = 346.69 \text{ MeV.}$$

The parity of these objects is equal to $P = -1$.

In particles built of objects **a**, **b**, and **b'**, the spins are oriented in accordance with the Hund law (the sign "+" denotes spin oriented up, the sign "-" denotes spin oriented down, and the word "and" separates succeeding shells), for example

+– and +– +++– – – and +– +++– – – +++++– – – – – and etc.

Because electrically neutral mesonic nuclei may consist of the above three different types of objects whereas only one of them contains the charged pions, the charged pions should, therefore, be two times less than the neutral pions. It is also obvious that there should be some analogy for mesonic and atomic nuclei. I will demonstrate this for the Upsilon meson and the Gallion. The Gal is composed of 31 protons and has an atomic mass equal to 69.72. To try to build a meson having a mesonic mass equal to 69.5 we can use the following equation:

$${}^{69.5}\text{Upsilon} = Y(1S) = 8\mathbf{a} + 14\mathbf{b} + 9\mathbf{b}' = 9464.92 \text{ MeV (vector).}$$

Such a mesonic nucleus contains 18 charged pions, 36 bound neutral pions, 31 FGLs, and contains $31 = 8 + 14 + 9$ objects.

2.20.1. Lightest mesonic nuclei

The Eta meson is an analog to the Helion-4. Since the Eta meson contains three pions there are two possibilities. Such a mesonic nucleus should contain one charged pion but such objects are not electrically neutral. This means that the Eta meson should contain two charged pions or zero

$${}^4\text{Eta} = \eta = \mathbf{a} + \mathbf{b}' = 549.20 \text{ MeV (pseudoscalar)},$$

$${}^4\text{Eta}_{\text{minimum}} = \eta_{\text{minimum}} = \mathbf{a} + \mathbf{b} = 539.99 \text{ MeV (pseudoscalar)}.$$

The Eta' meson is an analog to Lithion-7

$$\text{Eta}' = \eta'(958) = \mathbf{3a} + \mathbf{b}' = 954.22 \text{ MeV (pseudoscalar)}.$$

We see that there are in existence the following mesonic nuclei ($\mathbf{a} + \mathbf{b}'$) and ($\mathbf{3a} + \mathbf{b}'$) – it suggests that there should also be ($\mathbf{2a} + \mathbf{b}'$). However, an atomic nucleus does not exist which has an atomic mass equal to 5.5. Such a mesonic nucleus can, however, exist in a bound state, for example inside a binary system of mesons

$$\mathbf{X}' = \rho = \mathbf{2a} + \mathbf{b}' = 751.71 \text{ MeV (vector)}.$$

2.20.2. The K kaons

The core of baryons is indestructible at high energies so particles that are created also at high energies must be created inside the baryonic core. Kaons, pions, or Higgs bosons all are produced inside the core. Therefore we do not have much choice – there is the \mathbf{X}^\pm , \mathbf{Y} , m_{FGL} , ΔE_{Core} , there can be the bare electron, $m_{\text{e,bare}}$, on the circular axis of the torus, and there is the four fermion symmetry associated with \mathbf{Y} ($4 m_{\text{e,bare}}$ or $\mathbf{Y} \approx 4 \mu^\pm$ so we can the μ^\pm muons).

Assume that the spin-1 charged kaon \mathbf{K}^\pm is a result of following interactions

$$\mathbf{K}^\pm = \mathbf{Y} + m_{\text{FGL}} + 4 m_{\text{e,bare}} + \{m_{\text{e,bare}} + \text{neutrino}\}_{\text{virtual}} = 493.708 \text{ MeV}. \quad (2.20.1)$$

The spin-1 neutral kaon \mathbf{K}^0 is created because the \mathbf{K}^\pm attaches the electromagnetic mass and a virtual pair

$$\mathbf{K}^0 = \mathbf{K}^\pm (1 + \alpha_{\text{em,high}}) + \{m_{\text{e,bare}} + \text{neutrino}\}_{\text{virtual}} = 497.579 \text{ MeV}. \quad (2.20.2)$$

Due to the strong interactions, the neutral kaon decays into two pions (the coupling constant is equal to 1) or due to the weak interactions to three pions. The condensate of the proton is about π times greater than the rest mass of the neutral pion so the coupling constant of the weak interactions of two pions is π^2 times smaller than for the proton. This means that the \mathbf{K}_L^0 kaons should live approximately $\pi^2 / \alpha_{\text{w(p)}} = 527$ times longer than the \mathbf{K}_S^0 .

2.20.3. The selected D and B mesons

If we divide the mass of the neutral kaon by the mass of the bound neutral pion, we obtain the factor $F_x = 3.6867$.

The composition of some D and B mesons is as follows (we neglect the virtual particles)

$$\mathbf{D}^\pm = (\mathbf{Y} + m_{\text{FGL}} + \Delta E_{\text{Core}}) F_x = 1868 \text{ MeV}, \quad (2.20.3)$$

$$\mathbf{D}_s^\pm = (\mathbf{Y} + \mu^\pm + \Delta\pi) F_x = 1970 \text{ MeV}, \quad (2.20.4)$$

$$B_s^0 = [K^0(497.58) + \eta'(954.22)] F_x = 5352 \text{ MeV}, \quad (2.20.5)$$

$$B_c^+ = [\rho(751.71) + \eta'(954.22)] F_x = 6289 \text{ MeV}. \quad (2.20.6)$$

2.21. Hyperons

The $d = 2$ state is the ground state outside the Schwarzschild surface for the strong interactions and is responsible for the structure of hyperons. During the transition of the W_d pion from the $d = 2$ state into $d = 4$, in the $d = 2$ state, some vector bosons occur as a result of decay of the W_d pions into two loops. Each loop has a mean energy equal to the E

$$E = (W_{(-),d=2} + W_{(o),d=2} - W_{(-),d=4} - W_{(o),d=4}) / 2 = 19.367 \text{ MeV}. \quad (2.21.1)$$

The vector bosons interact with the W_d pions in the $d = 2$ state. The mean relativistic energy, E_W , of these bosons is

$$E_W = E / \{1 - A / (A + 2 B)\}^{1/2} = 25.213 \text{ MeV}. \quad (2.21.2)$$

Groups of the vector bosons can contain d loops. Then in the $d = 2$ state there may occur particles that have mass which can be calculated using the following formula

$$M_{(+o),k,d=2} = W_{(+o),d=2} + \sum_{d=0,1,2,4}^{d < 2^k} d E_W, \quad (2.21.3)$$

where $k = 0, 1, 2, 3$, and the k and d determine the quantum state of the particle having a mass $M_{(+o),k,d}$.

The mass of a hyperon is equal to the sum of the mass of a nucleon and of the masses calculated from (2.21.3). We obtain good conformity with the experimental data assuming that hyperons contain the following particles (the values of the mass are in MeV)

$$\Lambda = n + M_{(o),k=0,d=2} = 1115.3, \quad (2.21.4)$$

$$\Sigma^+ = p + M_{(o),k=2,d=2} = 1189.6, \quad (2.21.5)$$

$$\Sigma^0 = n + M_{(o),k=2,d=2} = 1190.9, \quad (2.21.6)$$

$$\Sigma^- = n + M_{(-),k=2,d=2} = 1196.9, \quad (2.21.7)$$

$$\Xi^0 = \Lambda + M_{(o),k=1,d=2} = 1316.2, \quad (2.21.8)$$

$$\Xi^- = \Lambda + M_{(-),k=1,d=2} = 1322.2, \quad (2.21.9)$$

$$\Omega^- = \Xi^{-,0} + M_{(o-),k=3,d=2} = 1674.4. \quad (2.21.10)$$

Using the formulae (2.21.3)-(2.21.10) we can summarise that for the given hyperon the following selection rules are satisfied:

- a) each addend in the sum in (2.21.3) contains d vectorial bosons,
- b) for the $d = 2$ state the sum of the values of the k numbers is equal to one of the d numbers,

- c) the sum of the following three numbers i.e. of the sum of the values of the k numbers in the $d = 2$ state plus the number of particles denoted by $M_{(+o),k,d=2}$ plus one nucleon is equal to one of the d numbers,
- d) there can be only one object in the nucleon or hyperon having the mass $M_{(+o),k,d}$ for which the numbers k and d have the same values,
- e) there cannot be vector bosons in the $d = 1$ state because this state lies under the Schwarzschild surface and transitions from the $d = 1$ state to the $d = 2$ or $d = 4$ states are forbidden, so in the $d = 1$ state there can only be one W_d pion,
- f) the mean charge of the torus of the nucleon is positive so if the relativistic pions are not charged positively then electric repulsion does not take place – there is, however, one exception to this rule: in the $d = 1$ state there can be a positively charged pion because during that time the torus of the proton is uncharged,
- g) to eliminate electric repulsion between pions in the $d = 2$ state there cannot be two or more pions charged negatively,
- h) there cannot be a negatively charged W_d pion that does not interact with the vector boson in the $d = 2$ state in the proton because this particle and the W_d pion in the $d = 1$ state would annihilate,
- i) there cannot be a neutral pion in the $d = 2$ state in the proton because the exchange of the charged positively pion in the $d = 1$ state and of the neutral pion in the $d = 2$ state takes place. This means that the proton transforms itself into the neutron. Following such an exchange the positively charged pion in the $d = 2$ state is removed from the neutron because of the positively charged torus. Such a situation does not take place in the hyperon lambda $\Lambda = n W_{(o),d=2}$.

Using these rules we can conclude that the structure of hyperons strongly depends on the d numbers associated with the Titius-Bode law for strong interactions (i.e. with symmetrical decays) and on the interactions of electric charges.

The above selection rules lead to the conclusion that there are in existence only two nucleons and seven hyperons.

The spins of the vector bosons are oriented in accordance with the Hund law. The angular momentums and the spins of the objects having the mass $M_{(+o),k,d}$ are oriented in such a way that the total angular momentum of the hyperon has minimal value. All of the relativistic pions, which appear in the tunnels of nucleon, are in the S ($l = 0$) state. This means that hyperons Λ , Σ , and Ξ have half-integral spin, whereas Ω has a spin equal to $3/2$.

The strangeness of the hyperon is equal to the number of particles having the masses $M_{(+o),k,d=2}$ taken with the sign “–”.

Notice also that the percentages for the main channels of the decay of Λ and Σ^+ hyperons are close to the x , $1-x$, y , $1-y$ probabilities. This suggests that in a hyperon, before it decays, the $W_{(o),d=2}$ pion transits to the $d = 1$ state and during its decay the pion appears which was in the $d = 1$ state.

2.22. Selected resonances

The distance of mass between the resonances, and between the mass of the resonances and the hyperons or nucleons, are close to the mass of the S_d bosons.

The lightest resonance $\Delta(1236)$ consists of the nucleon and the S_d boson in the $d = 2$ state, i.e. the $\Delta(1236)$ consists of $S_{(+o),d=2}$ ($2-$) and of a proton or neutron ($1/2+$). Mean

mass calculated of all charge states i.e. ++, +, 0, −, equals 1236.8 MeV (the number before the signs "+" and "-" denotes the approximate value of angular momentum, whereas the "+" and "-" denotes the orientations of the angular momentum respectively "up" and "down").

The parity of the $S_{(o),d}$ pions is assumed to be negative, and the parity of the lambda hyperon is assumed to be positive. For selected resonances we have

$$\begin{aligned} N(2650) &= 3S_{(o),d=1}(2+2+2-) + 1S_{(o),d=2}(2+) + 1S_{(o),d=4}(1+) + [1p(1/2+) \text{ or } 1n(1/2+)] = \\ &= 2688 \text{ MeV } (J^P = 11/2^-), \quad (2.22.1) \end{aligned}$$

$$\Lambda(1520) = 1S_{(o),d=1}(2-) + \Lambda(1115)(1/2+) = 1537 \text{ MeV } (J^P = 3/2^-), \quad (2.22.2)$$

$$\begin{aligned} \Lambda(2100) &= 2S_{(o),d=1}(2+2+) + 1S_{(o),d=4}(1-) + \Lambda(1115)(1/2+) = \\ &= 2145 \text{ MeV } (J^P = 7/2^-), \quad (2.22.3) \end{aligned}$$

$$\begin{aligned} \Lambda(2350) &= 2S_{(o),d=1}(2+2+) + 2S_{(o),d=4}(1+1-) + \Lambda(1115)(1/2+) = \\ &= 2332 \text{ MeV } (J^P = 9/2^+), \quad (2.22.4) \end{aligned}$$

$$\begin{aligned} \Sigma(1765) &= 3S_{(o),d=4}(1-1-1-) + \Sigma(1192.5) \text{ (mean mass)} (1/2+) = \\ &= 1753 \text{ MeV } (J^P = 5/2^-), \quad (2.22.5) \end{aligned}$$

$$\begin{aligned} \Sigma(1915) &= 4S_{(o),d=4}(1+1+1+1-) + \Sigma(1192.5)(1/2+) = \\ &= 1940 \text{ MeV } (J^P = 5/2^+). \quad (2.22.6) \end{aligned}$$

2.23. Masses of quarks

Within the 3-valence-quarks model of baryons we cannot calculate simultaneously the precise mass and spin of proton whereas it is possible within the SST. Here we showed that the quark theory is not important at low energy. But, of course, the masses of quarks should follow from presented here the atom-like structure of baryons. Most important are the masses of the quark-antiquark pairs.

Mass of the up quark ($M_{\text{Quark-u}} = 2.23 \text{ MeV}$) is equal to the half of the mass distance between the two states of proton.

Mass of the down quark ($M_{\text{Quark-d}} = 4.89 \text{ MeV}$) is equal to the half of the mass distance between the two states of neutron.

Mass of the strange quark ($M_{\text{Quark-s}} = 87.86 \text{ MeV}$) should be associated with the mass of the relativistic $W_{(o),d=2} = 175.710 \text{ MeV}$ pion – this state is responsible for the masses of strange hyperons so mass of the strange quark is equal to the half of this mass.

To calculate masses of the three heaviest quarks we must derive some formula.

Quark is a loop or a condensate of it. We showed that a loop has 10 degrees of freedom. A hypervolume of the phase space and its total mass (the mass is in proportion to the

hypervolume), i.e. the mass of the quark-antiquark pairs created in collisions, must be in proportion to the radius of a gluon loop to the power of 10.

On the equator of the torus, there arise the gluon condensates which masses are the same as the calculated within the atom-like structure of baryons. Range of a condensate is r_{range} . Then, there is created a loop with radius $r_{\text{loop}} = r_{\text{range}} + A$. Mass of such a loop we can calculate from following formula

$$M_{\text{Loop}} [\text{GeV}] = a_q (r_{\text{Loop}} [\text{fm}])^{10} = a_q (r_{\text{range}} [\text{fm}] + A [\text{fm}])^{10}, \quad (2.23.1)$$

where a_q is a factor whereas $A = 0.6974425 \text{ fm}$ is the radius of the equator of the torus in the core of baryons. For $H^\pm = 0.7274387 \text{ GeV}$ we should obtain $r_{\text{loop}} = A$ so then $a_q = 26.71236 \text{ GeV/fm}^{10}$.

Knowing that range of a mass equal to $S_{(+),d=4} = 187.5744 \text{ MeV}$ is $4B_{\text{mean}} = 2.007333 \text{ fm}$, we can calculate range for a gluon condensate from formula

$$r_{\text{range}} [\text{fm}] = S_{(+),d=4} [\text{MeV}] 4B [\text{fm}] / m_{\text{condensate}} [\text{MeV}] = b_q / m_{\text{condensate}} [\text{MeV}], \quad (2.23.2)$$

where $m_{\text{condensate}}$ is the mass of a gluon condensate whereas $b_q = 376.52430 \text{ fm} \cdot \text{MeV}$.

We can rewrite formula (2.23.1) as follows

$$M_{\text{Loop}} [\text{GeV}] = a_q (b_q / m_{\text{condensate}} [\text{MeV}] + A [\text{fm}])^{10}. \quad (2.23.3)$$

Mass of gluon condensate equal to mass of the Upsilon $Y(1S, 9460 \text{ MeV})$ leads to the mass of the charm quark ($M_{\text{Quark-c}} = 1267 \text{ MeV}$).

Mass of a loop overlapping with the $d = 0$ orbit is 727.4387 MeV . Calculate mass of a condensate that is equal to mass of a loop overlapping with the last orbit, $d = 4$, on assumption that linear density is the same as for the loop overlapping with the $d = 0$ state. We obtain $m_{\text{condensate}} = 2821.105 \text{ MeV}$. Applying formula (2.23.3) we obtain mass of the bottom quark ($M_{\text{Quark-b}} = 4190.34 \text{ MeV}$).

Mass of gluon condensate equal to sum of masses of the torus inside the core of baryons ($X^\pm = 318.2955 \text{ MeV}$) and the condensate ($Y = 424.1217 \text{ MeV}$), i.e. $m_{\text{condensate}} = 742.42 \text{ MeV}$, leads to the mass of the top quark ($M_{\text{Quark-t}} = 171.9 \text{ GeV}$).

2.24. The PMNS neutrino-mixing matrix

Since the SST parameters and the SM parameters concerning the PMNS neutrino-mixing matrix are the same so the SM mimics the properties and weak interactions of neutrinos described in SST.

The mixing angles are defined as follows.

A. The first fundamental phenomenon in the early nuclear plasma was the production of the charged pion-antipion pairs $F_{\pi\pi} = (\pi^- \pi^+) = 279.14 \text{ MeV}$ and next their decays to, first of all, electron-neutrinos and tau-neutrinos (see the explanation below) with the characteristic energy $E_{\text{o,neutrino}} = m_{\text{FGL}} / 2 = 33.77221 \text{ MeV}$. The ratio of these masses can define the

A_{13} angle which is a powerful discriminator of the neutrino theory because it appears in all three SST definitions of the mixing angles. We obtain

$$A_{13} [^\circ] = F_{\pi\pi} / E_{o,\text{neutrino}} = 8.2654 . \quad (2.24.1)$$

Notice that value of the first mixing angle is close to the ratio of the masses of the lightest hyperon (i.e. hyperon Λ that decays due to the nuclear weak interactions) and lightest meson (i.e. the bound neutral pion): $\Lambda / \pi_{\text{bound}}^0 = 8.264$.

B. The second fundamental phenomenon in the early Universe was and is the four-neutrino symmetry (there are the four stable neutrinos) that can lead to the transition of four protons into atomic nucleus of helium-4. We can call such mixing angle the solar angle because it is associated with the solar neutrinos – it is the mixing angle A_{12} . We can define the solar mixing angle using formula

$$A_{12} [^\circ] = 4 A_{13} = 33.0616 . \quad (2.24.2)$$

C. The third fundamental phenomenon in the early Universe was creation of objects composed of three entangled neutrinos with different flavours – such objects were composed of 5 stable neutrinos (see the explanation below) so the mixing angle A_{23} we can define using formula

$$A_{23} [^\circ] = 5 A_{13} = 41.3270 . \quad (2.24.3)$$

Such angles lead to the 9 SST PMNS-matrix elements.

In SST, the nuclear weak interactions are associated with the poloidal motions of the torus/electric-charge in the core of baryons – such motions change the direction of the particles' motion to the opposite, so the phase shift is 180 degrees, i.e. $\delta_{\text{weak}} [^\circ] = 180$ i.e. $\exp(i \delta_{\text{weak}}) = -1$.

According to SST, the tremendous non-gravitating energy inside the four stable neutrinos (i.e. the electron-neutrino, muon-neutrino and their antiparticles) causes that they are indestructible in the present-day inner Cosmos.

The charged pions can decay as follows

$$\pi^+ \rightarrow e^+ + \nu_e + \nu_{\mu,\text{anti}} + \nu_{\mu} , \quad (2.24.4)$$

$$\pi^- \rightarrow e^- + \nu_{e,\text{anti}} + \nu_{\mu} + \nu_{\mu,\text{anti}} . \quad (2.24.5)$$

There is a possibility that the three neutrinos that appear in the decays of charged pions will be entangled and will carry half-integral spin. We claim that such objects composed of three entangled stable neutrinos are the tau-neutrinos

$$\nu_{\tau} \equiv \nu_e (\nu_{\mu,\text{anti}} \nu_{\mu}) , \quad (2.24.6)$$

$$\nu_{\tau,\text{anti}} \equiv \nu_{e,\text{anti}} (\nu_{\mu} \nu_{\mu,\text{anti}}) . \quad (2.24.7)$$

The pair of neutrinos in the parentheses has the total weak charge and total internal helicity both equal to zero so the tau-neutrinos behave as the electron-neutrinos with shifted mass (mass is three times greater).

We can see that there are three flavours of neutrinos ν_n , where $n = e, \mu, \tau$.

Rotating neutrinos shift the zero-point of the local zero-energy field and such “mass” can be measured because of the very small size of the rotating neutrino.

Maximum “mass” of rotating electron- or muon-neutrino can be close to the Planck mass

$$M_{\text{neutrino,max}} = h \nu / c^2 = \hbar / (r_{\text{neutrino}} c) = 3.1451 \cdot 10^{-8} \text{ kg} . \quad (2.24.8)$$

The CMB neutrinos should have the mean “mass” equal to the geometric mean of the mass of the non-rotating-spin neutrino and of $M_{\text{neutrino,max}}$

$$M_{\text{neutrino,CMB}} = (M_{\text{neutrino,max}} m_{\text{neutrino}})^{1/2} = 1.0241 \cdot 10^{-37} \text{ kg} = 0.05745 \text{ eV} . \quad (2.24.8)$$

The sum of the CMB masses of the three degenerate neutrinos with different flavours is

$$M_{3,\text{CMB}} = \sum_{n=e,\mu,\tau} M_n = 5 M_{\text{neutrino,CMB}} = 0.2873 \text{ eV} . \quad (2.24.9)$$

This value is consistent with the observational facts [9]: $0.320 \pm 0.081 \text{ eV}$.

2.25. The CKM quark-mixing matrix

Contrary to the Standard Model (SM) of particle physics, we can test the Scale-Symmetric Theory (SST) via the experimental values of the elements of the CKM matrix. It follows from the fact that values of such elements result from the atom-like structure of baryons described in SST. In SM, such values are the free parameters.

Since the SST parameters and the SM parameters concerning the CKM quark-mixing matrix are the same so the SM mimics the true description of structure and interactions of hadrons described within SST.

The masses of quarks and mixings of quarks have the origin in the SST. In SST, the three mixing angles are defined by ratios of masses of the three characteristic masses for the atom-like structure of baryons to the mass of the torus/electric-charge in the core of baryons $X^\pm = 318.2955 \text{ MeV}$ that is the source of the Titius-Bode orbits for the nuclear strong interactions. The masses are as follows. The first virtual mass $M_{\text{TB}} = 750.2975 \text{ MeV}$ is created on the equator of the core of baryons (the $d = 0$ state) – its symmetrical decays are responsible for creation of the TB orbits for the nuclear strong interactions. The second virtual mass $m_{\text{FGL}} = 67.54441 \text{ MeV}$ is the mass of the fundamental gluon loop (FGL) created on the circular axis inside the core of baryons – it is responsible for the strong interactions inside hadrons. Above we showed that the third virtual mass $M_{\text{Quark-b}} = 4190 \text{ MeV}$ is the mass of the b quark which is associated with the last TB orbit for the strong interactions.

The mixing angles are defined as follows

$$A_{12} [^\circ] = M_{\text{Quark-b}} / X^\pm = 13.164 , \quad (2.25.1)$$

$$A_{13} [^\circ] = m_{\text{FGL}} / X^\pm = 0.2122 , \quad (2.25.2)$$

$$A_{23} [^\circ] = M_{TB} / X^\pm = 2.3572 . \quad (2.25.3)$$

Emphasize that in the SST CKM matrix, we need only mass of the **b** quark that is derived within the atom-like structure of baryons – other properties of quarks are useless.

Such angles lead to the 9 SST CKM-matrix elements.

In SST, the nuclear weak interactions are associated with the poloidal motions of the torus/electric-charge in the core of baryons – such motions change the direction of the particles' motion to the opposite, so the phase shift is 180 degrees, i.e. $\delta_{\text{weak}} [^\circ] = 180$ i.e. $\exp(i\delta_{\text{weak}}) = -1$. The SST nuclear strong interactions are associated with the radial motions of the gluons so the phase shift is equal to zero degrees, i.e. $\delta_{\text{strong}} [^\circ] = 0$ i.e. $\exp(i\delta_{\text{strong}}) = +1$. The SST electromagnetic interactions are associated with the toroidal motions of the torus/electric-charge.

Knowing that the phase shift for the nuclear strong interactions is zero degrees and applying the mainstream definitions of the CKM elements, we can calculate two of them needed here

$$|V_{ub}| = \sin A_{13} = 0.0037036 , \quad (2.25.4)$$

and

$$|V_{cb}| = \sin A_{23} \cos A_{13} = 0.0411129 , \quad (2.25.5)$$

i.e. the ratio of them is

$$\hat{f}_{\text{high}} = [|V_{ub}| / |V_{cb}|]_{\text{high}} = 0.090048 . \quad (2.25.6)$$

This is the SST ratio for the high q^2 ranges because for such ranges, the nucleon-nucleon collisions cause the transitions of quanta from infinity, $R \rightarrow \infty$, onto the equator of the core of baryons with a radius of $A = 0.6974425 \text{ fm}$ (i.e. the $\infty \rightarrow A$ transition).

The SST theoretical result (2.25.6) is consistent with experimental data: 0.095(8) [10].

For lower-range transitions, the q^2 is lower so the ratio $|V_{ub}|/|V_{cb}|$ is lower too.

The radii of the TB orbits are defined by formula

$$R = A + d B_{\text{mean}} , \quad (2.25.7)$$

where $B_{\text{mean}} = 0.5018333 \text{ fm}$, and $d = 0, 1, 2$ and 4 .

Here we calculated the ratios \hat{f} for the low q^2 ranges (i.e. for $A + B \rightarrow A$) and for decays of the Λ_b^0 baryons (i.e. for $A + 4B \rightarrow A$).

The experimental results are as follows. For the low q^2 ranges we have 0.061(4) [10] and for the **b** hyperons is 0.079(6) [11].

The relativistic spin speeds on the TB orbits we can calculate from the boundary condition that on the equator of the core of baryons (the radius is A) the spin speed is c . From formula $v^2 = GM / R$ we obtain

$$v^2 / c^2 = A / (A + d B_{\text{mean}}) . \quad (2.25.8)$$

On the other hand, the relativistic mass we can calculate from the Einstein formula (see our derivation of formula (1.4.7))

$$M_{\text{Rel}} / M_0 = 1 / (1 - v^2 / c^2)^{1/2}. \quad (2.25.9)$$

In SST, the resultant ratio $f_{\text{Resultant}}$ is the product of $f_{\text{high}} = [|V_{\text{ub}}|/|V_{\text{cb}}|]_{\text{high}}$ and the ratio M_0/M_{Rel} so from (2.25.8) and (2.25.9) we have

$$f_{\text{Resultant}} = [|V_{\text{ub}}|/|V_{\text{cb}}|]_{\text{high}} [1 - A / (A + d B_{\text{mean}})]^{1/2}. \quad (2.25.10)$$

For the **high** q^2 ranges ($\infty \rightarrow A$) we have $d \rightarrow \infty$ so from (2.25.6) and (2.25.10) we have

$$f_{\text{Resultant,high}} = 0.090048. \quad \text{exp. } 0.095(8) \quad (2.25.11)$$

For the **low** q^2 ranges ($A + B_{\text{mean}} \rightarrow A$) we have $d = 1$ so from (2.25.10) we have

$$f_{\text{Resultant,low}} = 0.05825. \quad \text{exp. } 0.061(4) \quad (2.25.12)$$

It is consistent with experimental data [10].

The mass of the **b** quark relates to the $d = 4$ state so for such **b-hyperon** q^2 ranges ($A + 4B_{\text{mean}} \rightarrow A$) from (2.25.10) we have

$$f_{\text{Resultant,hyperon-b}} = 0.07757. \quad \text{exp. } 0.079(6) \quad (2.25.13)$$

The LHCb measurement using the baryons decays of Λ_b^0 gives the ratio $|V_{\text{ub}}|/|V_{\text{cb}}| = 0.079 \pm 0.006$ [10], [11].

The CKM matrix is for the baryons, for example, we can use it to describe decays of the hyperons. Decays of kaons and pions can give values that differ from the values in the SST CKM-matrix.

2.26. Larger structures

The saturation of interactions via the SST Higgs field and the four-particle symmetry lead to the larger structures.

For the single objects such as, for example, fermions, and for the binary systems, as for example, the neutrino-antineutrino pairs or binary systems of massive galaxies, there are obligatory following formulae for number of constituents, N , in bigger composite structures

$$N = 4^d \quad (\text{for single objects}), \quad (2.26.1)$$

$$N = 2 \cdot 4^d \quad (\text{for binary systems}), \quad (2.26.2)$$

where $d = 1, 2, 4, 8, 16, 32$ are the Titius-Bode numbers. Such structures follow from the quantum entanglement, i.e. they result from the exchanges of the superluminal entanglons. We can see that simplest composite objects can contain 4 or 8 constituents.

It is easy to calculate that from energy equal to the rest mass of a nucleon can be produced at the very most six neutral pions. The simplest neutral pion consists of four rotating and

spinning in two loops neutrinos (two gluon loops). We showed as well that each nucleon has two different mass states. Moreover, the spin-1 gluon loops behave in the nuclear strong fields as the spin-1/2 electrons in atoms. These remarks lead to following formula for upper limit for number of neutrinos in a neutral pion

$$N_{\text{maximum}} = 2 \cdot 4^{32}. \quad (2.26.3)$$

2.27. The ultimate equation

We can write the ultimate equation which ties the properties of the pieces of space, i.e. tachyons, with the all masses/sources responsible for the all types of interactions.

The ultimate equation looks as follows

$$4 \pi m_t \rho_t / (3 \eta_t) = (2 m_1 / \hbar)^2 (2 m_{\text{neutrino}} / \rho_{\text{As}})^{1/3} (m_{\text{e,bare}} / 2) c (X^\pm / H^\pm)^{1/2}. \quad (2.27.1)$$

The $4\pi/3$ on the left side of the ultimate equation shows that the tachyons are the balls. The mean mass of tachyons is the mean mass of the source of the fundamental interaction that follows from the direct collisions of tachyons and their viscosity which results from smoothness of their surface. The ρ_t is the mass density of the pieces of space, i.e. of the tachyons (it is not the inertial mass density of the Higgs field). The η_t is the dynamic viscosity of the pieces of space, i.e. of the tachyons.

The two masses of the closed strings (i.e. the entanglon – its total spin is \hbar) on the right side of the ultimate equation are the carriers of the quantum entanglement. The two masses of neutrinos, i.e. the neutrino-antineutrino pair, are the source of the gravitational field, of the directional quantum entanglement and of the volumetric confinement. The mass of single lightest neutrino is the smallest gravitational mass. In the equation, the smallest gravitational mass is multiplied by 2 that points that the non-rotating-spin neutrino-antineutrino pairs are the components of the ground state of the SST absolute spacetime (the ρ_{As} in the denominator is the mass density of the SST-As). The half of the mass of the bare electron is the mass of the electric charge i.e. of the mass of the source of the electromagnetic interaction, but it is also mass of the central condensate of the electron, which is responsible for the weak interactions of the electrons. The c is the speed of photons and gluons. The X^\pm is the mass of the torus/electric-charge inside the core of baryons in which the FGLs arise – they are responsible for the nuclear strong interactions inside baryons. The H^\pm is the mass of the charged core of baryons which is equal to $H^\pm = X^\pm + Y - \Delta E_{\text{Core}}$, where the Y is the source of the nuclear weak interactions of the baryons.

The left and right side of the ultimate equation is $6.97611592430938 \cdot 10^{-159} \text{ kg s/m}^2$.

2.28. Turning points in the formulation of the Scale-Symmetric Theory

In 1976, I noticed that the following formula describes how to calculate the mass of a hyperon

$$m [\text{MeV}] = 939 + 176 n + 26 (d - 1), \quad (2.28.1)$$

where $n = 0, 1, 2, 3$, and $d = 1, 2, 4, 8$ are the Titius-Bode numbers.

For a nucleon it is $n = 0$ and $d = 1$ which gives 939 MeV . For hyperon Λ is $n = 1$ and $d = 1$ which gives 1115 MeV . For hyperons Σ is $n = 1$ and $d = 4$ which gives 1193 MeV .

For hyperons Ξ is $n = 2$ and $d = 2$ which gives **1317 MeV**. For hyperon Ω is $n = 3$ and $d = 8$ which gives **1649 MeV**.

I also noticed that the mass distances between the resonances and mass distances between the resonances and hyperons is approximately **200 MeV**, **300 MeV**, **400 MeV**, and **700 MeV**.

In 1985, I grasped that in order to obtain positive theoretical results for hadrons, we should assume that outside the core of a nucleon is in force the Titius-Bode law for nuclear strong interactions. On orbits are relativistic pions.

The year 1997 was the most productive for me because I described the phase transitions of the SST Higgs field. In this eventful year, I practically formulated new particle physics and new cosmology.

2.29. Summary

Both quantum mechanics and general relativity are highly incomplete theories due to the internal structure and interactions of fundamental particles and larger systems.

Moreover, these theories are partially based on incorrect initial conditions. Namely, the speed of light c is invariant only in relation to the object with which the photons are entangled, while the concept of many worlds is erroneous due to the superluminal quantum entanglement.

The SST absolute spacetime consist of the neutrino-antineutrino pairs. The electromagnetic, weak and strong interactions are directly associated with excitations of the SST-As. On the other hand, the neutrinos produce gradients/gravitational-fields in the superluminal SST Higgs field. From (2.1.26) follows that the constants of interactions G_i are directly proportional to densities of fields so the gravitational constant G is tens of orders of magnitude lower than the constants of interactions for electromagnetic, weak and strong interactions. Moreover, properties of the SST-As and SST-Hf are very different so unification of the four mentioned interactions within the same methods is impossible. We also emphasize that the waves wrongly called “gravitational waves” in mainstream physics are actually flows in the SST absolute spacetime.

The ratio of the superluminal energy of the entanglons frozen inside each neutrino in the SST-As spacetime to gravitational energy of the neutrino is $\sim 0.6 \cdot 10^{119}$ (see (2.3.3)). On the other hand, quantum mechanics predicts that the zero-point energy from virtual particles (the summation of energies of the virtual photons stops at the Planck length) is some 120 powers of ten more than the measured value of the zero-point energy (the dark energy). We can see that the considerations in quantum mechanics are not based on facts. SST shows that, generally, the zero-point energy is frozen in neutrinos – there is not a tremendous energy associated with virtual photons unless we will call the entanglons the dark photons. Just during interactions, due to the quantum entanglement and/or confinement, there are created virtual particles but their total energy is infinitesimal in comparison with the superluminal energy frozen inside the neutrinos. Practically the “zero-energy” field is very cold for an observer. Notice that the maximum value of the coupling constant for the strong interactions is for cold atomic nuclei – it is ~ 14.4 so then the total involved zero-point energy is $0.6 \cdot 10^{119} \cdot 14.4 \approx 0.9 \cdot 10^{120}$.

Within the Scale-Symmetric Theory we predict existence of new scalar boson and/or vector boson with a mass of **17.1 – 17.2 TeV** that results from structure of the core of baryons and density of the SST absolute spacetime (see Section **2.15**).

2.30. Tables

Table 5 *Theoretical results*

Physical quantity	Theoretical value*
Gravitational constant	6.6740007 E-11 m ³ /(kg s ²)
Unitary spin	1.05457154835 E-34 Js
Speed of light	2.99792458 E+8 m/s
Electric charge	1.60217643101205 E-19 C
F (kg \leftrightarrow MeV)	1.78266169577332 E-30
Mass of electron	0.51099880(49) MeV
Fine-structure constant for low energies	1/137.035998889
Mass of bound neutral pion	134.96608045 MeV
Mass of charged pion	139.57040(14) MeV
Mass of free neutral pion	134.97672(13) MeV 134.97668(13) MeV
Mass distance $\pi^{\pm} - \pi^0$	4.5936852(44) MeV 4.5937234(44) MeV
Radius of closed string	0.944240446 E-45 m
Linear speed of closed string	0.726925275 E+68 m/s
Mass of closed string	2.340078419 E-87 kg
External radius of neutrino	1.1184554825 E-35 m
Mass of neutrino	3.3349241 E-67 kg
Mass of core of Protoworld and superluminal energy frozen inside lightest neutrino	1.9607584(19) E+52 kg
External radius of core of Protoworld	286.66348 E+6 light-years
Baryonic mass of the Universe	3.637912 E+51 kg
Radius of the early Universe loop	191.10899 E+6 light-years
External radius of torus of nucleon	0.697442473 fm
Constant K	0.7896685548 E+10
Mass of FGL	67.544410(65) MeV
Mass of torus of core of baryons	318.29553(31) MeV
Mass of condensate of the nucleon	424.12174(41) MeV
Range of weak interactions of the proton	8.7110239711 E-18 m
Binding energy of core of baryons	14.978575(15) MeV
Mass of charged core of baryons	727.4387032 MeV
Ratio of mass of the core of baryons to mass of FGL	10.769783932
Dark-matter/baryonic-matter ratio $\equiv H^{\pm} / \pi^0_{\text{bound}}$	5.38979
Mass of muon	105.65837503 MeV
A/B _{mean} in the Titius-Bode law for strong interactions	1.389789055
Mass of proton	938.27188(90) MeV
Mass of free neutron	939.56580(90) MeV
Proton magnetic moment in nuclear magneton	+2.793595
Neutron magnetic moment in nuclear magneton	-1.913406

*E-15=10⁻¹⁵

Table 6 *Theoretical results*

Physical quantity	Theoretical value
Radius of last tunnel for strong interactions	2.704776 fm
Mean square charge for nucleon	0.29
Mean square charge for proton	0.25
Mean square charge for neutron	0.33
Mass of the dark-matter loop	2.0795801 E-47 kg 1.1665590 E-11 eV
Mass of the dark-matter torus	727.4387032 MeV
External radius of torus of electron	386.6071393 fm
Range of weak interactions of electron	0.73541849146 E-18 m
Weak constant	1.0355025 E+27 m ³ /(kg s ²)
Electromagnetic constant for electrons	2.7802538 E+32 m ³ /(kg s ²)
Coupling constant for weak interactions of the proton	0.01872290929
Coupling constant for electron-proton weak interaction	1.1194460558 E-5
Coupling constant for electron-muon weak interaction	0.9511186121 E-6
Coupling constant for strong-weak interactions inside the baryons	d=0: 0.993813 d=1: 0.762596 d=2: 0.640307 d=4: 0.507795
M _{TB} responsible for creation of the TB orbits	750.2975256 MeV
Ratio of the hidden energy to mass of the neutrino	0.59 E+119
Range of confinement	3510.1803464 r _{neutrino}
Electron radius of proton	0.87701081 fm
Muon radius of proton	0.84038927 fm

Table 7 *Lifetimes*

Physical quantity	Theoretical value
* p	Stable
* n	876.34 s
* n (beam)	888.80 s
* μ [±]	2.194937 E-6 s
* tauon	2.6972 E-13 s
* π [±]	2.797 E-8 s
* π ⁰	0.793 E-16 s
* hyperons (mean)	1.115022 E-10 s
* H	1.99 E-25 s
* W [±]	3.10 E-25 s
* Z ⁰	2.73 E-25 s

Table 8 *Values of the G_i*

Interaction	Relative value of the G_i
Strong	1 (for $G_S=5.45651 \cdot 10^{29} \text{ m}^3 \text{ s}^{-2} \text{ kg}^{-1}$)
Weak	$1.9 \cdot 10^{-3}$
Electromagnetic interaction of electrons	$5.1 \cdot 10^2$ (it is not a mistake)
Gravitational	$1.2 \cdot 10^{-40}$
XXXXXXXXXXXXXXXXXXXX	XXXXXXX
Coupling constant for strong interactions inside baryons and mesons at low energy	1
Coupling constant for strong interactions of nucleons at low energy	14.391185

Table 9 *New electroweak theory*

Physical quantity	Theoretical value
Electron magnetic moment in the Bohr magneton	1.00115965217649
Muon magnetic moment in the muon magneton	1.00116592150
Frequency of the spin-flip transition in hydrogen atom	1420.4060(14) MHz
Lamb-Retherford Shift	1057.8384 MHz 1058.0789 MHz

Table 10 *Mesons*

Physical quantity	Theoretical value Mass
* H Higgs boson	125.00638(12) GeV
* W^\pm	80.379479(77) GeV
* Z^0	91.179756(87) GeV
* K^\pm	493.708 MeV
* K^0	497.579 MeV
Ratio of lifetimes K_L^0 / K_S^0	527
* Y(1S)	9464.92 MeV
* η	549.20 MeV
* $\eta'(958)$	954.22 MeV
* D^\pm	1868 MeV
* D_s^\pm	1970 MeV
* B_s^0	5352 MeV
* B_c^+	6289 MeV
Predicted particle	17.1 – 17.2 TeV

Table 11 *Hyperons and resonances*

Particle	Theoretical value Mass	Theoretical value		
		J	P	S
Hyperon Λ	1115.3 MeV	1/2	+1*	-1
Hyperon Σ^+	1189.6 MeV	1/2	+1	-1
Hyperon Σ^0	1190.9 MeV	1/2	+1	-1
Hyperon Σ^-	1196.9 MeV	1/2	+1	-1
Hyperon Ξ^0	1316.2 MeV	1/2	+1	-2
Hyperon Ξ^-	1322.2 MeV	1/2	+1	-2
Hyperon Ω^-	1674.4 MeV	3/2	+1	-3
Resonance $\Delta(1232)$	1236.8 MeV	3/2	+1	
Resonance N(2650)	2688 MeV	11/2	-1	
Resonance $\Lambda(1520)$	1537 MeV	3/2	-1	
Resonance $\Lambda(2100)$	2145 MeV	7/2	-1	
Resonance $\Lambda(2350)$	2332 MeV	9/2	+1	
Resonance $\Sigma(1765)$	1753 MeV	5/2	-1	
Resonance $\Sigma(1915)$	1940 MeV	5/2	+1	

*Assumed positive parity

Table 12 *Masses of quarks*

Physical quantity	Theoretical value
Up	2.23 MeV
Down	4.89 MeV
Strange	87.86 MeV
Charm	1267 MeV
Bottom	4190.34 MeV
Top	171.9 GeV

Table 13 *PMNS matrix and CKM matrix*

Physical quantity	Theoretical value
PMNS A_{12} [$^\circ$]	33.0616
PMNS A_{13} [$^\circ$]	8.2654
PMNS A_{23} [$^\circ$]	41.3270
PMNS phase shift δ [$^\circ$]	180
CKM A_{12} [$^\circ$]	13.164
CKM A_{13} [$^\circ$]	0.2122
CKM A_{23} [$^\circ$]	2.3572
CKM phase shift δ [$^\circ$]	0

References

- [1] Ramsey N. F. (1990).
Rev. Mod. Phys. **62** 541
- [2] G. W. Bennett, *et al.* (21 February 2004). “Measurement of the Negative Muon Anomalous Magnetic Moment to 0.7 ppm”
arXiv:hep-ex/0401008v3
G. W. Bennett, *et al.* (7 April 2006). “Final report of the E821 muon anomalous magnetic moment measurement at BNL”
Phys. Rev. D **73**, 072003
- [3] T. Aoyama, *et al.* (3 December 2020). “The anomalous magnetic moment of the muon in the Standard Model”
Physics Reports, Volume 887, 3 December 2020, Pages 1-166
- [4] K. A. Olive *et al.* (Particle Data Group),
Chin. Phys. **C38**, 090001 (2014)
<http://pdg.lbl.gov>
- [5] H el ene Fleurbaey, *et al.* (26 January 2018). “New Measurement of the 1S-3S Transition Frequency of Hydrogen: Contribution to the Proton Charge Radius Puzzle”
Phys. Rev. Lett. **120** (2018) 18, 183001
arXiv:1801.08816 [physics.atom-ph]
- [6] Ingo Sick (5 January 2018). “Proton charge radius from electron scattering”
arXiv:1801.01746 [nucl-ex]
- [7] Aldo Antognini, *et al.* (25 January 2013). “Proton Structure from the Measurement of 2S – 2P Transition Frequency of Muonic Hydrogen”
Science Vol. **339**, Issue 6118, pp. 417-420
- [8] N. Bezginov, *et al.* (7 September 2019). “A measurement of the atomic hydrogen Lamb shift and the proton charge radius”
Science Vol. **365** (2019) 6457, 1007-1012
- [9] Richard A. Battye and Adam Moss (6 February 2014). “Evidence for Massive Neutrinos from Cosmic Microwave Background and Lensing Observations”
Phys. Rev. Lett. **112**, 051303
- [10] LHCb Collaboration (9 December 2020). “First observation of the decay $B_s^0 \rightarrow K^- \mu^+ \nu_\mu$ and measurement of $|V_{ub}|/|V_{cb}|$ ”
arXiv:2012.05143 [hep-ex]
- [11] Heavy Flavor Averaging Group, Y. Amhis *et al.* (1 November 2019). “Averages of b-hadron, c-hadron, and τ -lepton properties as of 2018”
arXiv:1909.12524v2, updated results and plots available at <https://hflav.web.cern.ch>

Chapter 3

Cosmology

3.1. Introduction to the SST cosmology and abundances of baryonic matter (BM), dark matter (DM) and dark energy (DE)	74
3.2. Inflation, universes and radius of the inner Cosmos (i.e. of the SST absolute spacetime)	76
3.3. Neutron black holes (NBHs)	77
3.4. The large-scale structure of the very early Universe	79
3.5. The correct age of the Universe, Hubble constants and CMB	80
3.6. The origin of CMB power spectrum	83
3.7. Initial evolution of the expanding Universe	87
3.8. The standard ruler in cosmology	87
3.9. Black body spectrum	87
3.10. The hydrogen-to-helium-4 ratio in the expanding Universe	88
3.11. Summary	89
3.12. Tables	90
References	91

3.1. Introduction to the SST cosmology and abundances of baryonic matter (BM), dark matter (DM) and dark energy (DE)

In Chapter 2 we showed that the two-component spacetime (i.e. the SST Higgs field (SST-Hf) and the SST absolute spacetime (SST-As)) leads to a very simple and accurate description of particles. Properties of the two components are very different so unification of GR (gravitational fields are the gradients in the SST-Hf produced by neutrinos) and QM (we showed that the electrically charged leptons, the photons, gluons and hadrons are the excited states of the SST-As) within the same methods is impossible.

We showed also that the gravitational constant G is directly proportional to density of the SST-Hf. If both components of spacetime were free to expand, due to the enormous speed of the SST tachyons, the value of the G would change rapidly. The conclusion is simple, namely dark energy can expand while our two-component spacetime should be infinite or should have a solid boundary.

But endless and symmetrical spacetime does not lead to the observed matter-antimatter asymmetry. **So we assume that our inner Cosmos is the result of a collision of an asymmetric inflation field (i.e. with the left-handed external helicity) with a much larger cosmological object – this has led to the creation of the asymmetric inner Cosmos inside this larger cosmological object.** In the next Section, we calculated the radius of the inner Cosmos and we showed why it has a spherical symmetry.

Mainstream cosmology based on general relativity also has a big problem with the recession velocities v/c (more precisely we should call it the relative recession velocities) of galaxies in relation to their observed redshift z . When we neglect the peculiar velocity which is sensitive to the matter distribution, then the kinematic Doppler shift expression (KDSE) obtained within the Special Theory of Relativity (SR) for a motion in the line of sight looks as follows [1]

$$v / c = (z^2 + 2 z) / (z^2 + 2 z + 2) . \quad (3.1.1)$$

Intuition tells us that for the observed redshift of $z = 1$, the recession velocity should be 1 and this should be the maximum recession velocity in the Cosmos with a solid boundary. But in the distant Universe we see galaxies with $z > 1$. Why? Why from formula (3.1.1), for $z = 1$ is $v/c = 0.6$?

In SST there are galaxies with $v > c$ because at the beginning of the expansion of the Universe, the very high dynamic pressure and superfluidity of the SST absolute spacetime have contributed to the formation of superluminal protuberances in the SST-As, which accelerated the protogalaxies to superluminal speeds. We can observe today such protogalaxies because the superluminal protuberances were damped so their today recession velocities are below 1. The speed c is the speed of photons in relation to the object with which they are entangled so we can emphasize that we measure the redshift that directly follows from the speed of photons they had in relation to the Earth when they were emitted, i.e. we measure $z > 1$. It is the reason that GR incorrectly describes the expansion of the Universe. A change in radial velocity of a galaxy in relation to the Earth (for example, due to the reduction in superluminal speed relative to the Earth) causes the same change in velocities of photons entangled with such galaxy but the measured redshift is invariant, i.e. it does not depend on the change. Moreover, we will show that when we neglect the initial protuberances in the expanding Universe then the recession velocity on the surface/front of the expanding baryonic matter is $v_{\text{front,BM}}/c = 0.6469$, i.e. it is close to the $v/c = 0.6$ we obtain from (3.1.1).

Presented here cosmology is based on the assumption that the cosmological inflation was separated in time from the expansion of our Universe which is immersed in the inner Cosmos. The gravitational interaction and phase transitions described in Chapter 2 make our Universe cyclical and in the stage of its highest average density it is similar to the neutron, so we can use the calculations that concern it. We showed that the core of the Protoworld (the cosmological torus with central condensate) was composed of the entangled dark-matter (DM) tori. The baryonic part of the Universe appeared on the circular axis of the cosmological torus as the two cosmological loops composed of protogalaxies each built of the neutron black holes (NBHs) – it was like creating the bound neutral pion in the core of baryons.

Initially, the Protoworld was the SST gravitational black hole, i.e. on the equator of the Protoworld the spin speed was equal to c . The calculated mass of the DM-core of the Protoworld is (see (2.1.24))

$$H^+_{\text{Protoworld,DM}} = 1.96076 \cdot 10^{52} \text{ kg} . \quad (3.1.2)$$

Baryonic mass of the Universe relates to the mass of the bound neutral pion

$$M_{\text{BM}} = H^+_{\text{Protoworld,DM}} \pi^0_{\text{bound}} / H^+ = 0.363791 \cdot 10^{52} \text{ kg} . \quad (3.1.3)$$

The ratio of the dark matter to baryonic matter, $N_{\text{DM/BM}}$, is

$$N_{\text{DM/BM}} = H^+_{\text{Protoworld,DM}} / M_{\text{BM}} = 5.38979 . \quad (3.1.4)$$

In the $d = 1$ state of the Protoworld (i.e. $R = A_{\text{Protoworld}} + B_{\text{Protoworld}}$, where $A_{\text{Protoworld}} = 286.663 \text{ Mly}$ (see (2.1.25)), and $A_{\text{Protoworld}} / B_{\text{Protoworld}} = 1.38979$ (see 2.5.8)) there were the entangled photons and neutrinos with a total mass equal to

$$W_{(-),d=1,\text{Protoworld}} = H^+_{\text{Protoworld,DM}} W_{(-),d=1} / H^+ = 0.581569 \cdot 10^{52} \text{ kg} . \quad (3.1.5)$$

The total mass of the Protoworld was

$$M_{\text{Protoworld}} = H^+_{\text{Protoworld,DM}} + W_{(-),d=1,\text{Protoworld}} = 2.54233 \cdot 10^{52} \text{ kg} . \quad (3.1.6)$$

Dark energy segments were building blocks of dark matter – such transformation happened at the end of the SST inflation.

The Protoworld created virtual field, i.e. there was the positive mass of the virtual particle-antiparticle pairs equal to the mass of the Protoworld and there was the negative mass of the virtual holes created in the SST-As which absolute value was also equal to the mass of the Protoworld. We see that the total positive mass was two times higher than the mass of the Protoworld and such a mass of dark energy initially has been pushed out of the Protoworld.

In Chapter 2, we showed that the superluminal energy frozen inside the lightest neutrino is equal to the mass of the core of the Protoworld so a new lightest neutrino created in the Protoworld stole entanglons exchanged among other entangled particles, so the Protoworld decayed and the inflows of dark matter and dark energy into the baryonic part of the very early Universe forced the exit of the Universe from the black-hole state. From that moment on, we count the age of the Universe.

The decay of the Universe caused the dark energy with a mass twice that of the Protoworld to flow into its interior

$$M_{DE} = 2 M_{Protoworld} = 5.08466 \cdot 10^{52} \text{ kg} . \quad (3.1.7)$$

Now we can calculate the abundances of matter and energy just before the expansion of the Universe

$$\begin{aligned} & \text{BM} : \text{DM} : (\text{photons} + \text{neutrinos}) = \\ & = M_{BM} : H^+_{Protoworld,DM} : W_{(-),d=1,Protoworld} = \\ & = 12.52\% : 67.47\% : 20.01\% , \end{aligned} \quad (3.1.8)$$

and the abundance today

$$\begin{aligned} & \text{BM} : \text{DM} : \text{DE} = \\ & = M_{BM} : H^+_{Protoworld,DM} : M_{DE} = \\ & = 4.91\% : 26.46\% : 68.63\% . \end{aligned} \quad (3.1.9)$$

3.2. Inflation, universes and radius of the inner Cosmos (i.e. of the SST absolute spacetime)

During the SST inflation, due to the creations of entanglons (we described it by using the classical thermodynamics), due to the saturation symmetry, invariant surface-density symmetry, and the adoption symmetry, the inflation field transformed into the SST spacetime – such processes are described in Chapter 2. The inertia of the expanding in a superluminal way SST-As caused that after a very short period, on the surface of the expanding SST-As, the gravitational pressure inserted on a single neutrino had become higher than the dynamic pressure that was the cause of the expansion of the transforming inflation field. Compressive forces acting on the outer layer of the SST-As created a stable boundary of the inner-Cosmos/SST-As with spherical symmetry – it is placed inside the bigger cosmological object so there are two boundaries. Moreover, this compression produced a shockwave in which baryons and antibaryons, dark energy and dark matter were produced. The initial inflation field had a left-handed external helicity which was converted to the left-handed internal helicity of the tori/electric-charges in the cores of baryons – notice that the tori/electric-charges in antibaryons have right-handed internal helicity. Left-handedness led to the matter-antimatter asymmetry. Why did this asymmetry not appear in the production of neutrinos during the inflation? The reason was the enormous energy frozen inside the neutrinos, which made it impossible to break the symmetry.

The baryonic shockwave, which was moving towards the centre of the inner Cosmos, produced universes with spin speed equal to c on their equators, so they are closed universes, but matter and energy can move within them.

We can calculate radius of the SST absolute spacetime from the condition that gravitational pressure inserted on a single neutrino on surface of the spacetime cannot be higher than the dynamic pressure inside it.

The effective radius of a single lightest neutrino is $R_{\text{Confinement,Neutrino}} = 3.92598 \cdot 10^{-32} \text{ m}$ (see (2.14.1)). The gravitational force acts on area that is the cross-section so the gravitational pressure, p_{gr} , is (we neglect the baryonic mass of the inner Cosmos in comparison with the mass of the SST-As)

$$\begin{aligned} p_{\text{gr}} &= F_{\text{gr}} / S_{\text{eff}} = (G M_{\text{Cosmos}} m_{\text{neutrino}} / R_{\text{Cosmos}}^2) / (\pi R_{\text{Confinement,Neutrino}}^2) = \\ &= 4 G \pi \rho_{\text{As}} R_{\text{Cosmos}} m_{\text{neutrino}} / (3 \pi R_{\text{Confinement,Neutrino}}^2). \end{aligned} \quad (3.2.1)$$

On the other hand, the dynamic pressure of the SST-As, $p_{\text{dyn-As}}$, is

$$p_{\text{dyn-As}} = \rho_{\text{As}} c^2 / 2. \quad (3.2.2)$$

From equality of the pressures we obtain

$$R_{\text{Cosmos}} = 3 R_{\text{Confinement,Neutrino}}^2 c^2 / (8 G m_{\text{neutrino}}) = 2.334 \cdot 10^{30} \text{ m}. \quad (3.2.3)$$

Total mass of the SST-As in the inner Cosmos is

$$M_{\text{Cosmos}} = 4 \pi \rho_{\text{As}} R_{\text{Cosmos}}^3 / 3 = 5.870 \cdot 10^{119} \text{ kg}. \quad (3.2.4)$$

We can as well calculate the initial radius of the inflation field (i.e. of the field in which the tachyons were packed to maximum), R_{initial} , from which the SST spacetime was created (notice that in reality the radius was much bigger because there was created also the boundary)

$$R_{\text{initial}} = \{3 M_{\text{Cosmos}} / (4 \pi \rho_t)\}^{1/3} = 1.19 \cdot 10^{11} \text{ m}. \quad (3.2.5)$$

This radius is close to the radius of the orbit of the Venus.

3.3. Neutron black holes (NBHs)

We claim that the baryonic part of the Universe was created on the circular axis in the core of the Protoworld – there were two loops (it was an analog to the two gluon loops in neutral pion) composed of protogalaxies already grouped in bigger structures each composed of the NBHs – it causes that we need a theory of NBHs.

We claim that besides a very thin iron crust and very thin layer of nuclear plasma on surface of each neutron star (which we neglect in our calculations), the neutron lattice is composed of cubes with neutrons in their vertices (see Fig.12). Such neutron lattice is the very stable object because of the strong interactions also between pairs of neutrons located at the ends of diagonals of the side walls of the cubes. The length of the diagonals is equal to the effective range, $R_{\text{eff,NS}}$, of the neutron matter which in SST is equal to the radius of the last TB orbit for the nuclear strong interactions

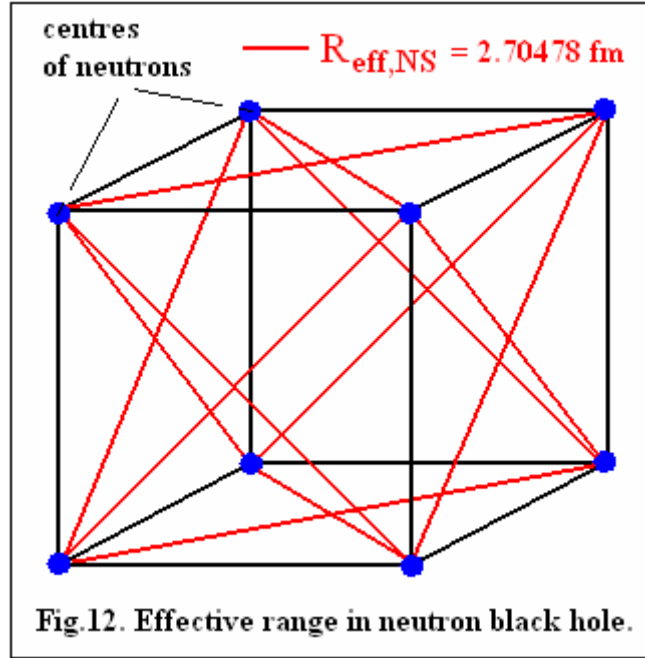
$$R_{\text{eff,NS}} = A + 4 B_{\text{mean}} = 2.70478 \text{ fm}. \quad (3.3.1)$$

This value is consistent with the mainstream value (~ 2.7 fm) [2] but due to the distribution of the neutrons, we get a different density of neutron matter ρ_{NS} . Our value, contrary to the mainstream values, is invariant

$$\rho_{\text{NS}} = n F / (\mathbf{R}_{\text{eff,NS}} / 2^{1/2})^3 = 2.39412 \cdot 10^{17} \text{ kg/m}^3, \quad (3.3.2)$$

where $n = 939.56580(90) \text{ MeV}$ is the mass of neutron (see (2.7.3)).

Why is the effective range $\mathbf{R}_{\text{eff,NS}}$ equal to the length of the diagonal and not of the side of the cubes and why is it equal to the radius of the last orbit for the strong interactions of baryons? For diagonals smaller than $\sim 2.7 \text{ fm}$ (there can be $\sim 1.7 \text{ fm}$, $\sim 1.2 \text{ fm}$, or $\sim 0.7 \text{ fm}$), the tori in the cores of baryons, which due to the very strong short-distance quantum entanglement cannot be destroyed (the half-integral spin and electric charge of such tori are conserved), partially overlap, which, because of the very high surface density of the tori, is forbidden. On the other hand, a cube with the side equal to $\mathbf{R}_{\text{eff,NS}}$ is not in its ground state.



The upper limit for mass, $M_{\text{NS,upper}}$, and radius, $R_{\text{NS,upper}}$, of neutron stars (NSs) we obtain from the boundary condition that spin speed on equator of NS should be equal to c . We have two equations

$$R_{\text{NS,upper}} = G M_{\text{NS,upper}} / c^2 \quad (3.3.3)$$

$$M_{\text{NS,upper}} = \rho_{\text{NS}} 4 \pi R_{\text{NS,upper}}^3 / 3, \quad (3.3.4)$$

which lead to following values

$$R_{\text{NS,upper}} = 36.64 \text{ km}, \quad (3.3.5)$$

$$M_{\text{NS,upper}} = 24.81 \text{ solar masses}. \quad (3.3.6)$$

Such a biggest neutron star we call “the neutron black hole (NBH)” because its equatorial spin speed is equal to c .

The binding energy of neutrons in neutron stars that follows from the nuclear strong interactions, due to the very short time of interactions ($\sim 10^{-23}$ s), is frozen inside the neutron star so there is no need to take it into account in calculations of NS mass.

But why can we also neglect the gravitational potential binding energy?

For example, let’s calculate the gravitational potential binding energy of a neutron, ΔE_g , located at the surface of the neutron black hole

$$\Delta E_g = -G M_{NS,upper} n F / R_{NS,upper} = -F n c^2 = -939.566 \text{ MeV} . \quad (3.3.7)$$

This value suggests that such neutron behaves as a virtual neutron because the sum of its mass and binding energy is equal to zero. So, do we really have to consider the change in mass due to gravitational interaction? Well, no, and this is due to phenomena occurring in the SST absolute spacetime.

When a star collapses into a neutron star or neutron stars collide, potential gravitational energy must be emitted, and this is due to the divergent flows in the SST-As, which the external observer observes as ripples in the SST-As. But due to the tremendous dynamic pressure in SST-As ($\sim 5 \cdot 10^{44}$ Pa), a reverse flow occurs that restores the initial state of local SST-As. Thus, it is the dynamic pressure in SST-As that means that we do not have to take into account the gravitational potential binding energy in the calculations of the mass of a neutron star.

We can say that neutrons in NBHs exchange virtual quanta composed of the SST-As components which are a part of the zero-energy field.

The colliding NSs with a total mass less or equal to 24.81 solar masses can merge into single neutron star, while NBHs cannot.

More massive black holes (BHs) consist of the NBHs and NSs.

The surface density of the torus in the core of baryons is about 300,000 times higher than in the SST-As – it causes that the moving cores try to drag the absolute spacetime. As a result the angular velocities of the NBH and of the SST-As inside NBH are the same so the NBH has always spherical symmetry and has not a relativistic mass resulting from its rotation.

3.4. The large-scale structure of the very early Universe

In Section 2.26, we showed that the four-object symmetry that follows from the superluminal quantum entanglement leads to following number of NBHs in groups of them or number of protogalaxies in larger structures: $N = 4^d$ for single objects, and $N = 2 \cdot 4^d$ for binary systems, where $d = 1, 2, 4, 8, 16, 32$ are the Titius-Bode numbers. We showed also that the upper limit for N is $N_{\text{maximum}} = 2 \cdot 4^{32}$.

Consider the binary systems of NBHs or protogalaxies. We have

$$N = 2 \cdot 4^d , \quad (3.4.1)$$

where $d = 0, 1, 2, 4, 8, 16$ is for a flattened spheroid-like structures, and $d = 3, 6, 12$ for a chain-like structures.

The cosmic structures composed of the binary systems of protogalaxies we will refer to as follows:

- $d = 0$ is for a binary system,
- $d = 1$ is for group,

$$\begin{aligned}
d = 2 & \text{ is for supergroup,} \\
d = 4 & \text{ is for cluster,} \\
d = 8 & \text{ is for supercluster,} \\
d = 16 & \text{ is for megacluster (the baryonic part of the Universe was the binary system} \\
& \text{of megaclusters composed of the binary systems of protogalaxies),} \\
d = 3 & \text{ is for chain,} \\
d = 6 & \text{ is for superchain,} \\
d = 12 & \text{ is for megachain.}
\end{aligned} \tag{3.4.2}$$

We can use formulae (3.4.1) and (3.3.6) to test the SST cosmology. Maximum number of NBHs in one cosmological loop can be $2 \cdot 4^{32}$ but the baryonic part of the early Universe was composed of two such loops so the total number of NBHs was 4^{33} . We can calculate mass of the two loops

$$M_{\text{baryonic}} = 4^{33} M_{\text{NS,upper}} = 0.3640 \cdot 10^{52} \text{ kg}. \tag{3.4.3}$$

This result is consistent with (3.1.3).

3.5. The correct age of the Universe, Hubble constants and CMB

Initially, the baryonic matter consisted of the neutrons placed in the NBHs but due to the decay of the Protoworld and the inflows of the dark matter and dark energy, it transformed into nuclear plasma. The most abundant ions were the hydrogen and helium-4 ions. It is very reasonable to assume that initially there was the equivalence in number density of nucleons in the two different ions.

When mean distance between the nucleons in baryonic plasma increased to the size of bare electrons, i.e. to $2\lambda_{\text{C,bare}}$ (from the Wien's displacement law follows that then temperature of the plasma was $3.748 \cdot 10^9 \text{ K}$), there appeared gas containing 50% of ionized hydrogen and 50% of ionized helium-4 by number of nucleons, i.e. there was 75% of the protons and 25% of the neutrons. The released energy per each initial neutron was (the mean binding energy of nucleon in helium-4 is 7.075 MeV [3] – it is calculated also within SST)

$$L_0 = 0.75 \cdot (n - p - m_e) + 0.5 \cdot 7.075 \text{ MeV} = 4.125 \text{ MeV}. \tag{3.5.1}$$

This energy leads to the CMB – the front of it was expanding with the radial speed equal to c .

The energy of the CMB is

$$E_{\text{CMB}} = M_{\text{BM}} L_0 c^2 / n = 1.435 \cdot 10^{66} \text{ J}. \tag{3.5.2}$$

We know that today the density of the energy of the CMB is equal to $\rho_{\text{CMB}} = 4.175(4) \cdot 10^{-14} \text{ J/m}^3$ [4]. By applying the following formula

$$4 \pi R_{\text{CMB}}^3 / 3 = E_{\text{CMB}} / \rho_{\text{CMB}} \tag{3.5.3}$$

we can calculate the radius of the sphere filled with CMB

$$R_{\text{CMB}} = 2.017 \cdot 10^{26} \text{ m, i.e. } 21.32(1) \text{ Gly} . \quad (3.5.4)$$

The front of CMB has the recession velocity equal to 1 so the correct age of the Universe is 21.32 Gyr, not the 13.8 Gyr! This means that the today spatial distance to the CMB front is 21.32 Gly.

In SST, due to the definition of the speed c , there are two different values of the Hubble constant, i.e. the spatial Hubble constant, $H_{\text{o,spatial}}$, and the time Hubble constant $H_{\text{o,time}}$ which depends on the time distance to the front of the baryonic matter.

The value from formula (3.5.4) leads to the spatial Hubble constant

$$H_{\text{o,spatial}} = c / R_{\text{CMB}} = 45.86 \text{ (km/s)/Mpc} . \quad (3.5.5)$$

To calculate the time Hubble constant notice that the Protoworld looked similar to the $H^+W_{(-),d=1}$ state of the neutron. The spin speed on the $d = 1$ TB orbit is $v_{\text{spin},d=1} = 0.7626c$ so the radial speeds, v_{rad} , of gluon/photon loops created on such orbit is

$$v_{\text{rad}} = (c^2 - v_{\text{spin},d=1}^2)^{1/2} = 0.6469c . \quad (3.5.6)$$

Such photon/gluon loops interacted with the baryonic matter so we can assume that the recession velocity of the front of the baryonic matter also is equal to 0.6469. This means that the time distance, $L_{\text{time,BM}}$, to the baryonic front is

$$L_{\text{time,BM}} = v_{\text{rad}} R_{\text{CMB}} / c = 13.79(1) \text{ Gly} . \quad (3.5.7)$$

From it we obtain the mean value of the time Hubble constant

$$H_{\text{o,time,MEAN}} = c / L_{\text{time,BM}} = 70.90 \text{ (km/s)/Mpc} . \quad (3.5.8)$$

The redshifts higher than $z > 0.6469$ are from the protuberances which with time were damped.

After the collapse of the Protoworld and the inflow of dark energy, the Universe transformed into an expanding cosmological ball filled with dark energy, dark matter, baryonic matter, neutrinos, photons and photon loops. Total mass/energy, M_{Total} , of it was (see formulae (3.1.3), (3.1.6) and (3.1.7))

$$M_{\text{Total}} = M_{\text{BM}} + M_{\text{Protoworld}} + M_{\text{DE}} = 0.7991 \cdot 10^{53} \text{ kg} . \quad (3.5.9)$$

Volume of the CMB is

$$V_{\text{CMB}} = 4 \pi R_{\text{CMB}}^3 / 3 = 3.437 \cdot 10^{79} \text{ m}^3 . \quad (3.5.10)$$

Today practically whole M_{Total} is inside a sphere with a spatial radius of 13.79 Gly so its total volume is

$$V_{\text{Matter-Energy}} = V_{\text{CMB}} (v_{\text{rad}} / c)^3 = 0.9304 \cdot 10^{79} \text{ m}^3 . \quad (3.5.11)$$

It means that the today critical density, ρ_c , is

$$\rho_c = M_{\text{Total}} / V_{\text{Matter-Energy}} = 8.5888 \cdot 10^{-27} \text{ kg/m}^3 . \quad (3.5.12)$$

In the mainstream cosmology, the H_0 is Hubble's constant that corresponds to the Hubble parameter, H , which is time dependent. From Friedmann equations for $\Lambda = k = 0$ we have

$$\rho_c = 3 H^2 / (8 \pi G) = 1.879 \cdot 10^{-26} h^2 \text{ kg/m}^3 , \quad (3.5.13)$$

where $h = H_0 / [100 \text{ (km/s)/Mpc}]$.

From (3.5.12) and (3.5.13) is

$$H_0 = 67.6 \text{ (km/s)/Mpc} . \quad (3.5.14)$$

Why there is a difference between (3.5.8) (the mean value is 70.9) and (3.5.14) (there is 67.6)? Energy density of photons in the initial cosmological ball was higher in its central parts and lower close to surface of it, i.e. pressure exerted by photons was higher in central parts. There some radial protuberances of the clusters of protogalaxies appeared to equalize the pressure in the initial cosmological ball. It caused the number density of the clusters in the centre to be slightly lower than at the surface of the ball. According to the SST, the Milky Way Galaxy should be near the centre of the expanding Universe, so the lower number density of clusters of galaxies is for the local Universe and the higher number density for the distant (earlier) Universe. The inner protuberances have made the Hubble constant for the local Universe higher, but that does not mean that the expansion of the Universe is accelerating – the mean time Hubble constant is **70.9 (km/s)/Mpc**.

We can roughly estimate the change of the Hubble parameter, ΔH , assuming that helium-4 (the binding energy per nucleon is about $\Delta E_{\text{Binding/N}} = 7.07 \text{ MeV}$) was created mainly in the central parts of the initial cosmological ball and that the squared relative change of the Hubble parameter is directly proportional to the excess energy density of the photons

$$\Delta H / H_0 = \{ \Delta E_{\text{Binding/N}} / 939 [\text{MeV}] \}^{1/2} = 0.0868 . \quad (3.5.15)$$

From (3.5.8) and (3.5.15) we have (the observational data are in [12])

$$H = 70.9 \pm 3.1 \text{ (km/s)/Mpc} . \quad (3.5.16)$$

Emphasize that when we neglect the short period (in the cosmological scale) of the inner protuberances then in the SST cosmology, the Hubble's parameter H depends on position in the Universe but it practically does not depend on time.

Density of baryonic matter is

$$\rho_{\text{BM}} = M_{\text{BM}} / V_{\text{Matter-Energy}} = 0.391 \cdot 10^{-27} \text{ kg/m}^3 . \quad (3.5.17)$$

The time distance between the true age of the Universe and the time distance to the most distant visible Universe is the period of evolution of protogalaxies which we cannot see

$$T_{\text{unobservable}} = 21.32 \text{ Gyr} - 13.79 \text{ Gyr} = 7.53 \text{ Gyr} . \quad (3.5.18)$$

The most distant massive galaxies are already **7.53 Gyr** old. We should not observe a “smooth field” of the dwarf galaxies as the first stage of the galaxies. Moreover, the Dark Ages are a scientific fiction.

We can see the CMB because the photons were scattered on the electron vortices with different recession velocities. Such vortices were produced in the very early Universe.

In paper [5] we can find a recapitulation concerning the ages of stars. There are cited the results obtained by Ludwig *et al.* (2009) [6]. Ludwig *et al.* derived solar ages from 1.7 to **22.3 Gyr**.

Initially number of the entangled SST-As components in the gluon/photon loops created in protons was $2 \cdot 4^{32}$ (we call such objects the supergluons or superphotons). Similar as it was in the baryonic cosmological loops (in each of them there were $2 \cdot 4^{16}$ protogalaxies), the supergluons or superphotons are built of $2 \cdot 4^{16}$ photon “galaxies” (photons) so number of the photons is about $2 \cdot 4^{16} = 0.86 \cdot 10^{10}$ times higher. On the assumption that each proton produced one supergluon we obtain the number of the photon galaxies in CMB (initially the abundance of protons was 0.75)

$$N_{\text{CMB-photons}} = 2 \cdot 4^{16} \cdot 0.75 M_{\text{BM}} / (n F) = 1.3993 \cdot 10^{88} . \quad (3.5.19)$$

Number density of the photon galaxies in CMB from supergluons is

$$\rho_{\text{CMB-photons}} = N_{\text{photon-galaxies}} / V_{\text{CMB}} = 407.1 \text{ per cubic centimetre} . \quad (3.5.20)$$

Outside the strong fields of baryons, the photon galaxies in the superphotons interacted electromagnetically not only with the bare electrons but also with their radiation masses so number of photon galaxies (photons) in CMB increased to

$$\begin{aligned} \rho_{\text{CMB-photons}}^* &= \rho_{\text{CMB-photons}} (1 + a_e)(\alpha_s + \alpha_{\text{em}}) / \alpha_s = \\ &= 410.6 \text{ per cubic centimetre} . \end{aligned} \quad (3.5.21)$$

3.6. The origin of CMB power spectrum

The temperature anisotropy in CMB follows from the atom-like structure of baryons which was excited by the inflows of the DM loops and by collisions of the NBHs.

Due to the decay of the Protoworld, there were three succeeding inflows of DM into the baryonic matter (Fig.13).

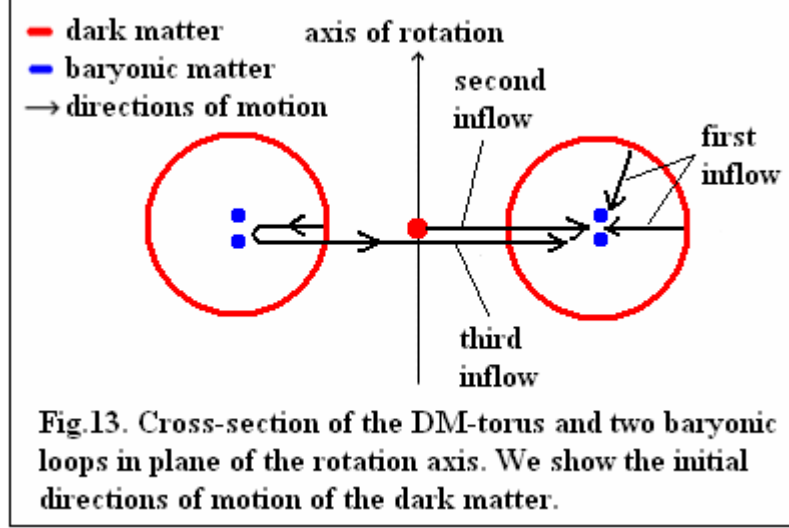
The weak interactions of the virtual electron-positron pairs in presence of DM lead to the present-day mean anisotropy power, $T_{\text{a,mean}}^2$

$$T_{\text{a,mean}}^2 = (T_{\text{Universe}} \alpha'_{\text{w(e),DM}})^2 \approx (30.5 \mu\text{K})^2 \approx 931 \mu\text{K}^2 , \quad (3.6.1)$$

where $T_{\text{Universe}} \approx 2.726 \text{ K}$ is the present-day temperature of the Universe [7], [11].

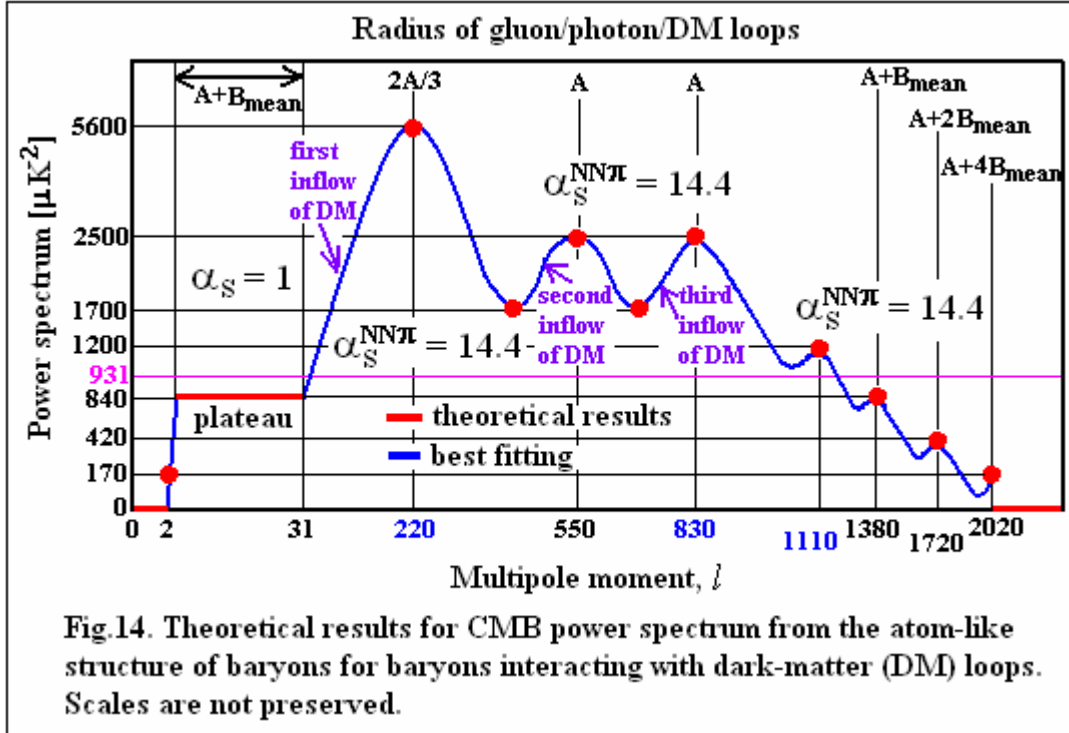
Initially, the baryonic matter consisted of the neutron black holes which are the cold objects, so there dominated the nuclear strong interactions at low energy. Initially, the inflow of DM was not intensive so the protons and neutrons interacted due to the exchanged fundamental gluon loops between pions in the $d = 1$ state. The coupling constant was $\alpha_s = \alpha_s^{\pi\pi, \text{FGL}} = 1$ (see formula (2.14.10)) and the created virtual gluon loops had the radius equal to $(A + B_{\text{mean}})$. Next there were the intensive inflows of the DM loops and creations of the

alpha particles. Coupling constant for strongly interacting protons, at low energies (as it is in the atomic nuclei), is $\alpha_s^{pp,\pi} = 14.39118$ (see formula (2.14.11)) whereas for strongly interacting neutrons is $\alpha_s^{nn,\pi} = 14.40991$. To the alpha particle, we can apply the mean value $\alpha_s^{NN,\pi} = 14.40055$.



Lifetimes are inversely proportional to coupling constants (see (1.4.29)) so we can divide the angular scale ($0^\circ - 90^\circ$) into two parts one related to the α_s (we denote it by $\Delta\phi_{FGL}$) and the second one related to the $\alpha_s^{NN,\pi}$ (we denote it by $\Delta\phi_\pi$)

$$\Delta\phi_{FGL} = 90^\circ \alpha_s^{NN,\pi} / (\alpha_s^{NN,\pi} + \alpha_s) = 84.2^\circ \text{ i.e. } \phi \text{ from } 90^\circ \text{ to } 5.8^\circ. \quad (3.6.2)$$



The definition which ties angular scale with multipole momentum, l , looks as follows

$$l = 180^\circ / \varphi, \quad (3.6.3)$$

so the SST plateau in CMB is from $l_{\text{pl,beginning}} = 2$ to

$$l_{\text{pl,end}} = 180^\circ / 5.8^\circ \approx 31. \quad (3.6.4)$$

We see that the SST plateau occupies almost whole angular scale so anisotropy power for the plateau should be only a little lower than the mean value. There is the largest triangle-like figure in Fig.14 so an excess in anisotropy temperature above the mean value is

$$\Delta T \approx \{(5600^{1/2} - 931^{1/2}) / 2\} (5.8^\circ / 90^\circ) \approx 1.43 \mu\text{K}. \quad (3.6.5)$$

Such a value we must subtract from the mean anisotropy temperature so for the plateau we have

$$T_{\text{pl}}^2 = T_{\text{A+B}}^2 = (T_{\text{Universe}} \alpha'_{\text{w(e),DM}} - \Delta T)^2 \approx (29 \mu\text{K})^2 \approx 840 \mu\text{K}^2. \quad (3.6.6)$$

Emphasize that this value is for $R = A + B_{\text{mean}}$.

Notice that similar results we obtain at high energies close to the rest mass of the Z^0 boson ($Q = Z^0$) for the electromagnetic interactions ($\alpha_{\text{em,high}} = 1 / 127.548$ – see formula (2.10.3)) and the strong-weak interactions ($\alpha_{\text{sw,Q=Z}} = 0.11795$ – see Table 4). It follows from the fact that the ratio $\alpha_{\text{sw,Q=Z}} / \alpha_{\text{em,high}} = 15.0$ is close to the ratio $\alpha_s^{\text{NN},\pi} / \alpha_s = 14.4$. Value of the fine structure constant increases at high energies because of the increase in surface density of the torus/electric charge in the core of baryons forced by the nuclear weak interactions – in such processes increases the effective electric charge.

It is easy to calculate the anisotropy powers for the FGL and the TB orbits because from the Wien's displacement law (see (1.4.11)) results that temperature is inversely proportional to a peak radius R_{Peak} which here is equal to one of the TB radii and to the radius of FGL. The curve should peak for following anisotropy powers

$$T^2 / T_{\text{pl}}^2 = \{(A + B_{\text{mean}}) / R\}^2. \quad (3.6.7)$$

For the FGL is $R = 2A/3$ so we have

$$T_{\text{FGL}}^2 = T_{\text{pl}}^2 \{(A + B_{\text{mean}}) / (2A/3)\}^2 \approx 5600 \mu\text{K}^2. \quad (3.6.8)$$

It is for the biggest peak that was created due to the first most intensive inflow of DM.

For $R = A$ is

$$T_{\text{FGL}}^2 = T_{\text{pl}}^2 \{(A + B_{\text{mean}}) / A\}^2 \approx 2500 \mu\text{K}^2. \quad (3.6.9)$$

It is for the second and third peaks that were created due to the second and third less intensive inflows of DM. All the time the loops created in the distinguished states were scattered.

For $R = A + 2B_{\text{mean}}$ is

$$T_{A+2B}^2 = T_{pl}^2 \{(A + B_{\text{mean}}) / (A + 2 B_{\text{mean}})\}^2 \approx 420 \mu\text{K}^2 . \quad (3.6.10)$$

For $R = A + 4B_{\text{mean}}$ is

$$T_{A+4B}^2 = T_{pl}^2 \{(A + B_{\text{mean}}) / (A + 4 B_{\text{mean}})\}^2 \approx 170 \mu\text{K}^2 . \quad (3.6.11)$$

We can see that the fourth peak does not relate to any TB orbit. It follows from the fact that for such a peak the energy was distributed among several orbits. Consider the first four orbits

$$R_{\text{mean}} = \{2A/3 + A + (A + B_{\text{mean}}) + (A + 2B_{\text{mean}})\} / 4 = 1.0157 \text{ fm} . \quad (3.6.12)$$

For $R = R_{\text{mean}}$ is

$$T_{R-\text{mean}}^2 = T_{pl}^2 \{(A + B_{\text{mean}}) / R_{\text{mean}}\}^2 \approx 1200 \mu\text{K}^2 . \quad (3.6.13)$$

During the scattering of loops from the $d = 0$ state (i.e. $R = A$) they first of all gather in distances equal to the muon radius of proton ($R_{p(\mu)} = 0.84039 \text{ fm}$ (see formula (2.19.7))). The anisotropy power for such distance is (it is a minimum)

$$T_{R-p(\mu)}^2 = T_{pl}^2 \{(A + B_{\text{mean}}) / R_{p(\mu)}\}^2 \approx 1700 \mu\text{K}^2 . \quad (3.6.14)$$

Calculate the increase in multipole moment per 1 MeV. Mass of the gluon loop in the $d = 0$ state (i.e. $R = A$) is $S_{(+o),d=0} \approx 727 \text{ MeV}$ – it relates to $l_A = 550$ while mass of the gluon loop in the $d = 4$ state (i.e. $R = A + 4B_{\text{mean}}$) is $S_{(+o),d=4} \approx 187 \text{ MeV}$ – it relates to $l_{A+4B} = 2020$ so we have

$$F_{\Delta/\text{MeV}} = (2020 - 550) / (727 - 187) = 2.72 \Delta/\text{MeV} . \quad (3.6.15)$$

Mass of the gluon loop in $A+B_{\text{mean}}$ is $S_{(+o),d=1} \approx 422 \text{ MeV}$ so we have

$$l_{A+B} = l_{A+4B} - (S_{(+o),d=1} - S_{(+o),d=4}) F_{\Delta/\text{MeV}} \approx 1380 . \quad (3.6.16)$$

Mass of the gluon loop in $A+2B_{\text{mean}}$ is $S_{(+o),d=2} \approx 298 \text{ MeV}$ so we have

$$l_{A+2B} = l_{A+4B} - (S_{(+o),d=2} - S_{(+o),d=4}) F_{\Delta/\text{MeV}} \approx 1720 . \quad (3.6.17)$$

Notice also that we should not observe anisotropy power for $l > l_{A+4B} = 2020$ because the $A+4B_{\text{mean}}$ is the last orbit – angular scale for the upper limit of l is

$$\varphi_{A+4B} = 180^\circ / l_{A+4B} = 0.0891^\circ . \quad (3.6.18)$$

The same is for following angular scales: $0 < \varphi < (90^\circ - \varphi_{A+4B})$, so we should have no anisotropy power for following multipole moments:

$$\text{for } 0 \leq l < \sim 2 \text{ is } T^2 = 0 . \quad (3.6.19)$$

Our results are in very good agreement with observational data [8].

3.7. Initial evolution of the expanding Universe

The initial state of the baryonic part of the Universe was the two cosmological loops with a radius $R_{\text{Cosmological}} = 0.191109 \text{ Gly}$ (the 2/3 of the equatorial radius of the core of the Protoworld (see (2.1.25))) both built of the NBHs which were the components of the protogalaxies. Collisions of the NBHs with DM and the mutual collisions of the NBHs caused that initially protogalaxies were embedded in a low-temperature baryonic-plasma ring (the NBHs are the cold objects). Such a ring, due to the nuclear strong interactions at low energy (the coupling constant for such interactions is $\alpha_s = 1$), had interacted with gluon loops that overlapped with the cosmological loops. It caused that the spin speed of the cosmological loops was close to c . So the period of rotation, $T_{\text{cosmological}}$, was

$$T_{\text{cosmological}} = 2 \pi R_{\text{Cosmological}} = 1.201 \text{ Gyr} . \quad (3.7.1)$$

The tidal locking (or a mutual spin-orbit resonance) of the Moon and the Earth caused that the rotation and revolution periods of the Moon are the same. Similar processes caused that the period of rotation of protogalaxies (so of the present-day massive galaxies as well) was (and still is) equal to the period of spinning of the two cosmological loops composed of the protogalaxies. Our exact result 1.201 Gly is close to the observational result $\sim 1 \text{ Gyr}$ [9].

Our Universe arose and developed as the double cosmic loop inside the torus of the core of the Protoworld. The magnetic axes of the neutrons in the cosmic structures were tangent to the double cosmic loop. Magnetic polarisation dominated because the neutrons are electrically neutral. The cosmic structures in the expanding Universe were mostly moving in radial directions. Due to the law of conservation of spin, the magnetic axes of the protogalaxies should be parallel or antiparallel to the direction of their acceleration. This means that there were the $\sim 90^\circ$ turns of the magnetic axes of the protogalaxies.

The dwarf galaxies appeared due to explosions of the protogalaxies.

The definition of the speed c leads to conclusion that we cannot see the initial period 7.53 Gyr of the evolution of the protogalaxies. It causes that in the most distant visible Universe, we should not see a field composed only of dwarf galaxies.

3.8. The standard ruler in cosmology

The radius of the $d = 1$ state in the Protoworld is 151.13 Mpc (see formulae (2.1.25) and (2.5.8)). There were produced photon loops and DM loops overlapping with this state

$$R_{\text{ruler-in-cosmology}} = A_{\text{Protoworld}} + B_{\text{Protoworld}} = 151.13 \text{ Mpc} . \quad (3.8.1)$$

It causes that radius of baryonic loops interacting with such loops is the standard ruler in cosmology.

The analysis of the WMAP data (CMB) yielded $146.8 \pm 1.8 \text{ Mpc}$ for the sound horizon at the photon decoupling epoch and $153.3 \pm 2.0 \text{ Mpc}$ at the end of the baryon drag epoch [10].

3.9. Black body spectrum

Superphotons consist of $2 \cdot 4^{32}$ neutrino-antineutrino pairs and are produced as the gluon loops on the orbits in baryons. Their wavelengths depend on the internal temperature of the baryons/black-body. Via the Wien's law we can calculate the λ_T peak wavelength: $\lambda_T T = 2.897771955 \cdot 10^{-3} \text{ [m K]}$ – it is the 2018 CODATA value of the Wien's-wavelength-

displacement-law constant numerically solved from Planck's law using Newton's method. Mostly such supergluons/superphotons transit from the $d = 0$ state (the equator) to the $d = 1$ state so the length of them increases to $2\pi(A + B_{\text{mean}})$ – emission is from the $d = 1$ state. From it we have

$$\lambda_T / \lambda_v = A / (A + B_{\text{mean}}) = 0.5815531 , \quad (3.9.1)$$

where λ_T is a peak wavelength from the Wien's law, and λ_v is a peak wavelength from the spectral radiance.

Using the central value of the today's temperature of the Universe from WMAP (2.7260(13) K [11]) we obtain $\lambda_T = 1.0630 \cdot 10^{-3}$ m, $\lambda_v = 1.8279 \cdot 10^{-3}$ m, and $\nu = 164.01$ GHz.

We can calculate the λ_v within the SST.

Outside the nuclear strong fields, the supergluons behave as superphotons and they decayed to the SST photon galaxies so length of them increased $N_1 = 2 \cdot 4^{16}$ times.

The superphotons were emitted, first of all, from surface of the initial ball which radius was equal to $A_{\text{Protoworld}} + B_{\text{Protoworld}} = 0.4929262$ Mly (see formulae (2.1.25) and (2.5.8)). Radius of such surface increased to R_{CMB} , so length of the CMB photons increased additionally $N_2 = R_{\text{CMB}} / (A_{\text{Protoworld}} + B_{\text{Protoworld}}) = 43.252(20)$ times – accuracy of this value is limited by the measured energy density of CMB which is very low (there are only four digits in the central value (see (3.6.2))).

Assume that supergluons appear on the three orbits that lie below the Schwarzschild surface for the nuclear strong interactions, so the mean wavelength of the emitted supergluons was $\lambda_{\text{mean}} = 2 \pi \{2A/3 + A + (A + B_{\text{mean}})\} / 3 = 4.946291$ fm.

Notice also that first of all the superphotons produced the $\mu^+ \mu^-$ pairs that decayed to the electron-positron pairs. The ratio of anomalous magnetic moments a_μ/a_e is $N_3 = 1.0054$ (see Chapter 2.8), so energy of the superphotons increased a little so their wavelength decreased N_3 times.

For λ_v we obtain

$$\lambda_v = \lambda_{\text{mean}} N_1 N_2 / N_3 = 1.8278(9) \cdot 10^{-3} \text{ m} . \quad (3.9.2)$$

Due to the different weak interactions of muons and electrons and the decays of the $\mu^+ \mu^-$ pairs into the electron-positron pairs, we should observe an excess in quanta with energy equal to

$$E_{\text{predicted}} = m_e (N_3 - 1) = 2.76 \text{ keV} . \quad (3.9.3)$$

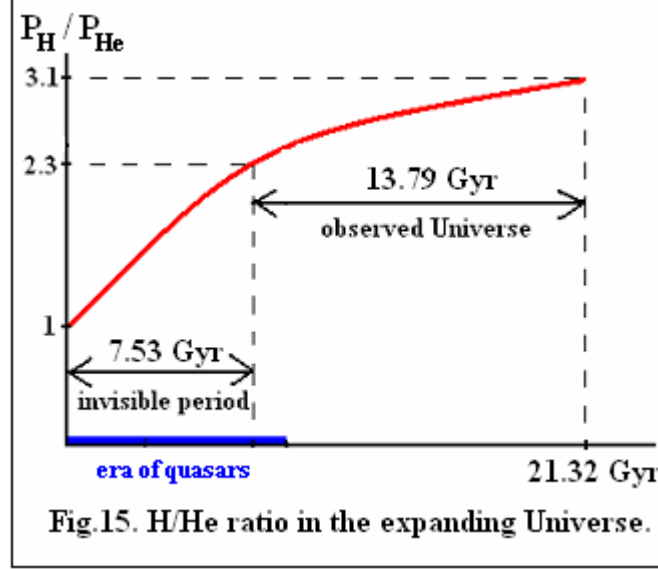
3.10. The hydrogen-to-helium-4 ratio in the expanding Universe

Due to evolution of the Universe, hydrogen transforms into helium whereas helium transforms into more massive atomic nuclei. It suggests that it can be that with time mass abundance of helium in relation to hydrogen can slowly decrease – it should not increase as it is assumed in the mainstream cosmology.

We use in this Section the Stefan-Boltzmann law which is derived within SST (see formula (1.4.20)). Assume that due to the big stars, a change in abundance of helium-4 (He-4), ΔP_{He} [%], is directly proportional to the temperature T (higher temperature means higher changes

in abundance) whereas that total emitted energy is directly proportional to age of the Universe, τ_{Universe} [Gyr]. Then, we have

$$\Delta P_{\text{He}} [\%] = f (\tau_{\text{Universe}} [\text{Gyr}])^{1/4}. \quad (3.10.1)$$



The resultant abundance of helium-4 is

$$P_{\text{He}} = P_{\text{initial,He}} - \Delta P_{\text{He}} [\%] = P_{\text{initial,He}} - f (\tau_{\text{Universe}} [\text{Gyr}])^{1/4}, \quad (3.10.2)$$

where $P_{\text{initial,He}} = 50\%$ is the primordial mass abundance of helium. On the assumption that the today abundances of helium-4 and hydrogen are respectively 24.5% and 75.5%, we obtain that the factor f is equal to $f = 11.87$.

From (3.10.2) we have that abundance of helium-4 in most distant observed Universe (i.e. $\tau_{\text{Universe-distant}} [\text{Gyr}] = 7.53$) should be 30.3% so abundance of hydrogen should be about $50\% + (50\% - 30.3\%) = 69.7\%$, so the ratio $P_{\text{H}}/P_{\text{He}} = 2.3$. The SST results are collected in Fig.15.

Above surfaces of the neutron stars and in the symmetrical decays of nuclei in the supernova explosions there appear protons so in such regions, with time, abundance of hydrogen increases.

3.11. Summary

The creation of the Protoworld and the expansion of the Universe were separated in time from the SST inflation that created the inner Cosmos.

The initial Universe was highly anisotropic because there were two baryonic loops and a rotating dark-matter torus. Protuberances inside and on the front of the early expanding Universe and the anisotropic inflows of the dark energy and dark matter into the baryonic part of the Universe caused that anisotropies of some regions of the Universe are higher. Only the creation of new neutrino (it took over most of the Protoworld rotational energy) and the damping of protuberances by a fairly symmetrical expansion of dark energy partially reduced the anisotropy.

The Universe is practically flat because the density of the isotropic SST absolute spacetime exceeds by many orders of magnitude the average density of matter and dark energy.

The Universe is 21.32(1) **Gyr** old, not 13.8 **Gyr**. We cannot see the initial period 7.53 **Gyr** of evolution of protogalaxies. We should observe the massive galaxies and quasars with supermassive black hole in their centre already in the most distant visible Universe.

Due to the different weak interactions of muons and electrons and the decays of the $\mu^+\mu^-$ pairs into the electron-positron pairs, we should observe an excess in quanta with energy equal to 2.76 keV (see Sections 3.9 and 2.8).

3.12. Tables

Table 14 *Inner Cosmos*

Cosmological quantity	Theoretical value*
Inertial-mass density of the initial inflation field	8.32192 E+85 kg/m ³
Radius of the inner Cosmos	2.3 E+30 m
Mass of the SST spacetime	5.9 E+119 kg

*2.3 E+30 = 2.3·10³⁰

Table 15 *Protoworld and early Universe*

Cosmological quantity	Theoretical value
Mass of the core of the Protoworld \approx \approx mass of the dark matter	1.96076 E+52 kg
Equatorial radius of the core of the Protoworld	0.286663 Gly
Radius of the standard ruler in cosmology	151.13 Mpc
Mass of baryonic matter	0.36379 E+51 kg
Radius of the initial baryon-matter loops	0.1911 Gyr
Mass of protogalaxy	1.0656 E+11 solar masses
Mass of neutron black hole (NBH)	4.933 E+31 kg i.e. about 24.81 solar masses
Radius of NBH	3.664 E+4 m

Table 16 *Universe*

Cosmological quantity	Theoretical value
Present-day abundance of baryonic matter	4.91 %
Present-day abundance of dark matter	26.46 %
Present-day abundance of dark energy	68.63 %
λ_T / λ_v for black body	0.5815531
λ_v	1.8278(9) E-3
Radius of the CMB sphere	21.32(1) Gly
Age of the Universe	21.32(1) Gyr
Time distance to the observed front of the sphere filled with BM, DM and DE	13.79(1) Gyr
Time Hubble constant	70.90 \pm 3.1 km·s ⁻¹ ·Mps ⁻¹
Spatial Hubble constant	45.86 km·s ⁻¹ ·Mps ⁻¹
Mean anisotropy power	931 μ K ²
Amplitude of the CMB temperature fluctuations	1.119446 E-5
Number of photon galaxies (photons) in cubic centimetre of CMB	410.6

References

- [1] H. S. Murdoch (14 October 1976). “Recession Velocities Greater than Light”
Q. Jl R. astr. Soc. (1977) **18**, 242-247
- [2] James M. Lattimer (28 June 2019). “Neutron Star Mass and Radius Measurements”
Universe **2019**, 5, 159
Doi:10.3390/universe5070159
- [3] sjsu.edu/faculty/Watkins/He4nuclide.htm
- [4] P. A. Zyla, *et al.* (Particle Data Group). ”2. Astrophysical Constants and Parameters”
Prog. Theor. Exp. Phys. **2020**, 083C01 (2020) 25th August, 2020
- [5] David R. Soderblom (31 March 2010). “The Ages of Stars”
arXiv:1003.6074v1 [astro-ph.SR]
- [6] Ludwig H-G, *et al.* (2009)
Astron. Astro-phys., in press
- [7] C. Patrignani *et al.* (Particle Data Group), Chin. Phys. C, **40**, 100001 (2016) and 2017
update, December 1, 2017
- [8] Planck Collaboration (15 September 2020). “Planck 2018 results. V. CMB power
spectra and likelihoods”
arXiv:1907.12875v2 [astro-ph.CO]
- [9] Gerhard R Meurer, *et al.* (9 March 2018). “Cosmic clocks: a tight radius-velocity
relationship for HI-selected galaxies”
MNRAS, Volume 476, Issue 2, May 2018, Pages 1624-1636
arXiv:1803.04716 [astro-ph.GA]
- [10] E. Komatsu *et al.* (2009). ”Five-Year Wilkinson Microwave Anisotropy Probe
Observations: Cosmological Interpretation”
ApJS, **180**, 330-376
- [11] D. J. Fixen (30 November 2009). “The Temperature of the Cosmic Microwave
Background”
ApJ **707** 916 (2009)
- [12] Wendy L. Freedman (29 June 2021). “Measurements of the Hubble Constant: Tensions
in Perspective”
arXiv:2106.15656 [astro-ph.CO]
Accepted to the Astrophysical Journal, 23 June 2021

Chapter 4

Applications

4.1. Particle physics	93
4.1.1. The origin of the transverse radii of hyperons at the LHC	93
4.2. Cosmology and astrophysics	94
4.2.1. Rotation curves of disc galaxies outside their bulges	94
4.2.2. Age of the Universe from the degree of curvature of the major arms of the massive spiral galaxies	96
4.2.3. Conditions for intensive evaporation of black holes	98
4.2.4. The main equation in theory of gamma-ray bursts (GRB)	99
4.2.5. New theory of the Solar System	101
4.2.6. Magnetars versus pulsars	106
4.3. Nuclear physics	109
4.3.1. The four-shell model of atomic nucleus	109
4.3.2. Coupling constants and binding energy	109
4.3.3. Model of dynamic supersymmetry for nuclei	112
4.4. Atomic physics	114
4.4.1. Derivation of the Pauli Exclusion Principle	114
4.4.2. Meaning simplification of the Dirac theory of the hydrogen atom	117
4.5. Brain-mind interactions	120
4.5.1. The brain-mind interactions	120
4.6. Chaos theory	121
4.6.1. Feigenbaum constants	121
4.7. Quantum physics	122
4.7.1. Quantum physics in SST	122
4.7.2. Testing the SST quantum gravity	125
4.8. Extraterrestrial communication	126
4.8.1. Wow! signal	126
4.9. Dark energy and dark matter	131
4.9.1. Creation of dark energy (DE) and dark matter (DM)	131

4.1. Particle physics

4.1.1. The origin of the transverse radii of hyperons at the LHC

Here we show that the effective Gaussian source radii for the proton-hyperon pairs obtained at the LHC follow from the atom-like structure of baryons.

The ALICE team at the LHC has shown that the source radii for the proton-hyperon pairs can be determined in proton-proton collisions via a function of the transverse mass m_T [GeV/c] [1]. They obtained an effective Gaussian source radius (we will call it the transverse radius) equal to $1.02(5)$ fm for $p-\Xi^-$ pairs and equal to $0.95(6)$ fm for $p-\Omega^-$ pairs. The average m_T of such pairs are 1.9 GeV/c and 2.2 GeV/c respectively.

In the relativistic proton-proton collisions, spins of protons are parallel or antiparallel to the direction of the collisions. On the other hand, the created gluon loops are in planes perpendicular to the direction of collisions. Thus, the breakdown of the gluon loops (or annihilation of the X^+X^- pairs) causes their masses to appear as transverse masses.

In interacting strongly hyperons, the gluon loops appear on the first four orbits with the radii equal to $R_{\text{FGL}} = 2A/3$, $R_{d=0} = A$, $R_{d=1} = A + B_{\text{mean}}$, and $R_{d=2} = A + 2B_{\text{mean}}$, so the mean transverse radius of all hyperons, $R_{\text{T,hyperons,SST}}$, should be

$$R_{\text{T,hyperons,SST}} = (R_{\text{FGL}} + R_{d=0} + R_{d=1} + R_{d=2}) / 4 = 1.0157 \text{ fm} \approx 1.02 \text{ fm} . \quad (4.1.1)$$

We can see that our result is equal to the central value for the LHC $p-\Xi^-$ pairs.

The SST transverse mass for all proton-hyperon pairs, $m_{\text{T,hyperons,SST}}$, should be – the hyperon interacts strongly with proton via π^0_{bound} (see Table 1)

$$\begin{aligned} m_{\text{T,hyperons,SST}} &= X^\pm + \pi^0_{\text{bound}} + S_{(+),d=0} + S_{(+),d=1} + S_{(+),d=2} = \\ &= 1902 \text{ MeV} \approx 1.9 \text{ GeV} . \end{aligned} \quad (4.1.2)$$

Why did the LHC experiment get different results for the $p-\Omega^-$ pairs?

Mass of the hyperon Ω^- is [2]

$$\Omega^- = 1672.45(29) \text{ MeV} . \quad (4.1.3)$$

It means that a $p-S_{(+),d=0}$ pair can mimic the mass of the hyperon Ω^- because the mass distance is very low

$$p + S_{(+),d=0} = 1665.71 \text{ MeV} . \quad (4.1.4)$$

In the $p-pS_{(+),d=0}$ pair, there are occupied only the states $d = 0$ and $d = 1$ (there does not appear an additional pion π^0_{bound} but there are two the $S_{(+),d=0}$ gluon loops) so we have

$$R_{\text{T,p-pS}(+),\text{SST}} = (R_{d=0} + R_{d=1}) / 2 = 0.948 \text{ fm} \approx 0.95 \text{ fm} . \quad (4.1.5)$$

We can see that our result is equal to the central value for the LHC $p-\Omega^-$ pairs.

The SST transverse mass for the $p-pS_{(+),d=0}$ pairs, $m_{\text{T,p-pS}(+),\text{SST}}$, should be

$$m_{\text{T,p-pS}(+),\text{SST}} = X^+ + 2S_{(+),d=0} + S_{(+),d=1} = 2196 \text{ MeV} \approx 2.2 \text{ GeV} . \quad (4.1.6)$$

It also is consistent with the LHC result.

References

- [1] ALICE Collaboration (9 December 2020). “Unveiling the strong interaction among hadrons at the LHC”
Nature **588**, 232-238 (9 December 2020)
 [2] P.A. Zyla, *et al.* (Particle Data Group)
 Prog. Theor. Exp. Phys. **2020**, 083C01 (2020)

4.2. Cosmology and astrophysics

4.2.1. Rotation curves of disc galaxies outside their bulges

The DM loops can interact weakly with baryonic matter. But in baryonic plasma can be created also the photon loops and gluon loops so in spinning galaxies, the other interactions can be realized as well.

Internal energy of a loop is defined as follows

$$\mathbf{E} = m_{\text{loop}} v_{\text{spin}}^2 . \quad (4.2.1)$$

Virtual mass m^* that is the mediator of the interactions of the DM loops with the actual baryonic mass, m_{BM} , of a vortex, is defined by the product of the baryonic mass m_{BM} and the coupling constant that defines a type of weak interactions. The DM loops interact via the virtual electron-positron pairs ($\alpha_{w(e)} = 0.9511186121 \cdot 10^{-6}$ (see (2.4.4)) and spin speed of loops and virtual pairs is equal to c so for the mediator we have

$$\mathbf{E} = 2 \alpha_{w(e)} m_{\text{BM}} c^2 , \quad (4.2.2)$$

where the factor 2 follows from the fact that there are virtual pairs, not single particles.

The energy defined by (4.2.2) was adopted by the spinning initial baryonic matter $m_{o,\text{BM}}$ so we have

$$\mathbf{E} = m_{o,\text{BM}} v_{\text{spin}}^2 , \quad (4.2.3)$$

where v_{spin} is the observed orbital speed of stars outside the bulge of spinning galaxies.

From (4.2.2) and (4.2.3) is

$$v_{\text{spin}} = c (2 \alpha_{w(e)} m_{\text{BM}} / m_{o,\text{BM}})^{1/2} . \quad (4.2.4)$$

Single protogalaxy was composed of 4^{16} NBHs so its baryonic mass was

$$M_{\text{Proto,BM}} = 4^{16} \cdot 24.81 M_{\text{Sun}} = 1.066 \cdot 10^{11} M_{\text{Sun}} , \quad (4.2.5)$$

where M_{Sun} is the mass of the Sun.

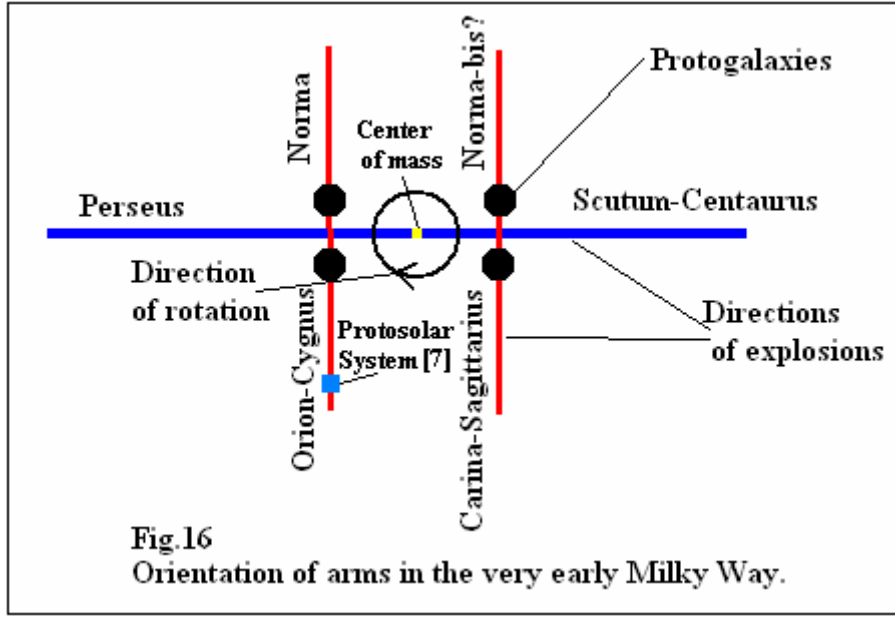
From (2.26.1) and (2.26.2) results that singlets, doublets, quadrupoles, and octopoles of protogalaxies were most numerous. From the structure of Milky Way (MW) Galaxy follows that initially there were 4 protogalaxies (Fig.16).

The MW initially was a quadrupole so it was a binary system of binary systems. It means that we should observe 2 major arms and 4 minor arms. The initial distance between the 2-protogalaxy systems was bigger than the distance between the protogalaxies in the single

binary systems. It caused that initially the temperature along the direction defined by Scutum-Centaurus arm and Perseus arm was lower than for the two other directions – it leads to conclusion that the two major arms should contain old stars while the four minor ones should contain younger stars and gas.

The observational data show that there are the two major arms (the Scutum-Centaurus and Perseus) containing old stars, and three or four minor ones (the Norma, Carina-Sagittarius, Orion-Cygnus, and ?) containing gas and young stars. Probably the Norma arm is composed today of two very close arms which practically overlap (Norma and Norma-bis?).

The spiral galaxies that evolved from binary systems of protogalaxies should have only two main arms. The M31 galaxy (Andromeda) evolved from 8 protogalaxies so the arrangement of the major and minor arms should be more complicated.



For MW from (4.2.4) we have

$$v_{\text{spin,MW}} = c \{ 2 \alpha_{w(e)} m_{\text{BM}} / (4 M_{\text{Proto,BM}}) \}^{1/2}. \quad (4.2.6)$$

Today the mean rotation velocity of the Milky Way for the approximately flat part of the rotation curve is [1]

$$v_{\text{spin,MW}} = 238 \pm 14 \text{ km/s}, \quad (4.2.7)$$

so from (4.2.6) we can calculate the present-day baryonic mass of MW

$$m_{\text{BM,MW}} = 1.41(17) \cdot 10^{11} M_{\text{Sun}}. \quad (4.2.8)$$

The rest of the initial baryonic mass is outside the MW halo – it is the mass of the dwarf galaxies and the intergalactic gas.

The mass of DM is about $N_{\text{DM/BM}} = 5.38979$ times higher than the baryonic mass (see (3.1.4)) so the total mass of MW should be close to

$$M_{\text{MW}} = m_{\text{BM,MW}} (1 + N_{\text{DM/BM}}) = 0.90(11) \cdot 10^{12} M_{\text{Sun}}. \quad (4.2.9)$$

Consider the initial stage of the baryonic part of the Universe. There were the two cosmological baryonic loops that created the gluon loops overlapping with the baryonic loops. Such plasma was cold because the NBHs are the cold objects. It means that the interactions between the gluon loops and baryonic loops were via the *single* FGLs at low energy so the coupling constant is $\alpha_s = 1$. From (4.2.6) we have

$$v_{\text{spin}} = c (\alpha_s)^{1/2} = c. \quad (4.2.10)$$

Radius of the two cosmological loops was $R_{\text{Cosmological}} = 0.1911 \text{ Gly}$ so the period of rotation, $T_{\text{cosmological}}$, was

$$T_{\text{cosmological}} = 2 \pi R_{\text{Cosmological}} = 1.201 \text{ Gyr}. \quad (4.2.11)$$

The tidal locking (or a mutual spin-orbit resonance) of the Moon and the Earth caused that the rotation and revolution periods of the Moon are the same. Similar processes caused that the period of rotation of protogalaxies (so of the present-day galaxies as well) was (and still is) equal to the period of spinning of the two cosmological loops composed of the protogalaxies.

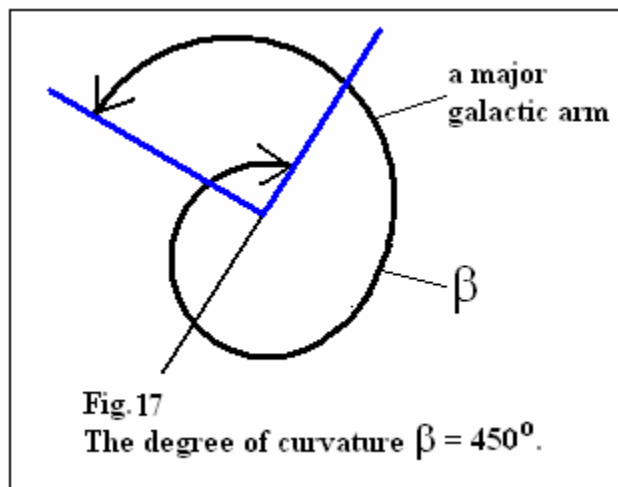
References

- [1] Mareki Honma, et al. (25 December 2012). “Fundamental Parameters of the Milky Way Galaxy Based on VLBI Astronomy”
 Publ. Astron. Soc. Japan (25 December 2012), Volume 64, Issue 6, 136
<https://doi.org/10.1093/pasj/64.6.136>

4.2.2. Age of the Universe from the degree of curvature of the major arms of the massive spiral galaxies

We already proved that the correct age of the Universe is $21.32(1) \text{ Gyr}$.

Ludwig et al. (2009) derived solar ages from 1.7 to 22.3 Gyr [1] – we can read it in some recapitulation concerning the ages of stars [2]. The upper limit is very close to the age of the Universe obtained within SST – we claim that we cannot see the initial period 7.53 Gyr of evolution of galaxies.



Here we show that the degree of curvature of the major arms of the massive spiral galaxies leads to the SST age of the Universe.

Here the degree of curvature β [$^\circ$] is the central angle defined by a major arm of a spiral galaxy (Fig.17).

The mutual spin-orbit resonance caused that the period of rotation of protogalaxies (so of the present-day galaxies as well) was (and still is) equal to the period of spinning of the baryonic part in the very early Universe (see (3.7.1) and (4.2.11))

$$T_{\text{cosmological}} = 1.201 \text{ Gyr} . \quad (4.2.12)$$

For a constant mass of a loop with increasing radius, from the conservation of spin, we have $r \sim 1/v_{\text{spin}}$. From definition of period of spinning is $T = 2\pi r/v_{\text{spin}}$ so we have $T \sim 1/v_{\text{spin}}^2$. From formula (2.14.9) is $\alpha \sim v_{\text{spin}}$ so we have

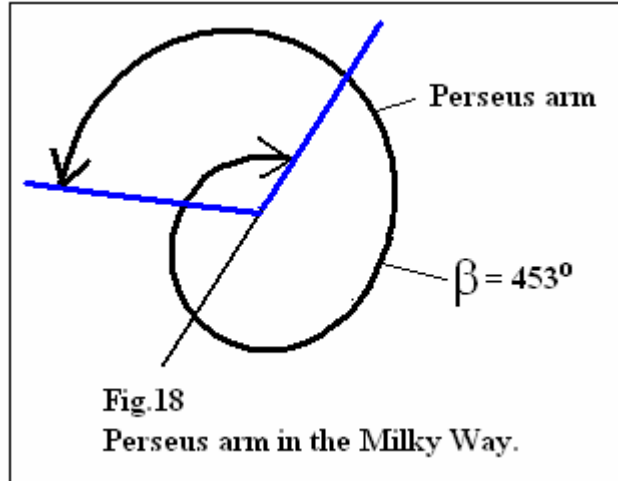
$$T \sim 1 / \alpha^2 . \quad (4.2.13)$$

The period of rotation $T_{\text{cosmological}} = 1.201 \text{ Gyr}$ should be characteristic for the edge of the galactic bulge or edge of the central bar where the galactic arms begin. On such edge, the nuclear strong ($\alpha_s = 1$) and nuclear weak interactions ($\alpha_{w(p)} = 0.0187229$) dominated. On the other hand, on the edge of the baryonic disc dominated the nuclear strong interactions so from (4.2.13) we have

$$f = T_{\text{end}} / T_{\text{cosmological}} = [(\alpha_s + 2 \alpha_{w(p)}) / \alpha_s]^2 = 1.0763 , \quad (4.2.14)$$

where T_{end} is the period of spinning of the end of the major arm, i.e. rotation on the end was a little slower than rotation near the central part. The delay is

$$\Delta\beta = 360^\circ - 360^\circ / f = 25.52 \text{ degrees per } 1.20 \text{ Gyr} . \quad (4.2.15)$$

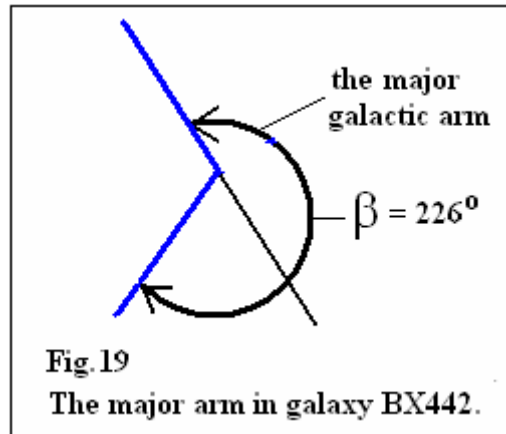


We can see that the Milky Way has already turned $N \approx 17.8$ times ($21.32 \text{ Gyr} / 1.20 \text{ Gyr} \approx 17.8$) so the degree of curvature for the major arm (Perseus arm) should be

$$\beta_{\text{MW}} = \Delta\beta N = 453^\circ \text{ or so} . \quad (4.2.16)$$

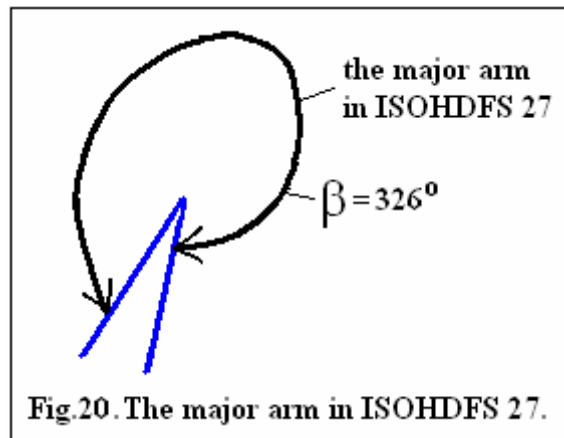
And it is (Fig. 18 and [3]).

For the spiral galaxy BX442 at the time distance 10.7 **Gyr** we obtain $\beta_{\text{BX442}} = 226^\circ$ or so – and it is (Fig.19 and [4]).



For the spiral galaxy ISOHDFS 27 at the distance 6 **Gyr** from the Earth we obtain $\beta_{\text{ISOHDFS27}} = 326^\circ$ or so – and it is (Fig.20 and [5]).

We showed that both the energy density of CMB and the curvatures of the major arms in massive spiral galaxies lead to the age of the Universe about 21.3 **Gyr**. Moreover, curvature of arms of such galaxies in most distant observed Universe, because we cannot see the initial period 7.53 **Gyr** of evolution of the protogalaxies, should be about 160 degrees.



References

- [1] Ludwig H-G, Caffau E, Steffen M, Bonifacio P, Sbordone L. (2009) Astron. Astro-phys., in press
- [2] David R. Soderblom (31 March 2010). "The Ages of Stars" arXiv:1003.6074v1 [astro-ph.SR]
- [3] en.wikipedia.org/wiki/Milky_Way
- [4] <http://astronoo.com/en/articles/galaxies-oldest.html>
- [5] European Southern Observatory (8 December 2000) www.eso.org/public/poland/images/eso0041a/?lang

4.2.3. Conditions for intensive evaporation of black holes

The SST black holes (BHs) are the NBHs or are the associations of NBHs and neutron stars. It follows from the fact that the very strong short-distance quantum entanglement between the

SST-As components on the torus in the core of baryons causes that the cores are indestructible in conditions that can happen in the today inner Cosmos. Moreover, the strong interactions in the neutron stars between the neutrons fix the effective distance between them in such a way that the cores of neutrons do not overlap even partially.

In spinning nuclear plasma are conditions to create the dark-matter loops and the gluon loops that outside the nuclear strong fields behave as the photon loops. They all are composed of the SST-As components so their resultant speed must be equal to c . It leads to conclusion that when spin speed of the loops cannot be equal to c (due to their interactions with matter which is spinning with speeds lower than c) then there are forced their motions in direction perpendicular to the plane on which they lie.

Accretion discs of BHs lie on planes parallel to planes of the equators of BHs so the created loops are concentric and their centres overlap with the BH axis of rotation. It leads to conclusion that the created loops and matter interacting with them move along the rotation axis of BH. Mass of NBHs must be invariant and due to the tremendous dynamic pressure in the SST-As, such spacetime should be flat. This means that the accreting baryonic matter can create new NBHs or/and such matter is intensively emitted along the BH rotation axis.

The collapse of the Protoworld forced the inflows of the DM loops into the SST BHs – this caused their collisions so some BHs were eaten by others, which converted neutron matter into nuclear plasma. The mass of the black holes decreased rapidly. Only their central parts have survived.

The Universe swelled at the expense of the zero-energy field thickening by incoming dark energy and partly due to the pressure exerted by the CMB created.

4.2.4. The main equation in theory of gamma-ray bursts (GRB)

Here, using the SST, we derived the main equation in theory of GRBs and used it to describe the GRB 080916C. Such theory is closely related to the theory of NBHs which is related to the theory of baryons.

From formulae (1.4.25) we have

$$t_{\text{Burst}} = \tau_{\text{Lifetime}} \sim 1 / m^4, \quad . \quad (4.2.17)$$

where m is the mass of a condensate or loop composed of the SST-As components or of a star, and t_{Burst} is the duration of a burst.

Emission during creation of a ball/condensate is due to the weak interactions.

The weak mass of NBH is

$$M_{\text{Weak}} = \alpha_{w(p)} M_{\text{NBH}}, \quad (4.2.18)$$

where $\alpha_{w(p)} = 0.0187229$, and $M_{\text{NBH}} = 24.81$ **solar masses**.

The strong mass of NBH at low energy (the NBHs are the cold objects) is

$$M_{\text{Strong}} = \alpha_s M_{\text{NBH}}, \quad (4.2.19)$$

where $\alpha_s = 1$.

The period of transition of a mass from the $A_{i(\text{NBH})} + B_{i(\text{NBH})}$ state to $A_{i(\text{NBH})} = 36.64$ **km** state, where $A_{i(\text{NBH})} / B_{i(\text{NBH})} = 1.3898$, due to the strong interactions, is

$$t_{\text{strong}} = B_i / c. \quad (4.2.20)$$

For the weak interaction, which is weaker, the speed of transition is lower. From formulae (4.2.17)-(4.2.20) we have

$$t_{\text{Burst,NBH}} / t_{\text{strong}} = (M_{\text{NBH}} / M_{\text{Weak}})^4 . \quad (4.2.21)$$

It leads to

$$t_{\text{Burst,NBH}} = (B_{i(\text{NBH})} / c) / \alpha_{w(p)}^4 = 716 \text{ s} . \quad (4.2.22)$$

From (4.2.17) and (4.2.22) we have

$$t_{\text{Burst}} = 716 (m / M_{\text{NBH}})^4 [\text{seconds}] , \quad (4.2.23)$$

where m [solar masses] is mass of captured star by NBH.

Equation (4.2.23) is the main equation in the theory of GRBs.

Some baryonic analog to stars captured by NBH looks as follows

$$m / M_{\text{NBH}} = m_{\text{particle}} / M_{\text{Neutron}} . \quad (4.2.24)$$

Number density of GRBs should be higher for stars that masses relate to the uncharged scalars (they are the Y central condensate in baryons and the $\mu_{\text{bare}}^{\pm}/2$ central condensate in muons) and uncharged pseudoscalars (they are the neutral pions) – from formulae (4.2.23) and (4.2.24) we obtain that durations of such GRBs are **30 seconds**, **0.007 second**, and **0.3 second respectively** which is consistent with observational data. Higher number density of GRBs follows from the fact that the nuclear energy produced in center of stars is easier transferred to their surface by uncharged and spin-0 objects so such stars are less stable – it leads to higher abundances of such GRBs.

Consider a star or binary system of stars with total mass which relates to mass of the hyperon $\Lambda = 1115.3 \text{ MeV}$. From formulae (4.2.23) and (4.2.24) we obtain that some stellar analog to the hyperon Λ has mass equal to $M_{\Lambda} = 24.81 \cdot 1115.3 / 939.56 = 29.45 \text{ solar masses}$, i.e. such star is more massive than NBH. From (4.2.24) we obtain that the burst should last

$$t_{\text{Burst,GRB080916C}} = 716 (M_{\Lambda} / M_{\text{NBH}})^4 = 1422 \text{ s} = 23.7 \text{ min} . \quad (4.2.25)$$

In the final stage there should appear new NBH while the mass equal to $29.45 - 24.81 = 4.64$ [solar masses] should be emitted as the gamma rays. Since total energy of the Sun is about $1.8 \cdot 10^{54} \text{ erg}$ so emitted isotropic energy should be about $4.64 \cdot 1.8 \cdot 10^{54} = 8.4 \cdot 10^{54} \text{ erg}$.

We can compare these results with data obtained by the Fermi LAT and Fermi GBM Collaborations [1]. They obtained $\sim 1400 \text{ s}$ and $\sim 8.8 \cdot 10^{54} \text{ erg}$ respectively.

References

- [1] The Fermi LAT and Fermi GBM Collaborations (27 March 2009). “Fermi Observations of High-Energy Gamma-Ray Emission from GRB 080916C”
Science VOL 323, pp: 1688-1693
https://www.openu.ac.il/personal_sites/yoni-granot/papers/GRB080916C_Science.pdf

4.2.5. New Theory of the Solar System

Here we show that the Titius-Bode (TB) law is a characteristic feature of the surroundings of various types of black holes. Only a star that is a remnant of a black hole may be surrounded by rings (or planets) whose radii (or semi-major axes) are defined by TB law. We explained the origin of Neptune and other massive planets, Kuiper belt and Oort cloud.

In the TB law for the Solar System, we have

$$A / B_{\text{mean}} = 1.3898 , \quad (4.2.26)$$

$$A + 2B_{\text{mean}} = 1 \text{ au} , \quad (4.2.27)$$

so we obtain $A = 0.41 \text{ au}$ and $B_{\text{mean}} = 0.295 \text{ au}$.

We claim that the initial rings in accretion disc around a black hole were produced due to the successive symmetrical decays of the nuclei containing 256 nucleons.

Ranges of objects are inversely proportional to their masses so we have:

A relates to atomic mass number equal to 256 – it is the semi-major axis of Mercury,

$A + B_{\text{mean}}$ relates to atomic mass number 256 **too** but it decays to two parts (for Venus),

$A + 2B_{\text{mean}}$ relates to 128 (for Earth),

$A + 4B_{\text{mean}}$ relates to 64 (for Mars),

$A + 8B_{\text{mean}}$ relates to 32 (for the asteroid/dwarf-planet Ceres),

$A + 16B_{\text{mean}}$ relates to 16 (for Jupiter),

$A + 32B$ relates to 8 (for Saturn),

$A + 64B_{\text{mean}}$ relates to 4 (for Uranus),

$A + 96B_{\text{mean}}$ relates to 3 (for Neptune): it is not the TB orbit,

$A + 128B_{\text{mean}}$ relates to 2 (for Pluto),

$A + 256B_{\text{mean}}$ relates to 1: it is outside the Kuiper cliff so such orbit can be empty. (4.2.28)

Assume that a progenitor of the Solar System was a black hole composed of $4^4 = 256$ NBHs so the mass of the progenitor was

$$M_{\text{Progenitor}} = 4^4 m_{\text{NBH}} = 1.263 \cdot 10^{34} \text{ kg} , \quad (4.2.29)$$

where $m_{\text{NBH}} = 24.81 \text{ solar masses}$.

Now the central mass is

$$M_{\text{Sun}} = 1.9885 \cdot 10^{30} \text{ kg} . \quad (4.2.30)$$

Range is inversely proportional to mass so the semi-major axes of the rings increased following number of times

$$F = M_{\text{Progenitor}} / M_{\text{Sun}} = 6352 . \quad (4.2.31)$$

At the beginning, the radius of the Mercury ring, $A_{\text{Beginning}}$, was equal to

$$A_{\text{Beginning}} = G M_{\text{Progenitor}} / c^2 = 9.379 \cdot 10^6 \text{ m} . \quad (4.2.32)$$

Now the semi-major axis of Mercury should be

$$A_{\text{Now}} = F A_{\text{Beginning}} = 5.958 \cdot 10^{10} \text{ m} = 0.398 \text{ au} . \quad (4.2.33)$$

This value is very close to the actual semi-major axis of Mercury $A_{\text{Mercury,actual}} = 0.387 \text{ au}$. The difference is $\sim 3\%$.

Can we show that the relationships between the gravitational black holes and the strong black holes in baryons are not only related to the TB law?

Mass of the charged core of baryons is $H^\pm = 727.4387 \text{ MeV}$. It interacts electromagnetically via the bare electron-positron pair which mass is $2m_{e,\text{bare}} = 1.0208 \text{ MeV}$. Assume that mass of the Sun, M_{Sun} , relates to H^\pm while the sum of the masses H^\pm and $2m_{e,\text{bare}}$ relates to the total mass of the Solar System $M_{\text{Solar-System}}$ – then we obtain

$$M_{\text{Sun}} / M_{\text{Solar-System}} = H^\pm / (H^\pm + 2m_{e,\text{bare}}) = 0.9986 . \quad (4.2.34)$$

This value is in perfect agreement with the observational data (see page 10 in [1]).

The Oort cloud contains the long period comets and extends from between $\sim 2,000$ and $\sim 5,000 \text{ au}$ to $\sim 200,000 \text{ au}$ from the Sun [2]. The models based on the observations of the comets suggest that the Oort cloud is divided into two regions: a spherical outer cloud and a scattered disc [3]. As the distance from the Sun increases, the scattered disc expands more and more in the directions transverse to the disc.

With time, the initial black hole was replaced by the Type-Ia supernova. Here we show that the Oort cloud was formed due to the scattering of matter on the Mercury orbit during the Type-Ia supernova (SN) explosion.

In SST, the key role in fermions plays torus. The strong interactions in baryons are associated with the radial motions of gluons emitted by a torus – such interactions, because of the internal structure of the torus, are possible only in hadrons. The electromagnetic interactions relate to the toroidal motions in the plane of the equator of the torus, while the weak interactions relate to the poloidal motions. We can see that the three motions are orthogonal! The poloidal motions are perpendicular to the equatorial plane of the torus so they scatter the radial and toroidal motions.

Most of matter on the Mercury orbit, because of the conservation of the angular momentum, was scattered in the plane of the Mercury orbit. The scattered disc-like region in the Oort cloud is a result of the increasing spin speed of the thin matter torus that overlapped with the Mercury orbit so it was due to the electromagnetic interactions at high energy. On the other hand, the spherical region in the Oort cloud is a result of a volumetric expansion of the thin torus – there appeared the radial motions so it was due to the nuclear strong interactions.

The radius of the Mercury orbit, $A_{\text{SN-Ia}}$, just before the supernova explosion, was

$$A_{\text{SN-Ia}} = A_{\text{Now}} M_{\text{Sun}} / M_{\text{SN-Ia}} = 0.2856 \text{ au} , \quad (4.2.35)$$

where $M_{\text{SN-Ia}} = 1.3934 \text{ solar masses}$ (see formula (4.2.24) for $\mu_{\text{bare}}^\pm/2$).

The inner radius, $R_{\text{Oort,inner}}$, of the inner edge of the scattered disc in the Oort cloud follows from the transition from the electromagnetic interactions at high energy on the Mercury orbit to the weak interactions of electrons on the inner edge of the scattered disc. Radius is inversely proportional to coupling constant so we have

$$R_{\text{Oort,inner}} = A_{\text{SN-Ia}} \alpha_{\text{em,high}} / \alpha_{\text{w(e)}} \approx 2,350 \text{ au} , \quad (4.2.36)$$

where $\alpha_{w(e)} = 0.9511186121 \cdot 10^{-6}$ is the coupling constant of the weak interactions of electrons, and $\alpha_{em,high} = 1 / 127.548$ (see formula 2.10.3). The “mixture” of the toroidal electromagnetic motions and the radial strong motions caused that with increasing distance from the Sun, the scattered disc expands more and more in the directions transverse to the disc.

The intermediate semi-major axes for the objects in the scattered disc we obtain for the mixed interactions in the Mercury orbit – here they are the strong and electromagnetic interactions.

The inner radius, $R_{Oort,inner-sphere}$, and outer radius, $R_{Oort,outer-sphere}$, of the spherical region in the Oort cloud result from the transition from the nuclear strong interactions on the Mercury orbit to the weak interactions of electrons on the most distant sphere. But during the supernova explosion, on the Mercury orbit appeared the turbulent motions so baryons had the relativistic masses. In such nuclear plasma, the coupling constant of the nuclear strong interactions is the running coupling – inside baryons it changes from $\alpha_{sw,asymptote} = 0.1138$ (see c_u in (2.14.20)) to $\alpha_s = 1$. Such values define the inner radius and outer radius of the spherical region in the Oort cloud

$$R_{Oort,inner-sphere} = A_{SN-Ia} \alpha_{sw,asymptote} / \alpha_{w(e)} \approx 34,000 \text{ au} , \quad (4.2.37)$$

$$R_{Oort,outer-sphere} = A_{SN-Ia} \alpha_s / \alpha_{w(e)} \approx 300,000 \text{ au} = 4.75 \text{ ly} . \quad (4.2.38)$$

The weak interactions of the electrons are very weak in relation to the strong and electromagnetic interactions of baryons so we neglect a deformation of the Oort cloud resulting from the poloidal motions.

We can see also that the mass of the Oort cloud should be close to the mass of the thin torus which overlapped with the Mercury orbit so it should be close to masses of planets.

Notice also that for the weak interactions of nucleons we obtain

$$R^*_{Oort} = A_{SN-Ia} \alpha_{w(p)} / \alpha_{w(e)} \approx 5,600 \text{ au} , \quad (4.2.39)$$

so for such and bigger distances, the number density of comets should be higher. Moreover, such a region should be deformed due to the poloidal motions.

We showed that SST leads to a spherical outer Oort cloud that should extend from $\sim 34,000 \text{ au}$ to $\sim 300,000 \text{ au}$, while a scattered-disc inner Oort cloud should extend from $\sim 2,350 \text{ au}$ to $\sim 34,000 \text{ au}$.

Why, unlike the radii of the planetary rings, did not the semi-major axes of the long-period comets in the Oort cloud increase in size following the SN-Ia explosion?

The thin torus of the nuclear plasma with its internal nuclear strong interactions, which overlapped with the orbit of Mercury, shielded the planetary ring system from destruction and mass changes during the supernova explosion.

Moreover, such a thin torus caused the disc part of the Oort cloud to be scattered.

Over time, as part of the ejected mass by the supernova (about 0.4 solar mass) flowed through the just formed Oort cloud, the masses of the components of this cloud increased, but on the other hand, the decreasing central mass decreased the orbital speeds of the comets. Since the orbital angular momentums of comets must be conserved, which is the product of mass, orbital velocity, and orbital radius, the semi-major axes of comets, contrary to the radii of the planetary rings, should not change significantly – they could decrease as well.

The mechanism of the formation and evolution of the Oort cloud described in this Paragraph differs significantly from that proposed in mainstream astrophysics. Under the mainstream

mechanism, unlike the one presented here, we cannot accurately predict the properties of the Oort cloud. We can see, however, that the appearing free parameters in the mainstream mechanism allow us to obtain values of some physical quantities consistent with the observations, but such additional parameters strongly distort the physical picture. Therefore, I warn against theories, models and simulations in which there are free parameters.

From the observations results that a mean mass of the long-period comets is about $5 \cdot 10^{12}$ kg – the estimated masses of a set of long-period comets are $[0.5, 10] \cdot 10^{12}$ kg [4]. The number of long-period comets is $\sim 10^{12}$ [5].

From observational data results that the more massive black holes (as, for example, in quasars) are surrounded by an opaque torus. Assume that our black hole composed of the 256 NBHs also was surrounded by such a torus. Assume also that the characteristic sizes of the black hole and its torus were directly proportional to the sizes in the core of baryons.

On the assumption that the radius of the central condensate in baryons relates to the present-day semi-major axis of Mercury, $A_{\text{Mercury,actual}} = 0.387 \text{ au}$, we obtain that the today mean distance of the initial opaque torus from the Sun, $R_{\text{Torus,mean}}$, should be

$$R_{\text{Torus,mean}} = A_{\text{Mercury,actual}} / \alpha_{w(p)} \approx 20.7 \text{ au} , \quad (4.2.40)$$

while its today equatorial radius, $R_{\text{Torus,equator}}$, should be

$$R_{\text{Torus,equator}} = R_{\text{Torus,mean}} \sqrt{3} \approx 31.0 \text{ au} . \quad (4.2.41)$$

We can see that the calculated distances are close to the present-day semi-major axes of the Uranus (19.2 au) and Neptune (30.1 au) respectively so there should be formed the Neptune even when the symmetry describing the symmetrical decays is not broken.

Today, the inner radius of the opaque torus, $R_{\text{Torus,inner}}$, should be equal to 1/3 of its equatorial radius

$$R_{\text{Torus,inner}} = R_{\text{Torus,equator}} / 3 \approx 10.3 \text{ au} . \quad (4.2.42)$$

Table 17 *Comparison of semi-major axes in [au]*

	$R_{\text{SM-O}}$ from observations	$R_{\text{SM-T}}$ from opaque torus	$R_{\text{SM-TB}}$ from TB
Saturn	9.6	10.3	9.9
Uranus	19.2	20.7	19.3
Neptune	30.1	31.0	28.7

The value in (4.2.42) is close to the semi-major axis of the Saturn (9.5 au).

In Table 17, we compared the observed semi-major axes, $R_{\text{SM-O}}$, of the Saturn, Uranus and Neptune with semi-major axes calculated from the sizes of the opaque torus, $R_{\text{SM-T}}$, and from the TB law that follows from the symmetrical decays of the atomic nuclei ($R_{\text{SM-TB}} [\text{au}] = 0.41 + d \cdot 0.295$, where $d = 32, 64$ and 96).

Table 1 shows that in the case of Neptune and Uranus, contrary to the Neptune, the distribution of matter that was a result of the symmetrical decays of the atomic nuclei dominated over the distribution of matter forced by the sizes of the opaque torus.

Initially, the orbits of Saturn, Uranus and Neptune were additionally fed with matter from the opaque torus so the three planets are today the massive planets. But why is the Jupiter the most massive planet? Initially, the inner accretion disc (i.e. from the black hole to the opaque

torus) also was fed with matter from the opaque torus. On the other hand, the Jupiter orbit was the closest orbit to the inner boundary of the opaque torus – it is the reason that today Jupiter is the most massive planet.

It is impossible to understand the cosmogony of the Solar System without two new symmetries described in SST (i.e. saturation of interactions and symmetrical decays of atomic nuclei in nuclear plasma) and the assumption that our Universe is cyclical.

The large-scale structure of the Universe we are seeing today was formed before it began to expand.

The cosmogony of the Solar System begins with a black hole containing 256 NBHs, which captures the extra NBH and converts it into an accretion disc.

Notice that there was a quantum resonance between the 256 NBHs in the black hole and the 256 nucleons in the atomic nuclei created in the nuclear plasma near the equator of the black hole.

The inflows of dark energy and dark-matter loops cause that the black hole evaporates, ejecting matter mainly along its axis of rotation. This mechanism causes protoplanet orbital radii to increase.

When the central star's mass decreased to about 1.4 solar masses, it exploded as a supernova, a key moment for the survival of the Solar System. Our Sun was formed about 4.6 Gyr ago from the remnants of such an explosion.

The question is: where are the remaining fragments of the original black hole? New stars were formed from the nuclear plasma ejected along the axis of rotation, and these are stars scattered around the Solar System inside a sphere with a radius of about 100 light-years.

The only planet whose semi-major axis does not obey the TB law is Neptune, but note that the symmetry of symmetrical decays relates to hot nuclear plasma. Thus, this symmetry at the periphery of the accretion disc can be broken. Helium-4 is for Uranus and deuterium is for Pluto, so the orbit for the stable He-3 should have a semi-major axis which is the arithmetic mean of the semi-major axes of Uranus and Pluto – this is consistent with the observational data for Neptune. Notice that the broken symmetry for Neptune was forced by the fact that the Neptune orbit had overlapped with the equatorial radius of the opaque torus.

The Kuiper belt is the remnant of the outer edge of the initial accretion disc, while the Oort cloud is the remnant of the type Ia supernova explosion.

The Solar System is unique because its history goes back to the origins of our Universe and its structure could have been damaged many times.

References

- [1] M M Woolfson (2000). "The Origin and Evolution of the Solar System"
Institute of Physics Publishing, Bristol and Philadelphia
ISBN 0 7503 0457 X (hbk)
ISBN 0 7503 0458 8 (pbk)
- [2] www.phys.org/news/2015-08-oort-cloud.html
- [3] The European Space Agency
www.esa.int/ESA_Multimedia/Images/2014/12/Kuiper_Belt_and_Oort_Cloud_in_context
- [4] Julio A. Fernández, Andrea Sosa (October 2011). "Mass estimates of long-period comets coming close to the Sun"
EPSC Abstracts, Vol. 6, EPSC-DPS2011-152-1, 2011, EPSC-OPS Joint Meeting 2011
- [5] The European Space Agency
www.esa.int/Science_Exploration/Space_Science/Rosetta/How_many_comets_are_there

4.2.6. Magnetars versus pulsars

Calculate the radius of the spin-1 dark-matter loops (see formula ())

$$R_{\text{DM-loop,spin=1}} = \hbar / (M_{\text{DM-loop}} c) = 16.915 \text{ km} . \quad (4.2.43)$$

Such a radius of neutron star leads to its mass equal to the TOV limit, i.e. 2.441 **solar masses** (see formulae (3.3.3) and (3.3.4)). The spin speed of the resting DM loops is equal to c .

We claim that magnetars are the neutron stars interacting weakly with the spin-1 DM loops i.e. the initial mass of magnetars should be close to the TOV limit: $M_{\text{Magnetar}} = 4.854 \cdot 10^{30}$ **kg**. Due to the weak interactions of the spin-1 DM loops with the nuclear-plasma vortex on surface of a magnetar, angular momentum of the vortex increases. We define the nuclear plasma as the plasma composed of 50% of protons and 50% of neutrons. Initially the weak interaction increases the spin speed of the nuclear-plasma vortex so there is created the very strong magnetic field, but as time goes on, the star's rotation slows down so the strong magnetic field weakens. Slowing the magnetar's rotation causes the radii of the DM loops to increase, separating them from the magnetar. Such increases in the radii of the DM loops combined with the weak interactions cause that the baryon matter is scattered, so with time mass of the magnetar decreases.

Magnetic axis of magnetar has the same direction as the angular momentum of the DM loops. In neutron-stars, there can be an angle different from zero between the magnetic axis and the axis of rotation.

Rotation of the free NSs is slowing down because of the friction between the rotating part of the SST absolute spacetime inside the NSs and the non-rotating part outside them (the spin down).

The friction in the SST-As together with strong magnetic field causes the emission of the polarized electromagnetic radiation.

The observed pulse periods of the so-called "normal pulsars" are between 0.3 s and 3 s. Assume that a pulsar with a mass of the TOV limit (so its radius is $R_{\text{Magnetar}} = 1.6915 \cdot 10^4$ **m**) has the pulse period equal to $t = 1$ s. Then the spin speed of the nuclear-plasma vortex, V_{Vortex} , is

$$V_{\text{Vortex}} = 2 \pi R_{\text{Magnetar}} / t = 1.0628 \cdot 10^5 \text{ m/s} . \quad (4.2.44)$$

On the other hand, from (4.2.10) follows (there instead the α_s is $2\alpha_{w(p)}$) that the DM loops, due to their weak interactions with the condensates in centres of baryons, increase the spin speed of the nuclear-plasma vortex to $V_{\text{Vortex-with-loops}}$

$$V_{\text{Vortex-with-loops}} = c (\alpha_{w(p)})^{1/2} = 5.8013 \cdot 10^7 \text{ m/s} . \quad (4.2.45)$$

It means that the DM loops increase the spin speed and decrease the vortex period, t^* , N times

$$N = V_{\text{Vortex-with-loops}} / V_{\text{Vortex}} = 546 , \quad (4.2.46)$$

$$t^* = t / N = 1.83 \cdot 10^{-3} \text{ s} . \quad (4.2.47)$$

The Biot-Savart law relates magnetic fields to the currents. The magnetic field (magnetic flux density), \mathbf{B} , at centre of a current loop (of the nuclear-plasma vortex) with a radius R is

$$\mathbf{B} = \mu_0 \mathbf{Q} / (2 R t) , \quad (4.2.48)$$

where t is the period (in magnetars it is the vortex period t^*), $\mu_0 \approx 1.26 \cdot 10^{-6} \text{ H/m}$ is the magnetic constant (the vacuum permeability), and \mathbf{Q} is the total charge of the loop/vortex.

From (4.2.48) results that magnetic field is inversely proportional to pulse period. Since the DM loops decrease the pulse period N times so magnetic field of a magnetar with such a mass is N times higher than the pulsar in the absence of the DM loops. We can see that magnetic fields of magnetars are indeed very strong.

The mass of the nuclear-plasma vortex, M_{Plasma} , should be as many times lower than the mass of the magnetar as the mass of the DM loop, $M_{\text{DM-loop}} = 2.0796 \cdot 10^{-47} \text{ kg}$, is lower than the mass n of the neutron

$$M_{\text{Plasma}} = M_{\text{Magnetar}} M_{\text{DM-loop}} / n = 6.027 \cdot 10^{10} \text{ kg} . \quad (4.2.49)$$

It leads to the total electric charge, Q , of the nuclear-plasma vortex

$$Q = e M_{\text{Plasma}} / (2 M_{\text{Nucleon}}) = 2.885 \cdot 10^{18} \text{ C} , \quad (4.2.50)$$

where e is the electric charge of proton, and M_{Nucleon} is the mean mass of proton and neutron.

From the Biot-Savart law with the vortex period t^* , we have

$$\mathbf{B}_{\text{Magnetar}} = \mu_0 \mathbf{Q} / (2 R_{\text{Magnetar}} t^*) = 5.87 \cdot 10^{10} \text{ T} . \quad (4.2.51)$$

This result is consistent with observational data because the magnetic field of magnetars is from 10^{10} to 10^{11} T .

The initial period of the nuclear-plasma vortex t^* in magnetar with the TOV-limit mass does not depend on initial period of pulsar

$$t^* = 2 \pi R_{\text{Magnetar}} / v_{\text{Vortex-with-loops}} = 1.83 \cdot 10^{-3} \text{ s} . \quad (4.2.52)$$

For such a magnetar, Q and R_{Magnetar} are the initially invariant values so the magnetic field equal to $\sim 6 \cdot 10^{10} \text{ T}$ is the upper limit **unless there appears an accretion disc** (it strengthens magnetic field).

From formulae (4.2.45) and (4.2.51) follows that the ratio of the magnetic field of the nuclear-plasma vortex, $\mathbf{B}_{\text{Nuclear}}$, to the magnetic field of the vortex of electrons, $\mathbf{B}_{\text{Electron}}$, is

$$\mathbf{B}_{\text{Nuclear}} / \mathbf{B}_{\text{Electron}} = t^*_{\text{Electron}} / t^*_{\text{Nuclear}} = (\alpha_{w(p)} / \alpha_{w(e)})^{1/2} = 140.3 , \quad (4.2.53)$$

so we can neglect the $\mathbf{B}_{\text{Electron}}$ in comparison with the $\mathbf{B}_{\text{Nuclear}}$.

The composition of the nuclear-plasma vortex suggests that there dominates ionized helium-4. Radius of the ground-state orbit/shell in helium, $R_{\text{Helium-4}}$, has the radius 4 times smaller than the Bohr first orbit in hydrogen

$$R_{\text{Helium-4}} = 0.52918 \cdot 10^{-10} \text{ m} / 4 = 0.1323 \cdot 10^{-10} \text{ m} . \quad (4.2.54)$$

From (4.2.52) results that the $P \sim r_{\text{Pulsar}}$ is a relationship between the period, P , of a pulsar and its radius r_{Pulsar} . Assume that the first-time derivative of the period for pulsars, dP/dt (it defines the changes over time in period of the pulsars) is defined by the ratio of the radius of the DM loops overlapping with the ground-state orbit in helium-4, $R_{\text{Helium-4}}$, to radius of the DM loops overlapping with the magnetic equator of the pulsar. For $r_{\text{Pulsar}} = R_{\text{Magnetar}}$, we obtain

$$(dP/dt)_{\text{Pulsar}} = R_{\text{Helium-4}} / R_{\text{Magnetar}} = 0.7821 \cdot 10^{-15} \text{ s/s} . \quad (4.2.55)$$

From (4.2.55) follows that pulsars with smaller the equatorial radii have the first-time derivative of the period higher. Such values for pulsars are consistent with the observational data – see Figure 1 in [1].

In the pulsars, there is the friction between the rotating and non-rotating parts of the Einstein spacetime. But the friction in magnetars is much stronger because there appears also the very strong friction between the neutron star and the nuclear-plasma vortex. We can assume that the friction in pulsars leads to the electroweak interactions so there are produced the electron-neutrino pairs with energy equal to the mass distance between the charged and neutral pions: it is $\Delta\pi \approx 4.6 \text{ MeV}$. On the other hand, the friction in magnetars leads to the nuclear strong interactions represented by the fundamental gluon loops with energy equal to $m_{\text{FGL}} = 67.544 \text{ MeV}$. We can assume that the thermodynamic temperature T in the Stefan-Boltzmann law (see formula (1.4.20)) is directly proportional to involved energy while the total emitted energy is directly proportional to the changes in period, so we have

$$(dP/dt)_{\text{Magnetar}} / (dP/dt)_{\text{Pulsar}} = (m_{\text{FGL}} / \Delta\pi)^4 = 4.6 \cdot 10^4 . \quad (4.2.56)$$

From (4.2.55) and (4.2.56) we obtain

$$(dP/dt)_{\text{Magnetar}} = 3.6 \cdot 10^{-11} \text{ s/s} . \quad (4.2.57)$$

From (4.2.55) and (4.2.56) results that magnetars with smaller the equatorial radii have the first-time derivative of the period higher. Such values for magnetars are consistent with the observational data – see [2] and figure 1 in [1].

Due to the strong friction in magnetars between the nuclear-plasma vortex and neutron star, the high temperature of the very thin iron crust below the vortex sometimes damages it almost simultaneously at two or more points, each with a diameter of several dozen metres. Through the damages, high-energy photons and neutrinos from beta decays are emitted. The damages are quickly repaired when the local pressure is reduced – such a mechanism produces millisecond pulses, and their time distance may be a second or so. Such a phenomenon was observed in magnetar SGR 1935+2154 [3].

References

- [1] Australia Telescope National Facility. “Pulsars, magnetars and RRATs”
www.atnf.csiro.au/news/newsletter/jun06/RRATs.htm
- [2] McGill Online Magnetar Catalog (1 September 2020).
www.physics.mcgill.ca/~pulsar/magnetar/main.html

- [3] F. Kirsten, et al. (16 November 2020). “Detection of two bright radio bursts from magnetar SGR 1935+2154”
Nature Astronomy (2020), <https://doi.org/10.1038/s41550-020-01246-3>
 arXiv:2007.0501v2 [astro-ph.HE] 9 October 2020

4.3. Nuclear physics

4.3.1. The four-shell model of atomic nucleus

The sum of the masses of the relativistic charged pion and neutral pion (the W_d masses) in the $d = 1$ state is 424.4051 MeV. The nucleons that an alpha particle is composed of, occupies the vertices of the square with the diagonal of the square equal to $A + 4B_{\text{mean}}$. The exchanged pions are most frequently located in the centre of this square. As $A / R_d = v^2 / c^2$, and $W_{(+o),d} = \pi_{\text{bound}}^{\pm 0} / [1 - (v^2 / c^2)]^{1/2}$, and here $R_d = (A + 4B_{\text{mean}}) / 2$, the sum of the masses of the charged and neutral W_d pions is 394.5011 MeV. The distance between the mass of the unbound and bound states is 29.90405 MeV per two nucleons, so the volumetric binding energy per nucleon is 14.9520 MeV.

The side of the square and side of a cube occupied by each nucleon is

$$a_c = (A + 4B_{\text{mean}}) / 2^{1/2} = 1.912565 \cdot 10^{-15} \text{ m} . \quad (4.3.1)$$

We can assume that the nucleons inside a nucleus are placed on the concentric spheres where the distances between them equal a_c . This means that the radius of the first sphere is equal to $a_c/2$. This, therefore, leads to the following formula for the radii of the spheres (they are not the radii of the nuclei because the spheres have a thickness)

$$r_{\text{sn}} = (s - 0.5) a_c , \quad (4.3.2)$$

where $s = 1, 2, 3, 4$.

The maximum number of nucleons placed on a sphere is (one nucleon occupies a square with the area equal to a_c^2)

$$A_n = 4 \pi r_{\text{sn}}^2 / a_c^2 = 4 \pi (s - 0.5)^2 \quad (4.3.3)$$

i.e. $A_1 = 3.14$, $A_2 = 28.27$, $A_3 = 78.54$ and $A_4 = 153.94$.

If we round these numbers to the nearest even number (nuclei containing an even number of nucleons are more stable), we obtain the following series: 4, 28, 78, and 154. This means that on the first four wholly filled spheres there are 264 nucleons. As we see by the first two numbers, the sum of the first and third and the result of subtracting the third and second, and the fourth and second numbers, we can see that the result is the well-known magic numbers of 4, 28, 82, 50, 126. This cannot be a coincidence which confirms that we are on the right path in order to build the correct theory of an atomic nucleus. When the number of neutrons becomes equal to one of the magic numbers then transitions of the protons between lower and higher spheres occurs. This increases the binding energy of a nucleus.

4.3.2. Coupling constants and binding energy

According to SST, the spacetime as a whole is flat. According to Newton's second law, in the regular 3-dimensional Euclidean space is

$$F_i = d p_i / d t . \quad (4.3.4)$$

According to SST, constants of interactions G_i are directly proportional to the inertial mass densities of fields carrying the interactions (see (2.1.26)). The following formula defines the coupling constants (or running couplings), α_i , of all interactions (see (2.14.9)) (notice that m_i can be both mass or massless energy responsible for interactions)

$$\alpha_i = G_i M_i m_i / (c \hbar) , \quad (4.3.5)$$

where M_i defines the sum of the mass of the sources of interaction plus the mass of the component of the field, whereas m_i defines the mass/energy of the carrier of interactions.

The strong coupling constant for pions exchanging the fundamental gluon loop (its mass is a little higher than a half of the mass of neutral pion, $m_{FGL} = 67.54441 \text{ MeV}$) is $\alpha_s^{\pi\pi, FGL} = 1$ (see (2.14.10)). Coupling constant for strongly interacting protons, at low energies (as it is in the atomic nuclei), is $\alpha_s^{pp, \pi} = 14.39118$ whereas for strongly interacting neutrons is $\alpha_s^{nn, \pi} = 14.40991$. To the alpha particle, we can apply the mean value $\alpha_s^{NN, \pi} = 14.40055$. When we accelerate a baryon, then there decreases the spin speed of the FGL so mass of it decreases as well – it leads to the running coupling for the nuclear strong interactions.

Assume that a carrier of interactions interacts simultaneously, for example, strongly and electromagnetically. Then, strong mass is $\alpha_s m$ whereas electromagnetic mass of the strong mass is $\alpha_{em} \alpha_s m$. It leads to conclusion that resultant coupling constant α is the product, Π , of coupling constants involved in the interactions

$$\alpha = \Pi \alpha_i . \quad (4.3.6)$$

When a carrier is a binary system then there appears the factor 2 i.e.

$$\alpha = 2 \Pi \alpha_i . \quad (4.3.7)$$

Due to the radial emissions of carriers of interactions or radial polarization of virtual pairs, there is the inverse square law

$$F_i = G_i M_i m_i / r^2 . \quad (4.3.8)$$

Applying formulae (4.3.4) – (4.3.8), we obtain

$$\int dp_i = \Pi \alpha_i c \hbar \int (1 / r^2) dt . \quad (4.3.9)$$

$$p v = \Pi \alpha_i c \hbar \int (1 / r^2) dr . \quad (4.3.10)$$

The radial kinetic energy, E_{kin} , transforms into radiation energy, $E_{radiation}$, so into binding energy, $E_{binding}$, as well i.e. $E_{kin} = p v / 2 = E_{radiation} = - E_{binding}$. We can rewrite formula (4.3.10) as follows

$$E_{binding} = - \Pi \alpha_i c \hbar / (2 r) . \quad (4.3.11)$$

When we express this energy in **MeV** then there appears the factor F

$$E_{\text{binding}} [\text{MeV}] = m_{\text{binding}} c^2 = - \Pi \alpha_i c \hbar / (2 r F), \quad (4.3.12)$$

where $F = 1.7826617 \cdot 10^{-30} \text{ kg/MeV}$.

Introduce symbol k

$$k = \hbar / (2 c F) = 9.866347 \cdot 10^{-14} [\text{MeV m}]. \quad (4.3.13)$$

Formulae (4.3.12) and (4.3.13) lead to

$$m_{\text{binding}} [\text{MeV}] = - k \Pi \alpha_i / r. \quad (4.3.14)$$

It is the main formula.

Calculate the binding energy of electron in the ground state in hydrogen atom. We have $\Pi \alpha_i = \alpha_{\text{em}} = 1/137.036$ and $r_B = 0.529177 \cdot 10^{-10} \text{ m}$. Applying formula (4.3.14), we obtain

$$m_{\text{binding}} [\text{MeV}] = - 13.606 \cdot 10^{-6} \text{ MeV}. \quad (4.3.15)$$

Calculate the binding energy and radius of the deuteron. The tori of nucleons in deuteron do not overlap even partially when the smallest distance is $r_{\text{np}} = A + 2B_{\text{mean}}$. Then at low energy we have $\alpha_s = 1$. When we assume that there are exchanged also the Y condensates then we obtain

$$m_{\text{binding,deuteron}} [\text{MeV}] = - 2 k \alpha_s \alpha_{w(p)} / r_{\text{np}} \approx - 2.2 \text{ MeV}. \quad (4.3.16)$$

Radii of the deuteron in the directions of the x-axis and y-axis are

$$R_{x,y} = r_{\text{np}} / 2 + (A + B_{\text{mean}}) \approx 2.05 \text{ fm}. \quad (4.3.17)$$

Calculate the mean binding energy per nucleon in the alpha particle.

According to the SST, the two protons and two neutrons are placed in vertices of square which diagonal is $D = A + 4B_{\text{mean}} = 2.704776 \text{ fm}$, where $A = 0.6974425 \text{ fm}$ is the equatorial radius of the core of baryons, whereas $B_{\text{mean}} = 0.5018333 \text{ fm}$. There are 6 directions of strong interactions i.e. the 4 sides of the square and its two diagonal directions. It leads to conclusion that mean distance of strong interactions is

$$R = [2 D + 4 D / 2^{1/2}] / 6 = 2.176636 \text{ fm}. \quad (4.3.18)$$

The strong interactions of the four nucleons follow from the exchanges of the pions. It means that they interact strongly, $\alpha_s^{\text{NN},\pi} = 14.40055$, and electromagnetically $\alpha_{\text{em}} = 1/137.036$ i.e.

$$\Pi \alpha_i = \alpha_{\text{em}} \alpha_s^{\text{NN},\pi} = 0.105086. \quad (4.3.19)$$

From formulae (4.3.16), (4.3.18) and (4.3.19) we obtain the total strong binding energy for the alpha particle

$$m_{\text{binding,total}} [\text{MeV}] = -6 k \alpha_{\text{em}} \alpha_s^{\text{NN},\pi} / R = -28.5803 \text{ MeV} . \quad (4.3.20)$$

From the obtained absolute value 28.606 MeV , we must subtract the energy E_{em} which follows from the electrostatic repulsion of the protons. On the assumption that probabilities of the two different distances are the same for the electromagnetic interactions, we obtain

$$E_{\text{em}} = k \alpha_{\text{em}} / (D + D / 2^{1/2}) = 0.31186 \text{ MeV} . \quad (4.3.21)$$

The mean binding energy per nucleon, ΔE , in the alpha particle is

$$\Delta E = (m_{\text{binding,total}} + E_{\text{em}}) / 4 = -7.0735 \text{ MeV} . \quad (4.3.22)$$

On the assumption that the height of the rectangular prisms composed of 5 neutrons and 3 protons is $D = A + 4B_{\text{mean}}$, we obtain correct binding energies for other nuclei.

4.3.3. Model of dynamic supersymmetry for nuclei

From [1] results that the nucleons in a nuclei are grouped in following way

$\Theta \equiv 2$ protons and 2 neutrons,

$\Phi \equiv 3$ protons and 5 neutrons,

$\Gamma \equiv 3$ protons and 4 neutrons,

$\Psi \equiv 1$ proton and 1 neutron.

The SST explains the above as follows

** A proton exists in two states with the probabilities:

$$y = 0.50838 \text{ and } 1 - y = 0.49162.$$

If we multiply these probabilities by two (for a deuteron) or by four (for an alpha particle), we obtain the integers (approximately) because the probabilities are that y and $1 - y$ have almost the same values.

** A neutron exists in two states with the probabilities:

$$x = 0.62554 \text{ and } 1 - x = 0.37446.$$

If we multiply these probabilities by eight, we obtain in the integers approximately 5 (5.004) and 3 (2.996). The 8 is the smallest integer which leads to integers (in approximation). Such structures are the rectangular-prisms.

** For a system containing 50% of the proton-type structures and 50% of the neutron-type structures, we obtain the following probabilities

$$(x + y) / 2 = 0.56696 \text{ and } (1 - x + 1 - y) / 2 = 0.43304.$$

This factor is equal to 7 – then we obtain 3.969 i.e. approximately 4, and 3.031 i.e. approximately 3.

A nucleus chooses a mixture of the states Θ , Φ , Γ and Ψ in such a manner the binding energy was the greatest. The Θ groups appear when the interactions of protons dominate whereas the Φ groups appear when the interactions of neutrons dominate.

Describe the path of stability

Applying the model of dynamic supersymmetry for nuclei, we showed the abundances of the structures Θ , Φ , Γ and Ψ in most stable nuclei (Table 18).

The consistency with the experimental data is very high – only one result is inconsistent with experimental data. SST shows that the abundance of the 78Pt194 should be slightly higher than the 78Pt195.

References

- [1] P. Van Isacker, J. Jolie, K. Heyde and A. Frank; *Extension of supersymmetry in nuclear structure*; Phys. Rev. Lett. **54** (1985) 653

Table 18 *Main path of stability of nuclei*

ZXA	Θ	Φ	Γ	Ψ	ZXA	Θ	Φ	Γ	Ψ	ZXA	Θ	Φ	Γ	Ψ
1H1					36Kr84	9	6			71Lu175	10	16	1	
2He4 \mathbf{m}	1				37Rb85	9	5	1	1	72Hf180	9	18		
3Li7			1		38Sr88 \mathbf{m}	10	6			73Ta181	9	17	1	1
4Be9			1	1	39Y89	10	5	1	1	74W184	10	18		
5B11	1		1		40Zr90 \mathbf{m}	12	5		1	75Re187	9	18	1	
6C12	3				41Nb93	11	5	1	1	76Os192	8	20		
7N14	3			1	42Mo98	10	7		1	77Ir193	8	19	1	1
8O16 \mathbf{m}	4				43Tc97	12	5	1	1	78Pt194 ?	10	19		1
9F19	3		1		44Ru102	11	7		1	79Au197	9	19	1	1
10Ne20	5				45Rh103	12	6	1		80Hg202	8	21		1
11Na23	4		1		46Pd106	12	7		1	81Tl205	7	21	1	1
12Mg24	6				47Ag107	13	6	1		82Pb208 \mathbf{m}	8	22		
13Al27	5		1		48Cd114	10	9		1	83Bi209	8	21	1	1
14Si28	7				49In115	11	8	1		84Po209	10	20	1	1
15P31	6		1		50Sn120 \mathbf{m}	10	10			85At210	12	20		1
16S32	8				51Sb121	10	9	1	1	86Rn222	5	25		1
17Cl35	7		1		52Te130	6	13		1	87Fr223	6	24	1	
18Ar40	6	2			53I127	10	10	1		88Ra226	6	25		1
19K39	8		1		54Xe132	9	12			89Ac227	7	24	1	
20Ca40 \mathbf{m}	10				55Cs133	9	11	1	1	90 Th 232	6	26		
21Sc45	7	1	1	1	56Ba138	8	13		1	91Pa231	8	24	1	
22Ti48	8	2			57La139	9	12	1		92U238	5	27		1
23V51 \mathbf{m}	7	2	1		58Ce140	11	12			93Np237	7	25	1	1
24Cr52 \mathbf{m}	9	2			59Pr141	11	11	1	1	94Pu244	5	28		
25Mn55	8	2	1		60Nd142	13	11		1	95Am243	7	26	1	
26Fe56	10	2			61Pm147	11	12	1		96Cm247	6	27	1	
27Co59	9	2	1		62Sm152	10	14			97Bk247	8	26	1	
28Ni58 \mathbf{m}	12	1		1	63Eu153	10	13	1	1	98Cf251	7	27	1	
29Cu63	10	2	1		64Gd158	9	15		1	99Es254	7	28		1
30Zn64	10	2	1	1	65Tb159	10	14	1		100Fm253	9	26	1	1
31Ga69	9	3	1	1	66Dy164	9	16			101Md258	8	28		1
32Ge74	8	5		1	67Ho165	9	15	1	1	102No256	12	26		
33As75	9	4	1		68Er166	11	15		1	103Lr256	14	25		
34Se80	8	6			69Tm169	10	15	1	1	104Ku260	13	26		
35Br79	10	4	1		70Yb174	9	17		1					

ZXA – denotes the atomic-number/symbol-of-element/mass-number
 $\Theta = 2p + 2n = 2\text{He}4$; $\Phi = 3p + 5n$; $\Gamma = 3p + 4n = 3\text{Li}7$; $\Psi = p + n = 1\text{D}2$
 ? - denotes the discrepancy with the results in the periodic table of elements
 \mathbf{m} – denotes magic-number nucleus

4.4. Atomic physics

4.4.1. Derivation of the Pauli Exclusion Principle

In general, the Pauli Exclusion Principle follows from the spectroscopy whereas its origin is not good understood. To understand fully this principle, most important is the origin of quantization of the azimuthal quantum number i.e. of the angular momentum quantum number. Here, applying the theory of ellipse and starting from very simple physical condition, we quantized the azimuthal quantum number. The presented model leads directly to the eigenvalue of the square of angular momentum and to the additional potential energy that appears in the equation for the modified wave function.

The Pauli Exclusion Principle says that no two identical half-integer-spin fermions may occupy the same quantum state simultaneously. For example, no two electrons in an atom can have the same four quantum numbers. They are the principal quantum number n that denotes the number of the de Broglie-wave lengths λ in a quantum state, the azimuthal quantum number l (i.e. the angular momentum quantum number), the magnetic quantum number m and the spin s .

On the base of the spectrums of atoms, placed in magnetic field as well, follows that the quantum numbers take the values:

$$n = 1, 2, 3, \dots$$

$$l = 0, 1, 2, \dots, n - 1$$

$$m = -l, \dots, +l$$

$$s = \pm 1 / 2.$$

The three first quantum numbers n , l , and m are the integer numbers and define a state in which can be maximum two electrons with opposite spins.

The magnetic quantum number m determines the projection of the azimuthal quantum number l on the arbitrary chosen axis. This axis can overlap with a diameter of the circle $l = 0$.

To understand fully the Pauli Exclusion Principle we must answer following questions concerning the azimuthal quantum number l :

1. What is physical meaning of this quantum number?
2. Why the l numbers are the natural numbers only?
3. Why the zero is the lower limit?
4. Why the $n - 1$ is the upper limit?

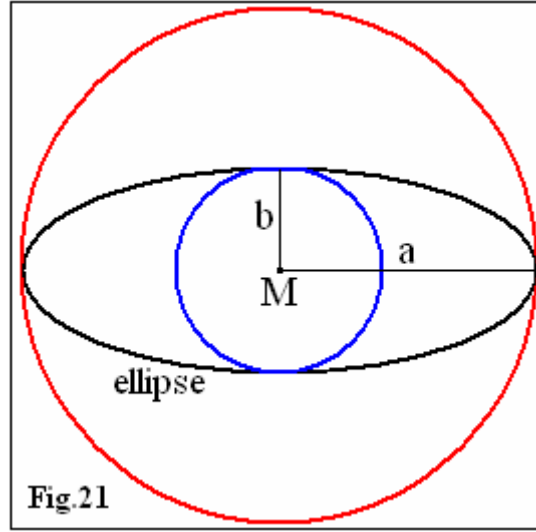
To answer these questions we must apply the theory of ellipse, especially the formula for its circumference C and eccentricity e . When we use the complete elliptic integral of the second kind and the Carlson symmetric form [1], we obtain for circumference C of an ellipse following formula

$$C = 2\pi a [1 - (1/2)^2 e^2 / 1 - (1 \cdot 3 / (2 \cdot 4))^2 e^4 / 3 - (1 \cdot 3 \cdot 5 / (2 \cdot 4 \cdot 6))^2 e^6 / 5 - \dots], \quad (4.4.1)$$

where a is the major radius and e is the eccentricity defined as follows

$$e = (a^2 - b^2)^{1/2} / a, \quad (4.4.2)$$

where b is the minor radius.



In the Fig.21, the circumference of the ellipse $C_{de-Broglie}$ is $C_{de-Broglie} = n \lambda = 2 \pi n \lambda$, where the n is the principal quantum number whereas the λ is the reduced de Broglie-wave length. Assume that there are allowed only ellipses that circumference is the arithmetic mean of the circumferences of two circles that radii are equal to the major and minor radii of the ellipse.

Similarly as for the circumference of the ellipse, the circumferences of the circles must be equal to a natural number multiplied by the de Broglie-wave length. This leads to following definitions

$$a = j \lambda \text{ and } b = k \lambda. \quad (4.4.3)$$

Notice that $j = k = 0$ has no sense.

Then, we can rewrite formula (4.4.2) as follows

$$e = (j^2 - k^2)^{1/2} / j. \quad (4.4.4)$$

It is the natural assumption that the allowed circumferences of the ellipse should be the arithmetic mean of the sum of the circumferences of the two circles. It leads to following conclusion

$$(j + k) / 2 = n. \quad (4.4.5)$$

Define some number l as follows

$$(j - k) / 2 = l. \quad (4.4.6)$$

Formulae (4.4.5) and (4.4.6) lead to following relations

$$j = n + l, \quad (4.4.7)$$

$$k = n - l. \quad (4.4.8)$$

Since the j , k and n are the integers so the number l must be an integer as well. Applying formulae (4.4.7) and (4.4.8) we can rewrite formula (4.4.4) as follows

$$e = 2 (n l)^{1/2} / (n + l). \quad (4.4.9)$$

We can see that due to the square root, this formula has no real sense for $l < 0$. Since the l cannot be negative then from formulae (4.4.5) and (4.4.6) we have $l < n$.

Applying formulae (4.4.3) and (4.4.7), we can rewrite formula (4.4.1) as follows

$$C_K = 2\pi(n + l)\lambda[1 - (1/2)^2 e^2/1 - (1 \cdot 3/(2 \cdot 4))^2 e^4/3 - (1 \cdot 3 \cdot 5/(2 \cdot 4 \cdot 6))^2 e^6/5 - \dots]. \quad (4.4.10)$$

Notice that for $n = l$ is $e = 1$ and then $C_{de-Broglie} > C_K$ i.e. l cannot be equal to n . For $l = 0$ is $C_{de-Broglie} = C_K$ and because l cannot be negative then the $l = 0$ is the lower limit for l .

Some recapitulation is as follows. We proved that the azimuthal quantum number l

- 1) is associated with transitions between the states j and k ,
- 2) is the integer,
- 3) cannot be negative and the lower limit is zero,
- 4) the $n - 1$ is the upper limit.

Some abbreviation of it is as follows

$$l = 0, 1, 2, \dots, n - 1.$$

The Quantum Physics is timeless because a quantum particle disappears in one region of a field or spacetime and appears in another one, and so on. There are no trajectories of individual quantum particles. Quantum Physics concerns the statistical shapes and their allowed orientations. Such procedure simplifies considerably the Quantum Physics.

An ellipse/electron-state we can resolve into two circles that radii are defined by the semi-axes of the ellipse. The two circles in a pair are entangled due to the exchanges of the binary systems of the closed strings (entanglons) the SST-As components (from which are built all the Principle-of-Equivalence particles) consist of. The spin-1 entanglons are responsible for the infinitesimal transformations that lead to the commutators. Calculate a change in the azimuthal quantum number l when the smaller circle or one of identical two circles emits one entanglon (since in this paper is $j \geq k$ so there is the transition $k \rightarrow k - 1$) whereas the second circle in the pair almost simultaneously absorbs the emitted entanglon (there is the transition $j \rightarrow j + 1$). Such transition causes that ratio of the major radius to the minor radius of the ellipse (or circle) increases. From formula (4.4.5) follows that such emission-absorption does not change the principal quantum number n whereas from formula (4.4.6) follows that there is following transition for the azimuthal quantum number l : $l \rightarrow l + 1$. The geometric mean is $(l(l + 1))^{1/2}$ and this expression multiplied by \hbar is the mean angular momentum L for the described transition. This leads to conclusion that eigenvalue of the square of angular momentum L^2 is $l(l + 1)\hbar^2$.

The eigenvalue of the square of angular momentum leads to the additional potential energy E_A (it follows from the radial transitions i.e. from the changes in shape of the ellipses) equal to

$$E_A = L^2 / (2 m r^2) = l(l + 1) \hbar^2 / (2 m r^2). \quad (4.4.11)$$

The energy E_A appears in the equation for the modified wave function.

The SST shows that inside the baryons are only the $l = 0$ states (i.e. there are only the circles) so the quantum mechanics describing baryons is much simpler than for atoms.

References

- [1] Carlson, B. C. (1995). “Computation of real or complex elliptic integrals”
Numerical Algorithms **10**: 13-26. arXiv:math/9409227

4.4.2. Meaning simplification of the Dirac theory of the hydrogen atom

We showed that the Lamb shift follows from the fact that the charged relativistic pion in proton interacts due to the nuclear weak interactions while the electron interacts due to the electromagnetic and weak interactions in presence of dark matter (see Section 2.17).

We showed that the hyperfine splitting in the ground state of hydrogen (it leads to the ~21 cm line) follows from different binding energies of two vortices/spinning-tori (see Section 2.16). When spins are parallel but their directions does not overlap (it is in hydrogen atom) then the singlet state (spin = 0) has lower energy because binding energy is higher.

The Schrödinger equation with a Coulomb potential leads to the Bohr hydrogen atom. Here we show that the Dirac-Sommerfeld fine structure of hydrogen atom is a result of creations and exchanges of the virtual electron-positron pairs. Moreover, it is associated also with the fact that the atom-like structure of proton leads to an effective value of the base of the natural logarithm $e_{\text{eff}} = 2.66666\dots$

The fermions consist, at least for period of spinning, of the stable/classical structures/bare-fermions plus the quantum fields, so the semiclassical theories are simplest, most fruitful and contain least parameters. And such method is not a mathematical trick – just in such a way behaves Nature. We formulated a very simple semiclassical analog to the Dirac and Sommerfeld theories of the hydrogen atom.

Gravity is associated with the inverse square law. It is because gravitational fields are the gradients produced by masses in the superluminal SST Higgs field. There are the divergently moving classical tachyons so there appears the inverse square law

$$F \sim 1 / R^2 . \quad (4.4.12)$$

Today, in the Higgs field cannot be created any virtual pairs as it is in the SST absolute spacetime. Polarisation and distribution of the virtual pairs in a field ψ composed of the SST-As components causes that such a field is defined by following function

$$\psi = \psi_0 \exp^{-R} , \quad (4.4.13)$$

where $\exp \approx 2.718\dots$ is close to the base of the natural logarithm. In reality, this formula is more complicated for $R \rightarrow 0$ because there appears a torus/charge/spin and central condensate.

We claim that the atom-like structure of baryons leads to an effective value, e_{eff} , of the base of the natural logarithm. We can define it as the sum of the inverses of the relative distances between the TB orbits in the baryons (it defines a slope of the field ψ in proton). There are the four TB orbits for the nuclear strong interactions – the relative distances between them are 1, 1 and 2. But there is also one photonic TB orbit outside the nuclear strong field. Outside such field, the virtual FGL behaves as virtual photon loop which can create one or two virtual electron-positron pairs – when spin of the pair is zero then there is created one pair while is

equal to 1 then to conserve spin of the virtual photon loop there are created two virtual pairs with antiparallel spins. The range of the FGL due to its circumference is $2\pi(2A/3)$, but due to its energy, when we subtract energies of the created virtual pairs (their mean energy is $3m_{e,bare}$) is very close to $A + 10B_{mean}$ (precisely, because the range of the M_{TB} is B_{mean} , there instead the 10 is 9.889 for one pair and 10.065 for two pairs, so the mean is $9.977 \approx 10$). We see that the relative distance of the photonic orbit from the $d = 4$ TB orbit is very close to 6. So we have for baryons the series $\mathbf{1, 1, 2, 6} = \mathbf{0!, 1!, 2!, 3!}$ (to be precise, there is $\mathbf{1, 1, 2, 5.977}$) which leads to following effective value for the base of the natural logarithm for baryons (it is for a mixture of the strong and electromagnetic interactions)

$$e_{eff} = 1 / 0! + 1 / 1! + 1 / 2! + 1 / 5.977 = 2.667 \approx \\ \approx 8 / 3 = 1 / (\mathbf{1} - 1 / \mathbf{2} - 1 / \mathbf{8}) . \quad (4.4.14)$$

Define a following factor associated with the internal structure of proton

$$F_{SST} = 1 / e_{eff} \approx 0.375 . \quad (4.4.15)$$

Can we quantize the value F_{SST} , i.e. can we write an expression that leads to F_{SST} ? Such expression is showed in (4.4.14)

$$F_{SST} = (\mathbf{1} - 1 / \mathbf{2} - 1 / \mathbf{8}) = 0.375 . \quad (4.4.16)$$

Such expression quantizes the factors (1, 1/2, and 1/8) that can appear in formula for energy of the proton-electron system. Formula (4.4.16) suggests as well that we should expand energy into a series because of the interactions via the exchanged virtual pairs. Such virtual pairs produce the holes in SST-As so their masses are negative – it leads to conclusion that the electromagnetic interactions via the virtual pairs must be associated with the second and third factor. With the second factor are associated two virtual electron-positron pairs (one from H^+ and one from electron). Radiation mass can create the second virtual pair so with the third factor are associated four virtual pairs (two from H^+ and two from electron).

In SST, the electromagnetic mass/energy of a mass/energy E is defined as

$$E_{em} = \alpha_{em} E , \quad (4.4.17)$$

where α_{em} is the fine structure constant.

The succeeding k interactions of virtual pairs (in a group of them) with some energy decrease the initial energy the α_{em}^k times.

Energy associated with a loop is inversely proportional to length of wave which is directly proportional to the principal quantum number n : $E \sim 1 / \lambda \sim 1 / n$. It leads to conclusion that each virtual electron-positron pair produced in state defined by n decreases energy (α_{em} / n) times.

The above remarks lead to following formula for hydrogen atom

$$E = m c^2 [\mathbf{1} - (\alpha_{em} / n)^2 / \mathbf{2} - (\alpha_{em} / n)^4 / \mathbf{8}] , \quad (4.4.18)$$

where $m c^2 = 0.5109988 \text{ MeV}$ is the mass of electron.

Notice that for the transition from the electromagnetic interactions to the strong interactions at low energy ($\alpha_{em} \rightarrow \alpha_s = 1$) in the ground state ($n = 1$), the expression in parenthesis transforms into (4.4.16).

The second component

$$E_{B,n} = -m c^2 (\alpha_{em} / n)^2 / 2 \quad (4.4.19)$$

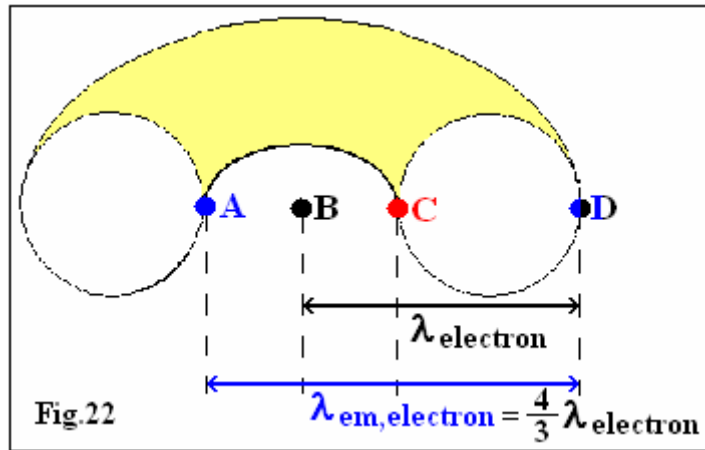
is equal to the energies of the Bohr orbits in the hydrogen atom and $E_{B,n=1} = -13.606 \text{ eV}$.

The third component is the fine structure energy

$$E_{FS,n} = -m c^2 (\alpha_{em} / n)^4 / 8. \quad (4.4.20)$$

This component depends on classical and quantum structure of electron so we must write it in such a way to interpret it correctly. Write the factor $1/8$ as follows

$$1 / 8 = (1 - 3 / 4) / 2. \quad (4.4.21)$$



The $3/4$ represents the classical mass of electron (see Fig.22) which relates to the $\lambda_{em,electron}$ (the points A and D are in the same state) while the quantum mass of electron relates to $\lambda_{electron}$.

We know that maximum azimuthal quantum number l is $l_{max} = n - 1$ so $n / (l_{max} + 1) = 1$. This means that we can rewrite formula (4.4.21) as follows

$$1 / 8 = [n / (l_{max} + 1) - 3 / 4] / 2. \quad (4.4.22)$$

The n and $(l_{max} + 1)$ define the lengths of the de Broglie waves but the additional potential energy $E_A = l(l + 1) \hbar^2 / (2 m r^2)$ (see (4.4.11)) suggests that for defined n there can appear spontaneously as well the other standing waves defined by $l + 1$. For smaller l waves are shorter so corresponding absolute energy is greater. Since in formula (4.4.20) is the sign “-” so the levels defined by smaller and smaller l are closer and closer to the ground state $n = 1$. Finally, we can rewrite formula (4.4.20) as follows

$$E_{FS,n} = -m c^2 (\alpha_{em} / n)^4 [n / (l + 1) - 3 / 4] / 2. \quad (4.4.23)$$

The ground state is shifted by $E_{FS,n=1} = -m c^2 \alpha_{em}^4 [1 - 3/4] / 2 = -1.81 \cdot 10^{-4} \text{ eV}$.
Calculate the energy distance between the states $l = 0, 1$ for defined n

$$\Delta E_{FS,n} = -m c^2 (\alpha_{em} / n)^4 (n / 2) / 2. \quad (4.4.24)$$

For $n = 2$ is $\Delta E_{FS,n=2} = -m c^2 (\alpha_{em} / 2)^4 (1) / 2 = -m c^2 \alpha_{em}^4 / 32 = -4.53 \cdot 10^{-5} \text{ eV}$.

Why we obtained results the same as in the Sommerfeld theory [1]? Why we obtained results the same as in the Dirac theory [2] neglecting the relativistic effects, the spin-orbit interactions, and so on?

It is due to the applied methods – just the standing waves defined by the quantum numbers cannot be changed by any phenomena. Just the quantum numbers define the total picture and must be conserved. The three theories are equivalent because the numbers n_θ in the Sommerfeld theory, $j + 1/2$ in the Dirac theory (the j is not the j in the last two Sections) and $l + 1$ in presented here theory, are the integers and change from 1 to n . But only presented here theory of hydrogen atom proves equivalence of the three theories and describes in all respects the physical origin of the final equation.

References

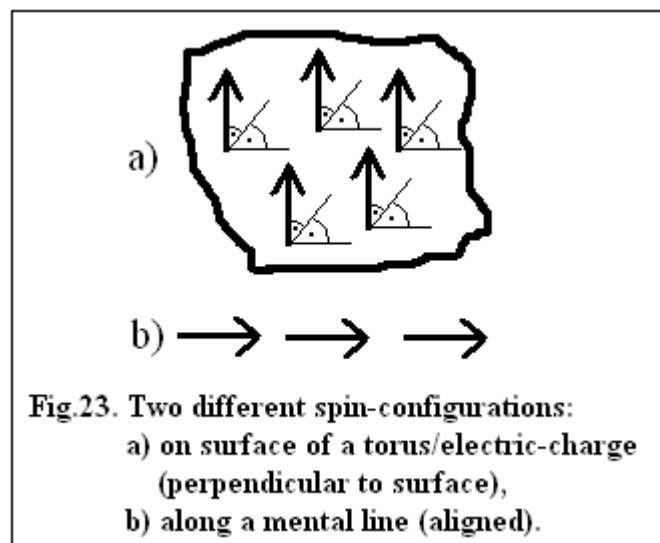
- [1] A. Sommerfeld (1916), *Ann. Physik*, **51**, 1
[2] P. A. M. Dirac (1928), *Proc. Roy. Soc.*, **A117**, 610 (London)

4.5. Brain-mind interactions

4.5.1. The brain-mind interactions

It is very important to unify the particle physics with the mental world via a single field. Consider arrangements of spins of the neutrino-antineutrino pairs in the SST-As.

There are two different spin-configurations of entangled non-rotating-spin neutrino-antineutrino pairs. One configuration leads to the tori/electric-charges whereas the second one leads to the mental lines that can be closed (Fig.23).



A mental soliton consists of crossing sets composed of concentric circles/loops built of the non-rotating-spin neutrino-antineutrino pairs with aligned spins. Such tangled solitons are the

3-dimensional dark-matter structures. They are the flexible but stable structures and baryonic matter is transparent for them.

Tangled circular electric currents, so those inside brains as well, create the mental solitons. Our minds consist of such DM solitons. Due to the current decays and circuit breakers (for example, neurons can do this), entangled smaller and smaller self-similar mental solitons are produced.

Identical parts in different mental solitons attract each other, so there is a struggle for dominance in the minds. Such processes are the origin of the mind-brain interactions.

Our memory is in the form of mental solitons in the mind.

By neglecting the dark-matter structures, we cannot fully understand Nature.

4.6. Chaos theory

4.6.1. Feigenbaum constants

Chaotic behaviour arises in simple non-linear dynamical systems [1].

The Logistic Map is written as follows

$$x_{n+1} = r x_n (1 - x_n), \quad (4.6.1)$$

where x_n is a number between zero and one (the interval $[0, 1]$) that represents the ratio of existing population to the maximum possible population, whereas r is a parameter. It leads to conclusion that r is defined by the interval $[0, 4]$. There are many different logistic maps that in the limit behave the same – it is the Feigenbaum universality. Such maps describe many physical phenomena. Such maps have a similar shape i.e. have a single quadratic maximum. The parameter r defines steepness of the maximum.

A single bifurcation is a splitting of one value into two values. Such bifurcations appear in the Logistic Map for different values of the parameter r . We let r_n be the value of r at which a stable 2^n cycle first appears. At $r = r_1 = 3$ there is a splitting of one a branch into two i.e. there appears an orbit of period $2^1 = 2$, at $r = r_2 \approx 3.4494897\dots$ there is a splitting of two branches into four (each branch splits into two) i.e. there appears an orbit of period $2^2 = 4$, at $r = r_3 \approx 3.54409\dots$ there is a splitting of four branches into eight (each branch splits into two) i.e. there appears an orbit of period $2^3 = 8$, at $r = r_4 \approx 3.5644\dots$ there is a splitting of eight branches into sixteen i.e. there appears an orbit of period $2^4 = 16$, and so on. At the end of the period-doubling cascade, i.e. at $r \approx 3.569946\dots$, there is the onset of chaos i.e. there appears an orbit of infinite period (solution does not contain a periodic orbit) but there sometimes appear islands of stability i.e. the period-doubling windows.

The bifurcation diagram for the Logistic Map is a function $x = f(r)$.

The first Feigenbaum constant results from a numerical work. It is given by the limit

$$\delta = \lim_{n \rightarrow \infty} (r_{n-1} - r_{n-2}) / (r_n - r_{n-1}) = 4.669201609\dots, \quad (4.6.2)$$

or

$$\delta = \lim_{n \rightarrow \infty} (r_{n-2} - r_{n-1}) / (r_{n-1} - r_n) = 4.669201609\dots, \quad (4.6.3)$$

where r_n are discrete values of r at the n th period-doubling. We can see that the successive bifurcations are separated by a distance that asymptotically decreases geometrically by the factor δ .

In the Chaos Theory there is defined an operator that performs the iteration and rescaling. Such operator has a fixed point solution for a particular value of α (it is the second Feigenbaum constant)

$$\alpha \approx 2.50281\dots \quad (4.6.4)$$

For the strong field in baryons we obtain (see formula (4.4.14))

$$\alpha \approx e_{\text{eff, strong}} = 1 / 0! + 1 / 1! + 1 / 2! = 2.500. \quad (4.6.5)$$

It is very close to the second Feigenbaum constant. The gluon loops outside the strong fields of baryons behave as the photon loops, so the structure of proton leaks outside the nuclear strong field and can have an influence on behaviour of physical systems.

The successive symmetrical decays of the boson $r_{n-2} = M_{\text{TB}} = 750.29753 \text{ MeV}$ (the bifurcation) lead to the TB orbits. The boson which reaches the last orbit for the strong interactions has mass $r_{n-1} = M_{\text{TB}}/4$. On the other hand, the fundamental gluon loops ($r_n = m_{\text{FGL}} = 67.54441 \text{ MeV}$) that outside the nuclear strong fields behave as the photon loops, leak outside the strong fields of baryons. So in SST, the first Feigenbaum constant can be defined as follows (it is an analog to formula (4.6.3))

$$\delta \approx (M_{\text{TB}} - M_{\text{TB}} / 4) / (M_{\text{TB}} / 4 - m_{\text{FGL}}) = 4.688. \quad (4.6.6)$$

Such phenomena should be characteristic also for the SST gravitational black holes.

Emphasize that the origin of the Chaos Theory is related to the leakage of the nuclear strong part of the atom-like structure of protons – there are the emissions of the virtual gluon loops that outside the nuclear strong fields behave as the photon loops that interact with the electrically charged particles/structures such as protons, ions, atomic nuclei and electrons.

References

- [1] Steven Strogatz (1994). “Nonlinear Dynamics and Chaos”
Addison-Wesley (1994)

4.7. Quantum physics

4.7.1. Quantum physics in SST

Here within the SST we derived the fundamental equation of the Matrix Quantum Mechanics i.e. the commutator. The fundamental equation results from the quantum entanglement that leads to the infinitesimal transformations. In reality, the Matrix Quantum Mechanics that describes excited states of fields (i.e. the quantum particles) is timeless and non-local i.e. non-deterministic. But the Matrix Quantum Mechanics leads to the time-dependent, so deterministic, wave functions that are characteristic for the Statistical Quantum Mechanics. It is the reason why the wave functions appear in the equations of motion. The Statistical Quantum Mechanics or the Quantum Theory of Fields, are the semiclassical/semi-quantum theories.

The presented here extended Matrix Quantum Mechanics leads to the methods applied in the Quantum Theory of Fields but there appear some limitations.

The idea of existence of many separated parallel worlds is incorrect.

In SST, in descriptions of interactions, most important are tori/charges and loops, especially the gluon loops and photon loops, so as it is in the Matrix Quantum Mechanics, we can start from the definition of commutator applied in the ring theory

$$[\mathbf{I}, \mathbf{B}] = \mathbf{I}\mathbf{U} - \mathbf{U}\mathbf{I}, \quad (4.7.1)$$

where \mathbf{I} and \mathbf{U} are some quantities associated with a ring.

For a spin-1 loop is

$$E_{\text{loop}} T_{\text{lifetime}} = \hbar, \quad (4.7.2)$$

where $E_{\text{loop}} = m_{\text{loop}} c^2$ defines the mass/energy of a loop, and T_{lifetime} is its lifetime (lifetime of a loop is equal to its period of spinning). Lifetime of a virtual loop is inversely proportional to its mass/energy.

There can be a virtual loop/system composed of n entangled spin-1 loops. Denote the energy/mass of a virtual loop, labeled by n , by iE_n ($i^2 = -1$ because virtual objects produce in field holes with negative mass) whereas its lifetime by T_n . Then we obtain

$$(i E_n) T_n = \hbar. \quad (4.7.3)$$

Emission or absorption of one entanglon (its mass is infinitesimal in relation to mass/energy of the loops) by a system changes its spin by $\pm 1\hbar$. Define a change (an amplitude) in mass under the infinitesimal transition from loop labeled by n to loop labeled by k by $E_{n,k}$ whereas a change (an amplitude) in lifetime due to the same transition by $T_{n,k}$. The set of the all $E_{n,k}$ elements is the matrix. The same concerns the $T_{n,k}$. Formula (4.7.3) for such a system looks as follows

$$(i E_{n,k}) T_{n,k} = n \hbar, \quad (4.7.4)$$

where n denotes the number of entangled loops whereas the pairs n,k label the amplitudes concerning masses and lifetimes. Such is the correct interpretation of the Heisenberg matrices. There can be matrices for other physical quantities such as energy, position, velocity, square of velocity, and so on. But for interactions described within the time-independent Matrix Quantum Mechanics most important is formula (4.7.4).

A measurement of, for example, lifetime of a system changes its configuration of mass/energy so the matrices for mass/energy and lifetime does not concern the same configuration. This means that these two physical quantities do not commute.

The generality of the derivation of the commutator will not be limited when we will start from the simpler formula (4.7.3). Calculate value of the commutator defined by formula (4.7.1) for $\mathbf{I} = E_n$ and $\mathbf{U} = T_n$. Assume that some observed/interacting system consists of n entangled spin-1 loops that spins are parallel (but there can be more loops that we can group in pairs and the spins of the constituents of the pairs are antiparallel). Then for the whole system labeled by n we obtain

$$(i E_n) T_n = n \hbar. \quad (4.7.5)$$

Assume that a component of the system emits the superluminal spin-1 entanglon so the change in spin is $m = n \pm 1$. Mass of the system decreases i.e. $E_m = E_n - E$ whereas

lifetime is longer $T_m = T_n + T$. Due to the entanglement, the changes are infinitesimal so $T \rightarrow 0$ and $E \rightarrow 0$. Due to the emission is

$$(i E_m) T_m = m \hbar . \quad (4.7.6)$$

Calculate the value of the commutator

$$[E_n , T_m] = E_n T_m - T_n E_m = \hbar \{ n (T_n + T) / T_n - (n \pm 1) T_n / ((T_n + T)) \} / i. \quad (4.7.7)$$

For $T \rightarrow 0$ and $E \rightarrow 0$, i.e. under infinitesimal transformation of the lifetime and energy of the system, we obtain

$$[E_n , T_m] = - (\pm \hbar / i) = \pm i \hbar . \quad (4.7.8)$$

It is easy to notice that equation (4.7.8) is valid for all quantum particles, i.e. for all values of n , when the changes in lifetime and mass are infinitesimal.

On the basis of equation (4.7.4), we can rewrite equation (4.7.8) as follows

$$[E_{n,k} , T_{m,l}] = \pm i \hbar . \quad (4.7.9)$$

The equation (4.7.9) is the fundamental equation in the Matrix Quantum Mechanics. We showed that this equation follows from the superluminal quantum entanglements with infinitesimal changes in energy and lifetime.

Denote the matrix $E_{n,k}$ by t_α , the matrix $T_{m,l}$ by t_β whereas ± 1 by $\varepsilon_{\gamma\alpha\beta}$, where $\varepsilon_{\gamma\alpha\beta}$ is $+1$ if γ, α, β is an even permutation or -1 if γ, α, β is an odd permutation. Then, for matrices that are the spin 1 (i.e. $1\hbar$) representation of the Lie algebra of the rotation group, we can rewrite equation (4.7.9) as follows

$$[t_\alpha , t_\beta] = i \varepsilon_{\gamma\alpha\beta} t_\gamma . \quad (4.7.10)$$

It is the fundamental equation applied in the non-Abelian gauge theories [1]. The gauge invariance we obtain assuming that the Lagrangian is invariant under a set of infinitesimal transformations on the matter fields. It is some analogy to the infinitesimal transformations on the masses of the loops in a set of entangled loops.

We can see that presented here the Matrix Quantum Mechanics based on the entanglement and constancy of spin of the loops in a set of entangled loops leads to the methods applied in the Quantum Theory of Fields (QTFs). Why we must apply the infinitesimal transformations in the Quantum Physics? It follows from the very small inertial mass of the carriers of the entanglement i.e. of the superluminal binary systems of closed strings. What is the physical meaning of the elements of the matrix $E_{n,k}$? The n and k numbers number the entangled loops in a system so the $E_{n,k}$ are the amplitudes of transitions between different or the same loops in the system. Their squares define the rates of the transitions. But the QTFs is the incomplete theory because of one weak point. Within this theory we neglect internal structure of the bare fermions. This causes that there appear the singularities and infinite energies of fields. The infinities are eliminated due to the procedure that we refer to as the renormalization. This procedure follows from the incorrect formula which can be written symbolically as follows: $\infty - \infty = C = \mathbf{constant} \neq 0$. The C can denote, for example, the bare mass of electron. It leads to conclusion that in reality the bare electron is not a sizeless point. The renormalization

partially corrects the wrong initial condition but we still neglect the internal structure of the bare particles, for example, the shapes and dynamics (that leads, for example, to the internal helicity) that are very important in the theory of the nuclear strong and weak interactions. This causes that the QTFs is the messy theory.

What is the correct interpretation of the wave function? Due to the superluminal entanglement of the SST-As components in their excited states, in this spacetime can appear the quantum particles. The initial configuration/distribution of the entangled constituents of a quantum system changes with time. We can say that some configuration disappears and there appears the next one, and so on. There are not continuous trajectories of the components of the quantum system between the succeeding configurations. The succeeding configurations depend stepwise on time. But in an approximation we can say about a time-dependent statistically averaged distribution that is coded by the wave function of the quantum system. In reality, due to the superluminal entanglement, for a defined time, the positions of the components of the quantum state are well-defined. Due to the superluminal quantum entanglement, we find a particle in a place of measurement – the measurement and entanglement cause that a set of entangled states collapses to one of allowed quantum states. Due to the stepwise dependence on time, the equations of motion for a wave function are only some approximation of the quantum reality, i.e. it is some statistical approximation.

Emphasize that according to SST, even pure energy, as for example the rotational energy, have to be carried by physical volumes and the smallest volumes/pieces-of-space (i.e. the SST tachyons) the other particles consist of cannot be simultaneously in two or more different states so the superposition is the wrong idea. But different parts of the same bigger particle can be simultaneously in different states – notice that it is not the superposition.

References

- [1] Steven Weinberg (1996). “The Quantum Theory of Fields”
Volume II, Modern Applications
The Press Syndicate of the University of Cambridge

4.7.2. Testing the SST quantum gravity

It is an extension of Paragraph 2.14.1 in which we described the SST Higgs-potential for neutrinos and baryons.

In SST, we showed that gravitational fields are the result of the viscid interactions of the SST Higgs field with the entanglons the neutrinos consist of. Inside the region of the SST Higgs potential, the spin-2 binary systems of entanglons (we call them the SST gravitons) are emitted and absorbed so such a region is described by the SST quantum gravity – its range is $\sim 3.925980 \cdot 10^{-32} \text{ m}$.

In Paragraph 2.14.1 we calculated a mass/energy which is responsible for creation of the SST Higgs potential by baryons – its mean mass is $\Delta m_{\text{mean}} \approx 0.15376987219 \text{ MeV}$. Phenomena forced by the neutrinos and the core of baryons are similar so the mass/energy counterparts and ranges are directly proportional. For example, proving the existence of a Higgs potential for baryons means that neutrinos and the SST-absolute-spacetime components create an analogous potential.

Assume that in baryons is a resonance of values of some coupling constants for electroweak interactions – then from the definition of coupling constants (see (2.14.9)) we have

$$M_1 m_1 = M_2 m_2 . \quad (4.7.11)$$

Assume that the bound neutral pion π_{bound}^0 (see (2.2.19)) attached the mass Δm_{mean} and both interact with the bare electron $m_{e,\text{bare}}$ (see (2.2.10)). On the other hand, assume that the binding energy of the core of baryons ΔE_{core} (see (2.5.18)) interacts with $\Delta\pi = \pi^{\pm} - \pi_{\text{bound}}^0$ (see (2.2.21)) and that there is a resonance between the two electroweak interactions, so we have

$$(\pi_{\text{bound}}^0 + \Delta m_{\text{mean}}) m_{e,\text{bare}} = \Delta E_{\text{core}} (\pi^{\pm} - \pi_{\text{bound}}^0). \quad (4.7.12)$$

From the last formula we obtain the mass of charged pion

$$\pi^{\pm} = 139.57039729 \approx 139.57040(14). \quad (4.7.13)$$

Calculated here mass of charged pion by using the mass/energy that is responsible for creation of the SST Higgs potential by baryons is consistent with that obtained by another method (see (2.2.20)) – this gives credence to the quantum gravity of neutrinos described in SST.

4.8. Extraterrestrial communication

4.8.1. Wow! signal

Here we show that in the Wow! signal, an extraterrestrial civilization coded the phase transitions of the initial inflation field and many other fundamental ideas.

The Wow! signal was a radio signal received on August 15, 1977, by Ohio State University's Big Ear radio telescope [1]. Most of its operation was in the 21-cm radio band. The receiver covered an 8-MHz bandwidth from 1411 to 1419 MHz.

The string of numbers and characters "6EQUJ5" we see in channel 2 of the printout [1].

The signal-strength sequence "6EQUJ5" in channel 2 of the computer printout represents the following sequence of signal-to-noise ratios [1]:

6: 6 (up to 7)
 E: 14 (up to 15)
 Q: 26 (up to 27)
 U: 30 (up to 31)
 J: 19 (up to 20)
 5: 5 (up to 6)

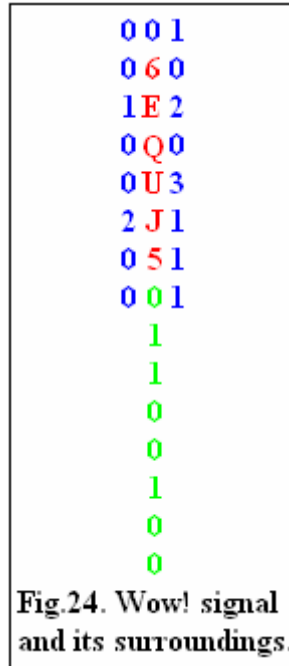
The intensity received (for example, "E") means that the signal was 14.5 ± 0.5 times stronger than the background noise.

Notice that each element in the signal is defined by two numbers (the lower and upper limit) differing by one.

In the printout, the noise is defined by empty place: we can assume that there is zero.

Notice that the two first numbers in the Wow! signal are 6 and 14 (E). Let's check if they can define the true length of the Wow! signal.

The first number 6 defines number of elements in the main part of the Wow! signal. On the other hand, we have $14 = 6 + 8$. This suggests that the signal sender indicates that he also uses eight numbers after the main part of the signal. A sequence of numbers immediately after it is 01100100 (see Fig.24 and [1]). The second part consists of the low-value signal-to-noise ratios.



How we can interpret it? We can assume that the second part of the string, i.e. the part composed of the zeros and ones, i.e. the part composed of the low-value signal-to-noise ratios: “01100100”, shows whether we correctly measured the signal-to-noise ratios for the main part “6EQUJ5”. We know that in the binary system, the sequence 01100100 represents the number 100. On the other hand, the sum of all numbers in the main part also is 100

$$6 + E + Q + U + J + 5 = 6 + 14 + 26 + 30 + 19 + 5 = 100.$$

It leads to conclusion that measured by the Ohio-State-University team the signal-to-noise ratios for “6EQUJ5” are correct.

The main part consists of 6 elements. Let’s create two groups each containing three elements and calculate the sum of numbers.

For “6EU” is

$$6 + E + U = 6 + 14 + 30 = 50,$$

and for “QJ5” is

$$Q + J + 5 = 26 + 19 + 5 = 50.$$

The sums are the same so such a division is justified.

We can use as well the English alphabet for our numerology analysis:

1 (A), 2 (B), 3 (C), 4 (D), 5 (E), 6 (F), 7 (G), 8 (H), 9 (I), 10 (J), 11 (K), 12 (L), 13 (M), 14 (N), 15 (O), 16 (P), 17 (Q), 18 (R), 19 (S), 20 (T), 21 (U), 22 (V), 23 (W), 24 (X), 25 (Y), 26 (Z).

Calculate the sums:

$$\text{“6EU”} = 6 + 5 (\text{E}) + 21 (\text{U}) = 32,$$

$$\text{“QJ5”} = 17 (\text{Q}) + 10 (\text{J}) + 5 = 32.$$

Such an incredible double coincidence must lead to important information.

In Section 2.13, we described the degrees of freedom of the fundamental objects that appeared in our Cosmos due to the phase transitions of the SST initial inflation field. To simplify the description we rewrite the main equation and Table 3.

If N denotes the degrees of freedom then for the rotating-spin loops/string and the SST cores is

$$N = | 8 (2d - 1) + 2 |, \quad (4.8.1)$$

where $d = 0, 1, 2, 4, 8$.

Table 3 *Degrees of freedom of fundamental objects*

Stable object	Co-ordinates and quantities needed to describe position, shape and motions
Tachyon	6 (they always are spinning)
Closed string Entanglon	10 for rotating spin or 8 for non-rotating spin
Neutrino Neutrino-antineutrino (NA) pair	26 or 24 : 8 for entanglons on torus 8 for entanglons in condensate 8 (or 10) for the core as a whole
Core of baryons Electron	58 or 56 : 24 for NA pairs on torus 24 for NA pairs in condensate 8 (or 10) for the core as a whole
An abstract core of Protoworld composed of the baryonic core-anticore (CA) pairs	122 or 120 : 56 for CA on torus 56 for CA in condensate 8 (or 10) for the core as a whole

From (4.8.1) we obtain respectively **6**, **10**, **26**, **58** and **122**. Notice that rotational energy has **2** degrees of freedom.

The Wow! signal is a sequence of the signal-to-noise ratios – each element changes its value from n to $(n + 1)$, for example, for **6** is **6** up to **7**. It suggests that following formula is very important in deciphering the Wow! signal

$$N = 2 \cdot [n + (n + 1)]. \quad (4.8.2)$$

We can use this formula for the transition from n to N or transformation from N to n .

For the all elements in the complete Wow! signal (i.e. the $14 = 6 + 8$ elements), i.e. for **6**, **E**, **Q**, **U**, **J**, **5**, **0** and **1**, and the elements in the closest surrounding of the signal we obtain

$$6 \text{ i.e. } n = 6 \text{ so } N = 2 \cdot (6 + 7) = 26$$

$$E \text{ i.e. } n = 14 \text{ so } N = 2 \cdot (14 + 15) = 58$$

$$Q \text{ i.e. } n = 26 \text{ so } N = 2 \cdot (26 + 27) = 106 \text{ i.e. } 10 \text{ and } 6$$

$$U \text{ i.e. } n = 30 \text{ so } N = 2 \cdot (30 + 31) = 122$$

$$J \text{ i.e. } n = 19 \text{ so } N = 2 \cdot (19 + 20) = 78$$

5 i.e. $n = 5$ so $N = 2 \cdot (5 + 6) = 22$

0 i.e. $n = 0$ so $N = 2 \cdot (0 + 1) = 2$

1 i.e. $n = 1$ so $N = 2 \cdot (1 + 2) = 6$

2 i.e. $n = 2$ so $N = 2 \cdot (2 + 3) = 10$

3 i.e. $n = 3$ so $N = 2 \cdot (3 + 4) = 14$ (it is the E that leads to 58)

We can see that the SST degrees of freedom are indeed encoded in the Wow! signal.

We can see that the numbers 106, 78 and 22 do not result from formula (4.8.1).

But notice that we have

$$N_{22} = \{[6 + 0] + [6 + 0] + 10\} = 22. \quad (4.8.3)$$

It is a “gaseous” torus with central ball/scalar both composed of the SST tachyons. The tachyons interact due to the dynamic viscosity which leads to the most fundamental force.

There also is

$$N_{78} = \{[24 + 10] + [24 + 10] + 10\} = 78. \quad (4.8.4)$$

It is a torus with central ball/scalar both composed of the non-rotating-spin SST-As components which exchange the rotating-spin entanglons (they are responsible for the quantum entanglement).

There also is

$$N_{106} = \{[24 + 24] + [24 + 24] + 10\} = 106. \quad (4.8.5)$$

It is a torus with central ball/scalar both composed of the non-rotating-spin SST-As components which exchange the SST-As components.

When we neglect the stable superluminal objects that cannot be observed directly (i.e. 6 and 10) then the SST leads to following sequence for stable objects

Stable: 26, 58, 122 (it relates to $6EU = 32$),

and to following sequence for meta-stable objects

Meta: 22, 78, 106 (it relates to $QJ5 = 32$).

Notice that sum of the numbers in each sequence is 206 i.e. is the same. The probability of such a strong coincidence (i.e. 32 and 32, and 206 and 206) as a result of the case is practically equal to zero. It suggests that the Wow! signal was emitted by an Extra-Terrestrial Intelligence (ETI).

Notice that two elements in Wow! signal with highest signal-to-noise ratios, i.e. Q(26) and U(30), are the numbers of protons and neutrons in iron ${}_{26}\text{Fe}^{(26+30)}$ whereas the two lowest ratios, i.e. 5 and 6, are the numbers of protons and neutrons in boron ${}_{5}\text{B}^{(5+6)}$. It forces the division of the Wow! signal into three pairs: QU, EJ and 65. On the other hand, according to SST, the ratios of the angles in the PMNS neutrino-mixing matrix are 4 : 5 : 1 (see the Section 2.24). We showed that an ETI suggests following pairing of the Wow! signal elements: QU,

EJ and 65. Differences in the signal-to-noise ratios for the components of the pairs are as follows:

$$U - Q = 30 - 26 = 4$$

$$J - E = 19 - 14 = 5$$

$$6 - 5 = 1$$

The ratios of obtained differences are $(U - Q) : (J - E) : (6 - 5) = 4 : 5 : 1$ as it is in the PMNS matrix.

We can show that also the fine-structure constant is encoded in the Wow! signal. The inverse of the fine-structure constant leads to a sequence: 1, 3, 7, 0, 3, 6. Using formula (4.8.2) two times to each cipher in this sequence, we obtain:

$$1 \text{ so } 2 \bullet (1 + 2) = 6 \text{ (Wow and Stable) so } 2 \bullet (6 + 7) = 26 \text{ (Wow and Stable)}$$

$$3 \text{ so } 2 \bullet (3 + 4) = 14 \text{ (Wow) so } 2 \bullet (14 + 15) = 58 \text{ (Stable)}$$

$$7 \text{ so } 2 \bullet (7 + 8) = 30 \text{ (Wow) so } 2 \bullet (30 + 31) = 122 \text{ (Stable)}$$

$$0 \text{ so } 2 \bullet (0 + 1) = 2 \text{ (rotation) so } 2 \bullet (2 + 3) = 10 \text{ (Stable)}$$

$$3 \text{ so } 2 \bullet (3 + 4) = 14 \text{ (Wow) so } 2 \bullet (14 + 15) = 58 \text{ (Stable)}$$

$$6 \text{ so } 2 \bullet (6 + 7) = 26 \text{ (Wow and Stable) so } 2 \bullet (26 + 27) = 106 \text{ (Meta)}$$

The probability of such a strong coincidence as a result of the case is very low. It suggests that the Wow! signal was emitted by an Extra-Terrestrial Intelligence (ETI).

Emphasize also that the Wow! signal leads to two isotopes i.e. ${}^6\text{C}^{14}$ and ${}^{14}\text{Si}^{30}$ which select the numbers 6, 14 (E) and 30 (U) in the order recorded here. Such order leads to the number 137.

The Wow! signal leads to discoverer of the Planck constant.

In SST, we showed that the reduced Planck constant is the most fundamental physical constant because it was set first at the start of inflation.

Rank the signal-to-noise ratios from the largest to the smallest

$$U, Q, J, E, 6, 5 = 30, 26, 19, 14, 6, 5 .$$

Let's consider the differences between the signal-to-noise ratios (for ratios arranged from the largest to the smallest): 4, 7, 5, 8, 1 or (for ratios arranged from the smallest to the largest): 1, 8, 5, 7, 4

The ciphers 4 and 7 lead to ${}_{19}47$ (date of M. Planck's death).

The ciphers 5 and 8 lead to ${}_{18}58$ (date of Planck's birth).

The ciphers 1 and 8 lead to ${}_{19}18$ (date in which the Nobel Prize for quantifying the radiation of a black body was awarded (received in 1919) to Max Karl Ernst Ludwig Planck).

Notice that the first ciphers 4, 5, 1, are the same as the ratios of the neutrino-mixing angles.

Many other coincidences suggest that the Earth is monitored by an ETI.

References

- [1] Dr. Jerry R. Ehman (Original Draft Completed: July 9, 2007; Last Revision: 28 May 2010). “The Big Ear Wow! Signal”
<http://www.bigear.org/Wow30th/wow30th.htm>

4.9. Dark energy and dark matter

4.9.1. Creation of dark energy (DE) and dark matter (DM)

Structure of the DM loops and DM tori we described in Section 2.1 – they were produced at the end of the SST inflation.

The increase in the relativistic mass of protons is a result of the formation of successive layers above the surface of the torus/electric-charge which is inside of the core of baryons. Such an increase does not cause a change in electric charge when the spins of the entangled neutrino-antineutrino pairs are polarized along electric-field lines (they are the DE segments) which converge on the circular axis (see Fig.2) of the torus/electric-charge.

To form DM loops, the relativistic mass of the proton torus must be about 81.3% of the Planck’s mass, $m_{\text{Planck}} = 2.1765 \cdot 10^{-8} \text{ kg}$, because then the DE segments contain K^2 of entangled stable neutrinos with spins polarized tangentially to the loop. The X^\pm torus has one layer built of the neutrino-antineutrino pairs so there must be created $K^2/2$ such layers. Then mass of such relativistic torus is

$$M_{\text{rel}} = X^\pm K^2 / 2 = 0.813 m_{\text{Planck}} . \quad (4.9.1)$$

The DE segments composed of K^2 stable neutrinos curl up into the DM loops while the DM loops were building blocks of the DM tori. To create the DM tori we need vortices excited in the SST absolute spacetime i.e. we need circular/poloidal flows on the torus/electric-charge in the cores of baryons because such flows force transformation of the DE segments into DM loops with sufficiently high linear density. **The DE segments wound around the proton torus.**

Due to the collapse of the outer shell of the expanding SST absolute spacetime at the end of the SST inflation, there was created the thickened SST-As near the front of the SST-As – it also had led to production of the DM tori by even resting baryons so probability of such phenomena was very high. But from (4.9.1) results that production of the DM tori in Earth laboratories is impossible. We would have to be very lucky to detect the cosmological DM tori with a mass of $\sim 727.44 \text{ MeV}$.

The Protoworld was destroyed because the DM tori decayed to the DM loops with a mass of $\sim 2.0796 \cdot 10^{-47} \text{ kg}$. The cosmological DM loops took the angular momentum of the baryon plasma, so their radii increased significantly. Today we can learn the origin of dark matter mainly by studying the rotation curves of galaxies.

From (1.4.26) follows that G_i (so field density, ρ , as well) is directly proportional to coupling constant. The DE segments were produced due to the nuclear weak interactions while the DM loops and the DM tori due to the electromagnetic interactions (there are the closed lines of electric field). We see that the ratio of abundances/densities of DE, ρ_{DE} , and DM, ρ_{DM} , should be close to

$$\rho_{\text{DE}} / \rho_{\text{DM}} = \alpha_{\text{w(p)}} / \alpha_{\text{em}} = 2.5657 . \quad (4.9.2)$$

It is consistent with observational data: $(\rho_{\text{DE}} / \rho_{\text{DM}})_{\text{obs}} = 68.63\% / 26.46\% \approx 2.59$.

DE segments have much larger surface area than the SST-As components, so virtual photons moving divergently effectively pushed the DE segments out of the interior and immediate surroundings of the Protoworld. **Initially, the Protoworld was free from DE composed of the DE segments.**

There, at low energies, due to the electroweak interactions of electrons, can be created low-density DM loops (LDDMLs). We need short-lived circular electric currents to produce LDDMLs with different masses and radii. The tangle of LDDMLs creates a DM soliton. Such solitons are produced by circular currents excited in the brain and they are components of the mind. But the linear densities are too low to create low-density DM tori.

Chapter 5

Interdisciplinary Problem

5.1. Space roar and the second mass of the bottom quark	134
5.2. Masses of the Upsilon and χ_b mesons	137
5.3. Absorption profile from the primordial cold hydrogen field	138
5.4. The SST large numbers law, Gravity versus the Standard Model, and the gravitational black holes	139

5.1. Space roar and the second mass of the bottom quark

The space roar is the unsolved problem in cosmology and particle physics. Here, applying the SST, we showed that the ARCADE 2 [1] and other literature the space roar for frequencies from 22 MHz to 10 GHz follows from the atom-like structure of baryons and from the expansion of the Universe (the wavelengths increased $F_U = 72.16$ times). Here as well we calculated the second mass of the bottom quark: $m_{b,2} = 4167.60 \text{ MeV}$.

The radio background from ARCADE 2 and radio surveys is a factor of ~ 6 brighter than the estimated contribution of radio point sources [1].

According to the SST, the expanding Universe is the result of evolution of the cosmic structure (the Protoworld) that appeared after the SST inflation. Initially, the baryonic part of the Universe was the double loop with a radius of $R_{\text{Cosmological}} = 0.191109 \text{ Gly}$ (see Section 3.7 and formula (2.1.25)). The today spatial radius of the sphere filled with baryonic matter is $R_{\text{BM, today}} = 13.79(1) \text{ Gly}$ (see (3.5.6) and (3.5.4)) so size of the baryonic part increased about F_U times

$$F_U = R_{\text{BM, today}} / R_{\text{Cosmological}} = 72.16(5), \quad (5.1.1)$$

and the same concerns the wavelengths that appeared at the beginning of the expansion of the Universe i.e. when the CMB was produced.

We showed that the black body spectrum (see Section 3.9) and the CMB anisotropy spectrum (see Section 3.6) are directly associated with the internal structure of baryons. On the other hand, the neutral pion ($\pi^0 = 134.9767 \text{ MeV}$ – see Section 2.9) is created on the circular axis which is the most inner orbit for the strong interactions in baryons while the SST bottom quark-antiquark pairs, $m_b m_{b, \text{anti}}$, are produced on the last TB orbit for the strong interactions (see Section 2.23).

The simplest neutral pion consists of four neutrinos, i.e. $E_{\text{neutrino}} = 33.74418 \text{ MeV}$, so at high energies, due to the four-object symmetry, it can create four the bottom quark-antiquark pairs – it is an octopole of bottom quarks that can decay to a photon pair. Due to the expansion of the Universe, frequency of such photons decreased F_U times. We see that the following transformations in the early Universe and in very hot baryonic plasma can appear

$$E_{\text{neutrino}} \rightarrow m_b m_{b, \text{anti}}. \quad (5.1.2)$$

Such transformations lead to following spectral index β

$$E_{\text{neutrino}}^\beta = 2 m_b. \quad (5.1.3)$$

In Section 2.23 we already calculated the first mass of the bottom quark

$$m_{b,1} = 4190.34 \text{ MeV} \quad (5.1.4)$$

so formula (5.1.3) leads to the index β equal to ~ 2.56726 . But the spectral index should result from some interactions. Notice that the spectral index is close to the ratio of the coupling constant of the nuclear weak interactions ($\alpha_{w(p)} = 0.0187229$) to the fine structure constant ($\alpha_{em} = 1/137.035999$)

$$\beta = \alpha_{w(p)} / \alpha_{em} = 2.56571. \quad (5.1.5)$$

From (5.1.3) and (5.1.5) we can calculate the second mass of the bottom quark

$$m_{b,2} = 4167.60 \text{ MeV} . \quad (5.1.6)$$

According to PDG [2], applying the minimal subtraction scheme to absorb the infinities that arise in perturbative calculations beyond leading order, introduced independently by Gerard 't Hooft (1973) and Steven Weinberg (1973), the mass of the bottom quark is $m_{b,\text{exp}} = 4.18(3) \text{ GeV}$ so both theoretical results are consistent with the PDG result.

In collisions of baryons at high energies are created strings composed of the X^+X^- pairs with spins tangent to the strings – they can collapse to the SST-As condensates. Mass of such string, m_{string} , is directly proportional to its length/wavelength, λ_{string} , and we have that frequency is directly proportional to mass of such string $v_{\text{string}} \sim m_{\text{string}}$

$$v_{\text{string}} \sim m_{\text{string}} \sim \lambda_{\text{string}} \quad (5.1.7)$$

so from the Wien's displacement law we have

$$\Delta T \sim 1 / v_{\text{string}} , \quad (5.1.8)$$

where ΔT is an excess temperature.

Due to the transition from the nuclear weak interactions to the electromagnetic interactions at low energy and because $m^\beta \sim v^\beta$, we have the transition

$$v_{\text{string}} \rightarrow v^\beta . \quad (5.1.9)$$

From the two last formulae we obtain

$$\Delta T v^\beta = T_o v_o^\beta . \quad (5.1.10)$$

i.e.

$$\Delta T = T_o (v / v_o)^{-\beta} . \quad (5.1.11)$$

Such power law distorts the frequency spectrum of the CMB.

Assume that at some temperature of the early Universe, from the strings were created octopoles of the $Y = 424.12174 \text{ MeV}$ condensates that decayed to photon pairs.

From (2.18.3) and because lifetime of a string is directly proportional to its length and mass we have

$$m_1 = m_2 (\alpha_2 / \alpha_1)^4 . \quad (5.1.12)$$

The transition from the nuclear weak interactions of the associations of the Y condensates to the weak interactions of the charged fermion-antifermion pairs in presence of dark matter ($\alpha'_{w(e),DM} = 1.1194461 \cdot 10^{-5}$) caused that the initial energy of the emitted photons was (see (5.1.12))

$$E_{\gamma, \text{initial}} = 4 Y (\alpha_{w(p)} / \alpha'_{w(e), DM})^4 = 2.1681 \cdot 10^{-10} \text{ MeV}, \quad (5.1.13)$$

i.e.

$$m_{\gamma, \text{initial}} = F E_{\gamma, \text{initial}} = 3.8649 \cdot 10^{-40} \text{ kg}. \quad (5.1.14)$$

The initial frequency was

$$\nu_{\gamma, \text{initial}} = m_{\gamma, \text{initial}} c^2 / (2 \pi \hbar) = 52.423 \text{ GHz}. \quad (5.1.15)$$

From (5.1.15) and (5.1.1) we obtain the today frequency

$$\nu_o = \nu_{\gamma, \text{initial}} / F_U = 726.5 \text{ MHz} \quad (5.1.16)$$

so it relates to the today CMB temperature [2]

$$T_o = 2.7255 \text{ K}. \quad (5.1.17)$$

Our power law looks as follows

$$\Delta T = 2.7255 \text{ [K]} (\nu / 726.5 \text{ [MHz]})^{-\beta}. \quad (5.1.18)$$

From it follows that when ν increases then the excess ΔT decreases.

Our results are collected in Table 19.

Table 19 *Today frequency and excess temperature*

Octopole of ...	Today frequency ν	Excess temperature ΔT (formula (5.1.18))
ΔE_{core}	$\sim 26 \text{ MHz}$	14,000 K
-----	310 MHz	24.2 K ARCADE 2 plus others: 24.1 ± 2.1 K [1]
Y	$\nu_o = 726.5 \text{ MHz}$	$T_o = 2.7255 \text{ K}$
-----	3.3 GHz	56 mK ARCADE 2: 54 ± 6 mK [1]
$m_{b,2}$	$\sim 7.1 \text{ GHz}$	7.9 mK

$$\beta = \alpha_{w(p)} / \alpha_{em} = 2.56571$$

References

- [1] D. J. Fixen, A. Kogut, *et al.* (17 May 2011). "ARCADE 2 Measurement of the Absolute Sky Brightness at 3–90 GHz"
The Astrophysical Journal, 734:5 (11pp)
- [2] P.A. Zyla, *et al.* (Particle Data Group)
Prog. Theor. Exp. Phys. **2020**, 083C01 (2020)

5.2. Masses of Upsilon and chi_b mesons

Here we described composition and calculated masses of the Upsilon (Y) and chi_b (χ_b) mesons.

According to SST, the Upsilon mesons are the mesonic nuclei (see Section 2.20) defined by the $I^G (J^{PC}) = 0^- (1^{--})$, where I is the isospin, G is the isoparity (G-parity), J is the spin, P is the parity, and C is the charge conjugation, while the chi_b mesons contain the bottom quark-antiquark pair and are denoted by $\chi_{bJ} ([J + 1]P)$ and defined by the $I^G (J^{PC}) = 0^+ (J^{++})$, where $J = 0, 1$ and 2 .

We already calculated the mass of the ground state of the Upsilon mesons: $Y(1S) = 9464.92 \text{ MeV}$ (see Section 2.20) and the two masses of the bottom quark: $m_{b,1} = 4190.34 \text{ MeV}$ and $m_{b,2} = 4167.60 \text{ MeV}$ (see Section 2.23 and (5.1.6) respectively).

To explain the mass spectrum of the Upsilon mesons we need some objects S_i defined by the $I^G (J^{PC}) = 0^+ (0^{++})$ which can be entangled with the ground state i.e. with $Y(1S)$ for which is $I^G (J^{PC}) = 0^- (1^{--})$. Such objects must satisfy the four-object symmetry so from Section 2.26 results that number of particles in the S_i objects should be 4, 8 or 16. Moreover, the total electric charge, Q , and total spin, J , of S_i both must be equal to zero.

To solve the problem we need following masses: mass of the charged pion: $\pi^\pm = 139.5704 \text{ MeV}$, mass of the fundamental gluon loop: $m_{\text{FGL}} = 67.5444 \text{ MeV}$, and mass/energy of the gluons created due to the transitions between the baryonic shells: $m_B = 25.213 \text{ MeV}$ (see formula (2.21.2)).

In Table 20 we present our results concerning the Upsilon mesons.

Table 20 *Upsilon mesons*

Upsilon meson	S_i 4, 8 or 16 particles, $Q = J = 0$	Composition	Theoretical mass [MeV]	Experimental mass [MeV] [1]
$Y(1S)$	----	$Y(1S)$	9464.92*	9460.30(26)
$Y(2S)$	$4 \pi^\pm$	$Y(1S) + S_i$	10023.20	10023.26(31)
$Y(3S)$	$6 \pi^\pm + 2 m_B$	$Y(1S) + S_i$	10352.77	10355.2(5)
$Y(?)$	$6 \pi^\pm + 2 m_{\text{FGL}}$	$Y(1S) + S_i$	10437.43	?
$Y(4S)$	$8 \pi^\pm$	$Y(1S) + S_i$	10581.48	10579.4(1.2)
$Y(10860)$	$8 \pi^\pm + 2 m_{\text{FGL}} + 6 m_B$	$Y(1S) + S_i$	10867.85	$10885.2^{+2.6}_{-1.6}$ $\Gamma = 37(4)$
$Y(11020)$	$8 \pi^\pm + 6 m_{\text{FGL}} + 2 m_B$	$Y(1S) + S_i$	11037.17	11000(4) $\Gamma = 24^{+8}_{-6}$
$Y(11700)$	$16 \pi^\pm$	$Y(1S) + S_i$	11698.05	?

*Notice that mass distance between our result and the experimental mass

is equal to $\pi^\pm - \pi^0$ so we can assume that our mass is the mass of the bound $Y(1S)$.

We claim that the ground state of the chi_b mesons consists of the bottom quark-antiquark pair and the pair of the bosons responsible for creation of the TB orbits for the nuclear strong interactions: $M_{\text{TB}} = 750.2975 \text{ MeV}$ (see formula (2.5.19)). The mean mass of the bottom quark is $m_{b,\text{mean}} = 4178.97 \text{ MeV}$ so we have

$$\chi_{b0}(1P) = 2 (m_{b,\text{mean}} + M_{\text{TB}}) = 9858.54 \text{ MeV} . \quad (5.2.1)$$

The quarks have antiparallel spins. The parity of χ_{b0} (1P) is positive while total spin and total charge are equal to zero.

We need some objects U_i defined by the $I^G (J^{PC}) = 0^+ (1^{++})$ to explain the spin distances between χ_{b1} and χ_{b0} and between χ_{b2} and χ_{b1} . We need also some objects W_i defined by the $I^G (J^{PC}) = 0^+ (0^{++})$ to explain the mass distance between χ_b (2P) and χ_b (1P) and between χ_b (3P) and χ_b (2P).

We claim that composition of the W_i objects is as follows (see Table 1)

$$W_{2P-1P} = 2 S_{(+),d=4} = 375.15 \text{ MeV} , \quad (5.2.2)$$

$$W_{3P-2P} = S_{(o),d=4} + m_{FGL} = 254.43 \text{ MeV} , \quad (5.2.3)$$

while composition of the U_i objects is as follows

$$U_{b1-b0} = m_B = 25.213 \text{ MeV} , \quad (5.2.4)$$

$$U_{b2-b1} = m_B \alpha_{em} / \alpha_{w(p)} = 9.827 \text{ MeV} . \quad (5.2.5)$$

Our results are collected in Table 21.

Table 21 *Chi_b mesons*

	χ_{b0} Theory [MeV]	χ_{b0} Exper. [1] [MeV]	χ_{b1} Theory [MeV]	χ_{b1} Exper. [1] [MeV]	χ_{b2} Theory [MeV]	χ_{b2} Exper. [1] [MeV]
1P	9858.54.	9859.44(73)	9883.75	9892.7(57)	9893.58	9912.21(57)
2P	10233.69	10232.5(9)	10258.90	10255.46(72)	10268.73	10268.65(72)
3P	10488.12	-----	10513.33	10513.4(7)	10523.16	10524.0(8)

References

- [1] P.A. Zyla, *et al.* (Particle Data Group)
Prog. Theor. Exp. Phys. **2020**, 083C01 (2020)

5.3. Absorption profile from the primordial cold hydrogen field

Within the SST we calculated the baryonic-matter (BM) density (see formula (3.5.17)) that is a little lower than the observed density. It suggests that outside the hot baryonic field of the Protoworld that relates to the nuclear strong field in baryons (radius of such cosmological field was $R_U = 2 \pi R_{\text{Cosmological}} = 1.201 \text{ Gly}$, where $R_{\text{Cosmological}} = 0.191109 \text{ Gly}$ (see Section 3.7 and formula (2.1.25)), there already before the expansion of the Universe was the primordial field of cold hydrogen. When the photons from the expanding Universe reached such field, there was created the absorption profile centred at $\nu_{\text{flip,initial}} = 1420.406 \text{ MHz}$ – it was due to the spin flip in the ground state of hydrogen atoms. There were absorbed photons with wavelength equal to $\lambda_{\text{flip}} = 0.21106 \text{ m}$. Since the today radius of the CMB is $R_{\text{CMB}} = 21.32(1) \text{ Gly}$ (see formula (3.5.4)) so the central frequency decreased to

$$\nu_{\text{flip,today}} = \nu_{\text{flip,initial}} R_U / R_{\text{CMB}} = 80.1 \text{ MHz} . \quad (5.3.1)$$

Due to the radius-circle transitions of the photons on the edge of the hot baryonic field i.e. at the distance R_U , the width of the absorption profile on its edge is today defined as follows

$$V_{\text{flip,today,width-on-edge}} = V_{\text{flip,initial}} \pm V_{\text{flip,initial}} / (2 \pi) \approx 80 \pm 13 \text{ MHz}. \quad (5.3.2)$$

This result is consistent with observational data [1].

The primordial hydrogen field outside the hot baryonic field of the Protoworld was very cold so the amplitude of the absorption profile must be today significantly high.

Notice also that described here phenomena did not lead to the mainstream Dark Ages in cosmology. When the Universe started to expand there was no a period called the Dark Ages.

References

- [1] Judd D. Bowman, *et al.* (13 October 2018). “An absorption profile centered at 78 megahertz in the sky-averaged spectrum”, arXiv:1810.05912 [astro-ph.CO]

5.4. The SST large numbers law, Gravity versus the Standard Model, and the gravitational black holes

In SST, the ratio of the constant of the electron-positron electromagnetic interactions, G_{em} , to the gravitational constant, G , is exactly equal to the ratio of the gravitational-mass density of the SST absolute spacetime, ρ_{As} , to the inertial-mass density of the SST Higgs field, ρ_{Hf}

$$N_{\text{em/gr}} = G_{\text{em}} / G = \rho_{\text{As}} / \rho_{\text{Hf}} = 4.165798 \cdot 10^{42}. \quad (5.4.1)$$

It is the SST large numbers law that follows from constancy of the SST initial parameters because there is the stable boundary of the inner Cosmos and very high dynamic pressure in the SST two-component spacetime.

We see that in the SST-As are created the electron-positron pairs i.e. this part of the SST spacetime relates to the electromagnetic interactions. On the other hand, in the SST superluminal Higgs field are created the gravitational fields i.e. this part of the SST spacetime relates to the gravitational interactions. Properties of the SST-As and SST-Hf are very different so unification of the electromagnetic interactions (also the weak and strong) with gravitational interactions (i.e. the Standard Model with Gravity) within the same methods is impossible.

The wrong assumption in the mainstream theories that the observed flows in the SST absolute spacetime (for example, by LIGO) are the gravitational waves suggests incorrectly that unification of the Standard Model and Gravity is possible.

Gravity appears because the neutrinos composed of the entanglons are placed in the SST Higgs field. On the other hand, the binary systems of neutrinos are the components of the SST absolute spacetime so SST shows that the internal structure of neutrinos marks the boundary between the gravitational fields and those described in the Standard Model.

The Schwarzschild surface is an abstract surface. Near the black holes (BHs) composed of the neutron black holes, the SST-As components, which have gravitational mass, spiral towards the centre of BH – it is because below equators of BHs ($R_{\text{equator,BH}} = GM/c^2$), orbital speed of the SST-As components should be higher than c . But due to the very high dynamic pressure ($\sim 10^{45} \text{ Pa}$) and constant speed of the neutrino-antineutrino pairs, these components are pulled along the BH's axis of rotation despite having a non-zero gravitational mass. The weak interactions between the SST-As jets and particles are the cause of the removal of gravitating matter from inside the black hole.

Chapter 6

Harbingers of a Revolution in Physics

The foundations of quantum physics and general relativity were formulated at the beginning of the 20th century, i.e. about a hundred years ago. There is a view that theoretical physics is practically complete. But when we ignore the Scale-Symmetric Theory, the truth is quite different. 95 percent of physics by mass/energy is dark matter and dark energy, and we still do not know the origin of these forms of matter and energy. The remaining 5 percent is mainly baryon matter and we still cannot calculate the exact masses and spins of the proton and neutron from the initial conditions used in the Standard Model. Moreover, these initial conditions cannot be considered fundamental. When we add to this the problems with the rate of formation of supermassive black holes in the early universe and dozens of unsolved fundamental problems such as, for example, the origin of masses of neutrinos or the matter-antimatter asymmetry, we can confidently say that we know very little, which contradicts the statement that theoretical physics is coming to an end.

What main mistakes are repeated by successive generations of physicists that the theory of everything is still beyond the horizon for them? The main mistake is to ignore the internal structure of bare fermions – it is straight path to infinite values in your calculations and the need to use mathematical tricks to match the theoretical results with your experimental data. But even such treatments do not lead to accurate results, as can be seen from the anomalous magnetic moment of the muon and the properties of the nucleons. Other errors are assumptions about the quantum superposition of a mathematical point, the coherence of wavefunctions without superluminal communication, the simultaneous constancy of the speed of light with respect to all inertial systems, or the smooth transformation from inflation (that created spacetime and boundary of the inner Cosmos) to the expansion of the universe, and so on.

Several experimental results lead directly to the Scale-Symmetric Theory.

The baryon-antibaryon strong interaction potential is [1]

$$r_{o,experiment,STAR} = 2.83 \pm 0.12 \text{ fm} . \quad (6.1)$$

On the other hand, radius of the SST last orbit for the strong interactions is $R_{d=4} = A + 4B_{mean} = 2.705 \text{ fm}$ – it is very close to the lower limit in (6.1), while the SST range of the nuclear strong interactions is $L_{Strong} = 2.958 \text{ fm}$ – it is very close to the upper limit in (6.1).

So-called “hard core of nucleons” of an infinite strength was first introduced phenomenologically by Jastrow in 1950 [2]. We assume that it concerns the SST fundamental gluon loop (FGL).

When a beam is flowing in direction of the spin of a target (i.e. the spins of the target components are polarized) then we should obtain the radius of FGL – it is at the zero-temperature limit and it is the upper limit for the radius of the hard core of nucleons in our model

$$R_{Hard-core,upper} = R_{FGL} = 2A/3 = 0.465 \text{ fm} . \quad (6.2)$$

On the other hand, for thermal nucleons (i.e. their spins are not polarized) we obtain the lower limit for radius of the hard core of nucleons. Along the x-axis and y-axis, the radius is R_{FGL} while along the z-axis the radius is zero so an approximate mean value that is the lower limit is

$$R_{\text{Hard-core,lower}} = (2 R_{\text{FGL}} + 0) / 3 = 0.31 \text{ fm} . \quad (6.3)$$

In paper [3], there are calculated the properties of a neutron star (NS) at zero-temperature limit (so spins of neutrons are polarized). They found the hard core radius for the baryons

$$0.425 \text{ fm} < R_{\text{Hard-core,NS,[3]}} < 0.476 \text{ fm} . \quad (6.4)$$

This result is consistent with our result (6.2).

In paper [4], authors claim that a comparison with the phenomenology of neutron stars implies that the hard-core radius of nucleons has to be temperature and density dependent. Their result for the hard-core radius of nucleons is

$$0.3 \text{ fm} < R_{\text{Hard-core,NS,[4]}} < 0.36 \text{ fm} . \quad (6.5)$$

This result is consistent with our result (6.3).

Consider the ATOMKI anomalies. In measurements of the angular correlation of electron-positron pairs in the isoscalar and isovector decays of atomic nuclei, a large deviation was found from quantum electrodynamics (QED) prediction for internal pair conversion (IPC). Applying the Scale-Symmetric Theory we show that such correlations are not associated with a fifth force but with creation of very unstable condensates from the SST-As components because of the nuclear weak interactions (the coupling constant is $\alpha_{w(p)} = 0.0187229$). They found a neutral boson with a mass around 9 MeV [5], neutral bosons with the dominant peaks at 12.42 MeV and 14.55 MeV [6], and around 17 MeV (the X17 particle) [7], and few others.

Our model is as follows. A weak mass, $\alpha_{w(p)}M$, of a characteristic mass, M , in the core of baryons attaches the electron-positron pair, $2m_e$, so the neutral resultant mass, M_{boson} , is

$$M_{\text{boson}} = \alpha_{w(p)} M + 2 m_e . \quad (6.6)$$

For the central condensate $M = Y = 424.17 \text{ MeV}$ we obtain $M_{\text{boson}} = 8.96 \text{ MeV}$.

For the pair of the tori/electric-charges $M = X^+X^- = 2X^\pm = 636.59 \text{ MeV}$ we obtain $M_{\text{boson}} = 12.94 \text{ MeV}$.

For the core of baryons $M = H^+ = 727.44 \text{ MeV}$ we obtain $M_{\text{boson}} = 14.64 \text{ MeV}$.

For the pair of the central condensates $M = 2Y = 848.34 \text{ MeV}$ we obtain $M_{\text{boson}} = 16.91 \text{ MeV} \equiv X17$.

But there are created also pions, muons and other objects so we should observe also the insignificant peaks.

We can see that the ATOMKI anomalies lead to the structure of the core of baryons.

In the future, we should observe the two following anomalies:

* Due to the different weak interactions of muons and electrons and the decays of the $\mu^+\mu^-$ pairs into the electron-positron pairs, we should observe an excess in quanta with energy equal to 2.76 keV (see Sections 3.9 and 2.8).

** Within the Scale-Symmetric Theory we predict existence of new scalar boson and/or vector boson with a mass of 17.1 – 17.2 TeV that results from structure of the core of baryons and density of the SST absolute spacetime (see Section 2.15) – there are four different formulae leading to such anomaly.

References

- [1] Adam Kisiel, *et al.* (3 March 2014). “Extracting baryon-antibaryon strong interaction potentials from $p\Lambda_{\text{anti}}$ femtosopic correlation function”
arXiv:1403.0433v1 [nucl-th]
J. Adams, *et al.* (STAR Collaboration)
Phys. Rev. **C74**, 064906 (2006), nucl-ex/0511003
- [2] R. Jastrow, Phys. Rev., **81**, 165 (1951).
- [3] Violetta V. Sagun and Ilídio Lopes (20 November 2017). “Neutron Stars: A Novel Equation of State with Induced Surface Tension”
The Astrophysical Journal, 850:75 (6pp), 2017 November 20
- [4] K. A. Bugaev, *et al.* (6 November 2018). “Hard-core Radius of Nucleons within the Induced Surface Tension Approach”
arXiv:1810.00486v2 [hep-ph]
- [5] F. W. N. de Boer, *et al.* (2001). “Further search for a neutral boson with a mass around 9 MeV/c²”
J. Phys. G: Nucl. Part. Phys. **27** L29
- [6] Fokke de Boer (6 January 2006). “Anomalous Internal Pair Conversion Signaling Elusive Light Neutral Particles”
arXiv:hep-ph/0511049v2
- [7] A. J. Krasznahorkay, *et al.* (29 January 2016). “Observation of Anomalous Internal Pair Creation in ⁸Be: A Possible Indication of a Light, Neutral Boson”
Phys. Rev. Lett., **116**, 042501 (2016)

A very short recapitulation

*The viscid interactions between the tachyons and between the tachyons and entanglons are the fundamental interactions and they follow from smoothness of surfaces of the tachyons – they lead to the gravitational fields. On the other hand, the quantum entanglement and the confinement of the SST-As components lead to the electromagnetic, weak, and strong interactions. Unification of Gravity and Quantum Mechanics is impossible.

*The structure of neutrinos and the atom-like structure of baryons are the fundamental structures in particle physics. Oscillations of neutrinos are an illusion.

*Due to the cosmological collision, the SST inflation was the explosion of space (of the initial inflation field).

*At the end of the SST inflation, the external left-handedness of the initial inflation field led to the emergence of the matter-antimatter asymmetry – just the baryons are internally left-handed.

*The expansion of the Universe was separated in time from the SST inflation – such expansion is the result of the evolution of the Protoworld composed of the SST-absolute-spacetime components.

*The Universe is anisotropic because of the initial anisotropies and protuberances. But mass density of the isotropic SST-As dominates so the Universe is practically flat.

*Dark matter and dark energy differ from matter in the arrangement of the spins of the components of the SST absolute spacetime.

*Quantum Mechanics wrongly describes structure and dynamics of the zero-energy field.

Chapter 7

Appendices

7.1. Appendix A: The neutron mean square charge radius and the origin of the Standard Model	144
7.2. Appendix B: Lepton universality	146

7.1. Appendix A: The neutron mean square charge radius and the origin of the Standard Model

Introduction

New measurements of the charge radius of the neutron show that the neutron has a mean square charge radius of [1]

$$\langle r_n^2 \rangle = -0.1101 \pm 0.0089 \text{ fm}^2. \quad (7.1.1)$$

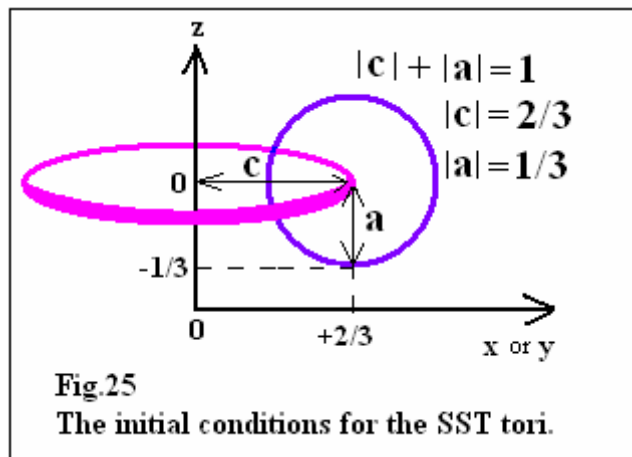
The negative sign in (7.1.1) refers to the negatively charged cloud created by the relativistic negative pion located in the outer part of the neutron [2]. In SST, such pion is in orbit with radius $A + B_{\text{mean}}$, where $A = 0.6974425 \text{ fm}$ (see formula 2.1.15) and $B_{\text{mean}} = 0.5018333 \text{ fm}$ (see formula 2.5.9).

Quantum chromodynamics (QCD) leads to a positive core and a negative outer region in the neutron [3] – the same we have in SST for one state of the two states of neutron (frequency of occurrence of this state is $\sim 62.6\%$: see Section 2.5). In the second state of the neutron ($\sim 37.4\%$), all main components of the neutron are neutral (see Section 2.5).

The origin of the Standard Model

In SST, electric charge is a photon loop with poloidal speed that forces a spherical symmetry of electromagnetic field at distances much greater than the radius of the photon loop. SST shows also that a photon loop can transform into a ring-torus/electric-charge with central condensate. The ring torus is most stable when for $|c| + |a| = 1$ (see Fig.25) is $|c| = 2/3$ and $|a| = 1/3$ (see Fig.2). Such values lead from the elementary electric charge, e , of a photon loop ($|e| = 1$) to the electric charges of quarks ($q_{u,c,t} = +2/3$ and $q_{d,s,b} = -1/3$) in the Standard Model (SM).

The Kasner metric is an exact solution to theory of general relativity (GR) for an anisotropic universe without matter so it is a spacetime solution. For the dimensions $D = 3 + 1$ and the Kasner conditions we have $(2/3, 2/3, -1/3)$ [4]. Notice that the three number fractions as well represent the electric charges of quarks in the proton and in particles built of two quarks carrying the charge $+2/3$ and one carrying the charge $-1/3$. So there is a link between GR (a spacetime solution) and the quarks in some particles in SM.



The mean square charge radius of the neutron

With time, a photon loop in a thermal neutron changes orientation of its plane so it leads to an abstract charged sphere. The negative pion in the $A + B_{\text{mean}}$ state creates the negatively charged cloud – it is a cylinder with the orthogonal radii equal to $R_x^- = R_y^- = A + B_{\text{mean}}$ and $R_z^- = A/3$ (see Section 2.19).

The arithmetic mean of the above orthogonal radii, which is the radius of the abstract negatively charged sphere, which is the mean negative charge radius of the neutron, $R_{o,n-}$, is

$$R_{o,n-} = (R_x^- + R_y^- + R_z^-) / 3 = [2 (A + B_{\text{mean}}) + A / 3] / 3 = 0.8770108 \text{ fm} . \quad (7.1.2)$$

Similar considerations for a positively charged photon loop (then the poloidal motion is left-handed) with a radius of $R_x^+ = R_y^+ = A$ (we assume that $R_z^+ = R_z^-$), which transforms into the torus/electric-charge in the core of baryons, lead to the mean positive charge radius of the neutron, $R_{o,n+}$

$$R_{o,n+} = (R_x^+ + R_y^+ + R_z^-) / 3 = (2 A + A / 3) / 3 = 0.5424553 \text{ fm} . \quad (7.1.3)$$

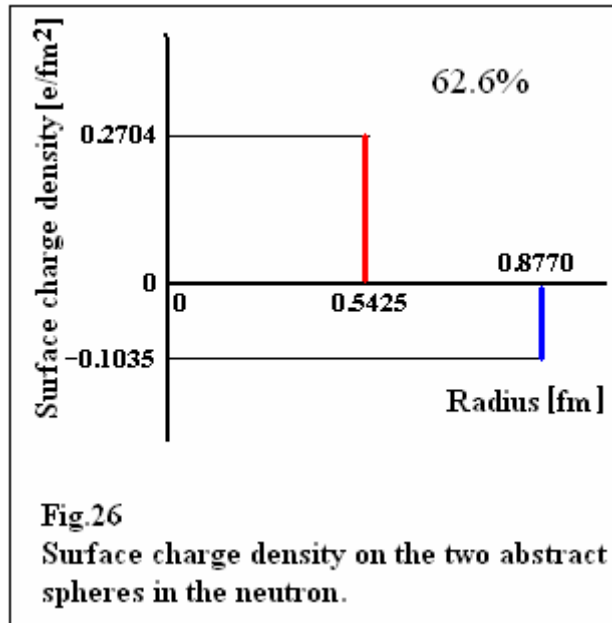
The neutron mean charge radius, r_n , is defined as the distance between the two abstract charged spheres

$$r_n = R_{o,n-} - R_{o,n+} = 0.3345555 \text{ fm} \quad (7.1.4)$$

so, in SST, the mean square charge radius of the neutron is

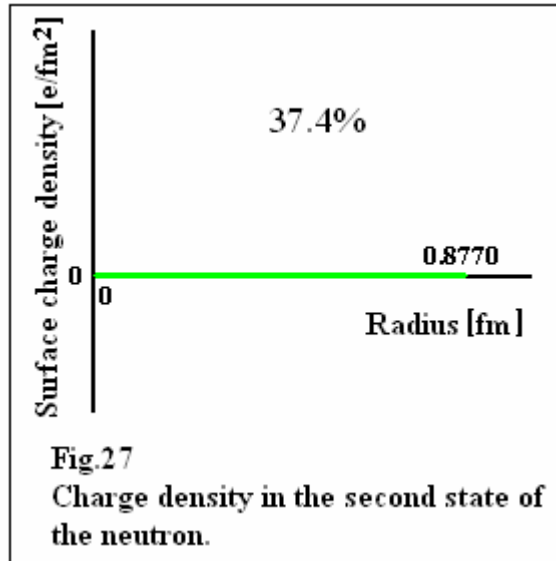
$$\langle r_n^2 \rangle = -0.11193 \text{ fm}^2 . \quad (7.1.5)$$

It is consistent with experimental data [1].



In Fig.26, we present the surface density of electric charges on the abstract spheres in the first state of the neutron.

In Fig.27, we present the surface density of electric charges in the second state of the neutron.



The ratio of the radii of the two abstract electrically charged spheres is close to the golden ratio (~ 1.618)

$$R_{o,n-} / R_{o,n+} \approx 1.617 . \quad (7.1.6)$$

References

- [1] Benjamin Heacock, *et al.* (10 September 2021). “Pendellösung interferometry probes the neutron charge radius, lattice dynamics, and fifth forces”
Science, 10 Sep 2021, Vol 373, Issue 6560, pp. 1239-1243,
DOI: 10.1126/science.abc2794
- [2] S. Kopecky, *et al.* (1995)
Phys. Rev. Lett. **74**, 2427 (1995)
- [3] Jo van den Brand, *et al.* (1996)
Physics World, February 35, 1996
- [4] Edward Kasner (1921). “Geometrical theorems on Einstein’s cosmological equations”
Am. J. Math. **43**, 217-221 (1921)

7.2. Appendix B: Lepton universality

According to SST, both the electron and muon have similar structures with different sizes of the components (a loop, or a torus with central condensate) but there is a difference: contrary to the electron, inside the muon central condensate, there are two energetic neutrinos (see Section 2.8). It causes that interactions of the two different leptons are not the same so the magnetic moment of the muon is higher than it should be (see Section 2.8).

Lepton universality is defined as follows: All three types of charged lepton particles interact in the same way with other particles.

SST shows that the **B** bosons are produced inside baryons.

We will show that the different branching ratios, BR, for the decays $B^0 \rightarrow K_S^0 \mu^+ \mu^-$ and $B^0 \rightarrow K_S^0 e^+ e^-$ follow from the structure and dynamics of baryons.

According to SST, the $\mu^+\mu^-$ pairs in B^0 are produced near the condensate Y in centre of the baryons so for the production of the $B_{\mu^+\mu^-}^0$ bosons (i.e. $K_S^0 \mu^+\mu^- \rightarrow B_{\mu^+\mu^-}^0$) are responsible the nuclear weak interactions ($\alpha_{w(p)} = 0.01872291$: see (2.2.27)). **Notice that particles “remember” which coupling constants were responsible for their production so in the decays of such $B_{\mu^+\mu^-}^0$ bosons appear the $\mu^+\mu^-$ pairs.**

On the other hand, the e^+e^- pairs are produced outside the electrically charged core of baryons so for the production of the $B_{e^+e^-}^0$ bosons (i.e. $K_S^0 e^+e^- \rightarrow B_{e^+e^-}^0$) are responsible the nuclear electroweak interactions ($\alpha_{w(p)} + \alpha_{em}$, where α_{em} is the fine structure constant).

We define the branching ratio as inversely proportional to lifetime so by applying formula (1.4.29) we have

$$BR \sim \alpha_i, \quad (7.2.1)$$

where α_i is the coupling constant responsible for production/decay of a particle.

Such remarks lead to the SST ratio, $R_{SST,low-energy}$, of the considered here two different branching ratios for decays of the B bosons at low energy

$$\begin{aligned} R_{SST,low-energy} (K_S^0 \text{ or } K^{*+}) &= BR(B_{\mu^+\mu^-}^0 \rightarrow K_S^0 \mu^+\mu^-) / BR(B_{e^+e^-}^0 \rightarrow K_S^0 e^+e^-) = \\ &= \alpha_{w(p)} / (\alpha_{w(p)} + \alpha_{em}) = 0.71955. \end{aligned} \quad (7.2.2)$$

Emphasize that the result $R_{SST,low-energy} = 0.71955$ follow from the fact that inside baryons the electron-positron pairs are created more frequently than the $\mu^+\mu^-$ pairs.

Value of the fine structure constant increases at high energies because there increases the effective electric charge. For value about $\alpha_{em,high-energy} = 1 / 128$ we obtain

$$R_{SST,high-energy} (K_S^0 \text{ or } K^{*+}) = \alpha_{w(p)} / (\alpha_{w(p)} + \alpha_{em,high-energy}) = 0.7056. \quad (7.2.3)$$

Our results, i.e. $R_{SST,low-energy} \approx 0.720$ and $R_{SST,high-energy} = 0.706$, are consistent with the last experimental data for $B^0 \rightarrow K_S^0 I^+ I^-$ decays and $B^+ \rightarrow K^{*+} I^+ I^-$ decays [1]

$$R(K_S^0) = 0.66^{+0.20}_{-0.14} \text{ (stat.) } ^{+0.02}_{-0.04} \text{ (syst.)}. \quad (7.2.4)$$

$$R(K^{*+}) = 0.70^{+0.18}_{-0.13} \text{ (stat.) } ^{+0.03}_{-0.04} \text{ (syst.)}. \quad (7.2.5)$$

More precise experimental data will show whether our atom-like structure and dynamics of baryons are correct.

References

[1] LHCb collaboration (19 October 2021).

“Tests of lepton universality using $B^0 \rightarrow K_S^0 I^+ I^-$ and $B^+ \rightarrow K^{*+} I^+ I^-$ decays”
arXiv:2110.09501v2 [hep-ex]

Index

3+ means “page 3 and beyond”

- absolute spacetime (SST-As) 6, 29
- astrophysics 94+
- atomic nucleus 109+
- atomic physics 114+
- ATOMKI 141
- atom-like structure of baryons 31+
- azimuthal number 14+-Fig.9

- baryonic matter 74+
- baryons 7+
- black body 87+
- black hole 98, 139

- chaos theory 121+
- charge conjugation 11-Fig.4
- chi_b mesons 137+
- closed string 6, 22
- CMB 83+
- condensates 25
- confinement 7, 44+
- core of baryons 23, 28
- cosmology 73+, 94+
- Cosmos 9, 76+
- coupling constant 28, 30

- dark-matter 9, 24, 74+, 131+
- dark energy 9, 74+, 131+
- degrees of freedom 42+
- dynamics of core of baryons 25+

- electron 19+, 26+, 29+, 31
- entanglement (quantum) 7
- entanglon 6

- fine-structure constant 27, 40+
- fundamental gluon loop 25

- galaxies 94+
- gluons 7, 41+
- gamma-ray bursts 99+
- gravitational constant 25

- half-jet asymmetry 11
- helicity 6
 - external 6
 - internal 6
- Higgs boson 49
- Higgs field (SST-Hf) 6
- Hubble constant 81+
- hydrogen atom 117+
- hyperons 58+

- inflation field (initial) 6, 22+, 76+
- initial conditions 10+
- interactions 43+, 47+
- iterative parameters 10, 22, 23, 31, 33

- Lamb-Retherford shift 50+
- large numbers law 139
- large structures 65+, 79+
- leptons (electrically charged) 7+
- lepton universality 146+
- lifetimes 18, 52+

- magnetars 106
- matrix 62+
 - PMNS 62+
 - CKM 63+
- mental world 120+
- mesons 56+
- muon 37+

- neutrinos 8, 23, 26
- neutron 35+
- neutron black holes (NBHs) 10, 77+
- neutron charge radius 144+
- nuclear physics 109+
- number K 22

- parity 12-Fig.5
- particle physics 21+, 93+
- Pauli Exclusion Principle 114+
- phase transitions 22+

- photons 7, 41+
- physical constants 22+
- pion 27, 37
- Planck constant 22
- proton 35+, 54+
- Protoworld 24
- pulsars 106

- quantum gravity 44+, 125+
- quantum physics 122+
- quarks 10, 61+, 134+

- range 14+
 - strong interactions 14-Fig.8
- relativistic mass 15+
- resonances 60+
- Reynolds number 22
- running coupling constant 47+

- Solar System 101
- space roar 134+
- spacetime (SST-S) 7
- speed c 9, 22
- spin-flip in hydrogen 49+
- Standard Model 144
- standard ruler 87
- Stefan-Boltzmann law 16+
- symmetries (new) 10+
 - adoption symmetry 11
 - decay symmetry 11
 - four-object symmetry 10
 - invariant surface-density symmetry 11
 - saturation symmetry 11

- tachyon 6
- tauon 40+
- thermodynamics 22+
- time reversal 12-Fig.6
- Titius-Bode law 13+
 - strong interactions 13+-Fig.7, 34
 - gravitational interactions 101+
- tori (fundamental) 8, 13, 23

- ultimate equation 66+
- uncertainty 20, 36+
- unification 139
- universes 76+
- Universe 80+, 86+, 88+, 96+
- Upsilon mesons 137+

- virtual particles 9-Fig.3

- W boson 42
- Wien's displacement law 16
- Wow! signal 126+

- Z boson 42
- zero-energy field 8, 67